INFORMATION TO USERS

This reproduction was made from a copy of a document sent to us for microfilming. While the most advanced technology has been used to photograph and reproduce this document, the quality of the reproduction is heavily dependent upon the quality of the material submitted.

The following explanation of techniques is provided to help clarify markings or notations which may appear on this reproduction.

1. The sign or "target" for pages apparently lacking from the document photographed is "Missing Page(s)". If it was possible to obtain the missing page(s) or section, they are spliced into the film along with adjacent pages. This may have necessitated cutting through an image and duplicating adjacent pages to assure complete continuity.

2. When an image on the film is obliterated with a round black mark, it is an indication of either blurred copy because of movement during exposure, duplicate copy, or copyrighted materials that should not have been filmed. For blurred pages, a good image of the page can be found in the adjacent frame. If copyrighted materials were deleted, a target note will appear listing the pages in the adjacent frame.

3. When a map, drawing or chart, etc., is part of the material being photographed, a definite method of "sectioning" the material has been followed. It is customary to begin filming at the upper left hand corner of a large sheet and to continue from left to right in equal sections with small overlaps. If necessary, sectioning is continued again—beginning below the first row and continuing on until complete.

4. For illustrations that cannot be satisfactorily reproduced by xerographic means, photographic prints can be purchased at additional cost and inserted into your xerographic copy. These prints are available upon request from the Dissertations Customer Services Department.

5. Some pages in any document may have indistinct print. In all cases the best available copy has been filmed.

University Microfilms International

300 N. Zeeb Road
Ann Arbor, MI 48106

8312372

Schuchman, Edward Howard

BIOCHEMICAL AND SOMATIC CELL GENETIC STUDIES OF HUMAN AND FELINE MUCOPOLYSACCHARIDOSES I

City University of New York PH.D. 1983

University
Microfilms
International 300 N. Zeeb Road, Ann Arbor, MI 48106

Copyright 1983

by

Schuchman, Edward Howard

All Rights Reserved

PLEASE NOTE:

In all cases this material has been filmed in the best possible way from the available copy. Problems encountered with this document have been identified here with a check mark ✓.

1. Glossy photographs or pages _____
2. Colored illustrations, paper or print _____
3. Photographs with dark background ✓
4. Illustrations are poor copy _____
5. Pages with black marks, not original copy _____
6. Print shows through as there is text on both sides of page _____
7. Indistinct, broken or small print on several pages ✓
8. Print exceeds margin requirements _____
9. Tightly bound copy with print lost in spine _____
10. Computer printout pages with indistinct print _____
11. Page(s) _____ lacking when material received, and not available from school or author.
12. Page(s) _____ seem to be missing in numbering only as text follows.
13. Two pages numbered _____. Text follows.
14. Curling and wrinkled pages ✓
15. Other _____

University
Microfilms
International

BIOCHEMICAL AND SOMATIC CELL GENETIC STUDIES OF HUMAN AND FELINE MUCOPOLYSACCHARIDOSES I

by

EDWARD HOWARD SCHUCHMAN

A dissertation submitted to the Graduate Faculty in Biomedical Sciences in partial fulfillment of the requirements for the degree of Doctor of Philosophy, The City University of New York.

1983

© Copyright by

EDWARD HOWARD SCHUCHMAN

1983

This manuscript has been read and accepted for the Graduate Faculty in Biomedical Sciences in satisfaction of the dissertation requirement for the degree of Doctor of Philosophy.

1/17/83
Date

Chairman of Examining Committee

1/18/83
Date

Executive Officer

David F. Bishop

Gregory A. Grabowski

Mark E. Haskins

Kurt Hirschhorn

Supervisory Committee

The City University of New York

BIOCHEMICAL AND SOMATIC CELL GENETIC STUDIES OF HUMAN AND FELINE MUCOPOLYSACCHARIDOSES I

by: Edward Howard Schuchman

Advisor: Professor R.J. Desnick

ABSTRACT

Biochemical and somatic cell genetic studies have been undertaken to initiate investigations into the molecular pathology of human and feline mucopolysaccharidoses I (α-L-iduronidase deficiency diseases). Towards this end a new, continuous, monodimensional cellulose acetate electrophoretic system was developed for the resolution of six major mammalian glycosaminoglycans. Using this micro-method, an extensive survey of the stored glycosaminoglycans in the tissues of homozygotes with human or feline mucopolysaccharidoses I was undertaken characterizing, for the first time, the distribution of the stored glycosaminoglycans in these disorders.

In addition, two major fractions containing α-L-iduronidase activity have been identified in normal human tissues and purified over 150,000-fold to homogeneity. The more electronegative form of the enzyme is membrane-associated and taken up rapidly by cultured α-L-iduronidase deficient fibroblasts ("high uptake"), while the more soluble form is "low uptake" enzyme. Isoelectric focusing studies of crude tissue homogenates revealed that a broad region (pI 5.85-7.35) stained for α-L-iduronidase activity. Two distinct, major bands (pI values of 6.00 and 6.85) were observed.

SDS polyacrylamide gel electrophoresis under denaturing conditions revealed that the low uptake fraction was composed of a 72,000 dalton doublet and a diffuse 43,000 component, while the high uptake fraction had a consistent 90,000 band in addition to the 72,000 and 43,000 molecular weight species. Further purification using high performance liquid chromatography, combined with these data, indicated that the homogeneous enzyme fractions contained a number of discrete polymeric and proteolytic intermediates, each of which retained catalytic activity.

Kinetic studies using artificial and natural substrates revealed that the K_m and apparent V_{max} values for both enzyme forms were nearly identical. The thermal stabilities of the two enzyme forms at 45°C, 52°C and 60°C and the pH optima using three different substrates were also nearly identical. Heparin was a potent non-competitive inhibitor of the 4-methylumbelliferyl α-L-iduronide activity for both the high and low uptake enzymes (K_i values of 0.13 mg/ml and 0.09 mg/ml, respectively). Interestingly, the inhibitory effect of each glycosaminoglycan was significantly less for the high uptake than the low uptake form despite their similar catalytic properties. Antibody raised in New Zealand white rabbits against the purified low uptake enzyme fraction recognized the high uptake form in both immunoprecipitation reactions and Ochterlony immunodiffusion gels. Amino acid composition analyses of the homogeneous enzyme fractions revealed significant differences.

The chromosomal locations of the structural genes for human and feline α-L-iduronidase were also determined. In all somatic cell hybrids examined the presence of human chromosome 22 was 100% concordant with the expression of human α-L-iduronidase activity. Studies of cell lines containing structural rearrangements of chromosome 22 further

localized the human gene to the region 22pter → 22q11. Finally, a cellulose acetate electrophoretic system was developed to discriminate the human and feline enzymes from their Chinese hamster counterpart in hamster-human or hamster-feline somatic cell hybrids; this method was used to confirm the assignment of the human structural gene to chromosome 22 and to map the feline structural gene to feline chromosome D4.

FORWORD

Portions of this thesis have been included in the following publications or manuscripts submitted for publication:

Schuchman, E.H. and Desnick, R.J.: A new continuous, monodimensional electrophoretic system for the separation and quantitation of individual glycosaminoglycans. Anal. Biochem. 117:419, 1981.

Desnick, R.J., McGovern, M.M., Schuchman, E.H., and Haskins, M.E.: Animal analogues of human inherited metabolic diseases: molecular pathology and therapeutic studies. In: Animal Models of Inherited Metabolic Diseases, Desnick, R.J., Patterson, D.F., and Scarpelli, D.F., eds., Alan R. Liss, Inc., New York, p 27-65, 1982.

Schuchman, E.H., Guzman, N.A., and Desnick, R.J.: Studies of human α-L-iduronidase. I. Identification and purification to homogeneity of high and low uptake forms from human lung. J. Biol. Chem., in review.

Schuchman, E.H., Guzman, N.A., and Desnick, R.J.: Studies of human α-L-iduronidase. II. Comparative biochemical and immunologic properties of purified high and low uptake forms from human lung. J. Biol. Chem., in review.

Schuchman, E.H., Astrin, K.A., Aula, P., and Desnick, R.J.: Regional gene assignment for human α-L-iduronidase. Proc. Natl. Acad. Sci., in review.

ACKNOWLEDGEMENTS

I wish to express my sincerest appreciation to Bob Desnick whose continual guidance, support and friendship have enabled me to pursue my education with professionalism and pleasure. His skillful creativity, perseverance and productivity will remain a model of excellence throughout my career.

I also wish to acknowledge the valuable intellectual and technical contributions of the following individuals: Norberto Guzman, Kenneth Astrin, Raman Reddy, David Bishop, Pepe Aula, Constantine Zamfirescu, Jessica Fuchs and Elizabeth Ginsburg. In addition, I am grateful to the following individuals for the supply of materials: Drs. M.B. Mathews, J.A. Cifonelli, Ruben Matalon, Bernard Weissman, Elizabeth Neufeld, Irwin Leder, Mark Haskins, Moyra Smith, Stephen O'Brien, Marcello Sinescalco, T. Mohandas and Diane Arthur.

An accomplishment of this sort cannot be completed without the warmth and companionship of many cherished friends and family. I want to especially express my deepest gratitude to my parents who have always been, and I trust will continue to be, my strongest supporters; I credit any future success to them.

Finally, I wish to express special thanks to Elof Carlson, who introduced me to the field of genetics and taught me the aesthetic art of science. His pursuit of scholarship and unique perspectives offer me a continually refreshing and valuable friendship.

TABLE OF CONTENTS

Page

APPROVAL PAGE.....iii

ABSTRACT.....iv

FORWARD.....vii

ACKNOWLEDGEMENTS.....viii

TABLE OF CONTENTS.....ix

LIST OF TABLES.....xiii

LIST OF FIGURES.....xv

LIST OF ABBREVIATIONS.....xvii

I. BACKGROUND AND RATIONALE.....1

A. BRIEF HISTORICAL PERSPECTIVE OF THE HUMAN TYPE I MUCOPOLYSACCHARIDE STORAGE DISEASES.....1

B. ANALYTICAL STUDIES OF GLYCOSAMINOGLYCANS IN NORMAL AND MUCOPOLYSACCHARIDOSIS I HOMOZYGOTES.....5

C. STUDIES OF LYSOSOMAL ENZYME PROCESSING AND TRANSPORT.....8

D. STUDIES OF HUMAN α-L-IDURONIDASE PURIFICATION AND CHARACTERIZATION.....11

E. COMPARATIVE GENE MAPPING AND STUDIES OF LYSOSOMAL ENZYME GENE REGULATION.....15

F. ANIMAL MODELS OF HUMAN LYSOSOMAL STORAGE DISEASES.....20

II. OBJECTIVES.....26

III. MATERIALS.....27

A. GLYCOSAMINOGLYCAN ANALYSES.....27

B. PURIFICATION AND CHARACTERIZATION OF LOW AND HIGH UPTAKE FORMS OF HUMAN α-L-IDURONIDASE.....27

C. COMPARATIVE GENE MAPPING OF HUMAN AND FELINE α-L-IDURONIDASE.....28

Page

IV. METHODS.....30

A. GLYCOSAMINOGLYCAN ANALYSES.....30

1. GLYCOSAMINOGLYCAN ELECTROPHORESIS.....30

2. EVALUATION OF OPTIMAL GLYCOSAMINOGLYCAN SEPARATION.....31

3. TISSUE ISOLATION OF GLYCOSAMINOGLYCANS.....32

B. PURIFICATION AND CHARACTERIZATION OF LOW AND HIGH UPTAKE FORMS OF HUMAN α-L-IDURONIDASE.....33

1. STANDARD ENZYME AND PROTEIN ASSAYS.....33

2. APPARENT MOLECULAR WEIGHT DETERMINATIONS.....33

3. FLAT-BED ISOELECTRIC FOCUSING.....34

4. NATIVE POLYACRYLAMIDE GEL ELECTROPHORESIS.....34

5. SDS POLYACRYLAMIDE SLAB GEL ELECTROPHORESIS.....35

6. ENZYME UPTAKE STUDIES.....36

7. ANTIBODY PRODUCTION AND CHARACTERIZATION.....36

8. AMINO ACID COMPOSITION ANALYSES.....37

9. PURIFICATION PROCEDURE.....37

10. HIGH PERFORMANCE LIQUID CHROMATOGRAPHY.....40

C. COMPARATIVE GENE MAPPING OF HUMAN AND FELINE α-L-IDURONIDASE.....41

1. PREPARATION OF SOMATIC CELL HYBRIDS.....41

2. DETERMINATION OF THE HUMAN AND FELINE CHROMOSOME CONSTITUTION IN SOMATIC CELL HYBRIDS.....41

3. IMMUNODISCRIMINATION OF HUMAN AND MURINE α-L-IDURONIDASE.....42

4. ELECTROPHORETIC SEPARATION OF α-L-IDURONIDASE FROM DIFFERENT SOURCES.....43

5. REGIONAL GENE MAPPING OF HUMAN α-L-IDURONIDASE.....43

Page

V. RESULTS....44

A. GLYCOSAMINOGLYCAN ANALYSES....44

1. DEVELOPMENT OF A NOVEL ELECTROPHORETIC SYSTEM FOR THE ANALYSIS OF GLYCOSAMINOGLYCANS....44

2. ANALYSIS OF STORED GLYCOSAMINOGLYCANS IN HOMOZYGOTES WITH HUMAN AND FELINE MUCOPOLY-SACCHARIDOSES I....54

B. PURIFICATION AND CHARACTERIZATION OF LOW AND HIGH UPTAKE FORMS OF HUMAN α-L-IDURONIDASE....60

1. OPTIMIZATION OF HUMAN ENZYME SOURCE....60

2. ION EXCHANGE CHROMATOGRAPHY....60

3. ISOELECTRIC FOCUSING....63

4. ENZYME UPTAKE STUDIES....63

5. PURIFICATION PROCEDURE....72

6. HIGH PERFORMANCE LIQUID CHROMATOGRAPHY....76

7. STABILITY OF HUMAN α-L-IDURONIDASE....82

8. NATIVE POLYACRYLAMIDE GEL ELECTROPHORESIS....82

9. SDS POLYACRYLAMIDE GEL ELECTROPHOREIS....82

10. APPARENT MOLECULAR WEIGHT DETERMINATIONS....88

11. KINETIC PROPERTIES....91

12. EFFECT OF GLYCOSAMINOGLYCANS....91

13. pH OPTIMA AND THERMAL STABILITY....98

14. EFFECT OF PROTEIN....98

15. AMINO ACID COMPOSITION ANALYSES....98

16. IMMUNOLOGIC FINDINGS....104

C. COMPARATIVE GENE MAPPING OF HUMAN AND FELINE α-L-IDURONIDASE....107

1. IMMUNODISCRIMINATION OF HUMAN AND MURINE α-L-IDURONIDASE....107

Page

2. CHROMOSOMAL ASSIGNMENT OF THE STRUCTURAL GENE FOR HUMAN α-L-IDURONIDASE.....107

3. REGIONAL GENE ASSIGNMENT FOR HUMAN α-L-IDURONIDASE....121

4. ELECTROPHORETIC SEPARATION OF α-L-IDURONIDASE ISOZYMES FROM DIFFERENT SOURCES AND CHROMOSOMAL ASSIGNMENT OF THE FELINE STRUCTURAL GENE.....127

VI. DISCUSSION.....133

A. GLYCOSAMINOGLYCAN ANALYSES.....133

B. PURIFICATION AND CHARACTERIZATION OF LOW AND HIGH UPTAKE FORMS OF HUMAN α-L-IDURONIDASE.....136

C. COMPARATIVE GENE MAPPING OF HUMAN AND FELINE α-L-IDURONIDASE.....145

VII. CONCLUDING REMARKS.....150

BIBLIOGRAPHY.....152

LIST OF TABLES

Page

1. Chemical Properties and Tissue Distribution of the Six Major Mammalian Glycosaminoglycans.....6

2. Chromosome Assignments of the Structural Genes for Human Lysosomal Enzymes.....19

3. Animal Models of Human Lysosomal Storage Diseases.....22

4. Effect of EDTA Tetrasodium Salt Concentration, Current and pH on the Relative Migration of Individual Glycosaminoglycans....45

5. Effect of Different EDTA Salts on the Relative Migration of Individual Glycosaminoglycans.....48

6. Resolution of Glycosaminoglycans in EDTA/Cationic Systems.....50

7. Effect of EDTA Concentration, LiCl Concentration and pH on the Relative Migration of Individual Glycosaminoglycans in EDTA/LiCl Systems.....51

8. Effect of Ethanol Precipitation on the Percent Recovery of Individual Glycosaminoglycans.....55

9. Analysis of Stored Glycosaminoglycans in the Human Mucopolysaccharidosis I-H Disease.....56

10. Analysis of Stored Glycosaminoglycans in the Feline Mucopolysaccharidosis I Disease.....59

11. α-L-Iduronidase Activity in a Variety of Different Human Tissues.....61

12. Optimization of α-L-Iduronidase Extraction from Human Lung.....62

13. Purification of Low and High Uptake Forms of α-L-Iduronidase from Human Lung.....73

14. Contaminating Glycosidases in the Purified Low and High Uptake Forms of Human α-L-Iduronidase Prior to HPLC.....79

15. Stability of the Low and High Uptake Forms of Human α-L-Iduronidase During the Purification Procedure.....83

16. K_m and V_{max} Values Obtained for Purified Low and High Uptake Forms of Human α-L-Iduronidase Using Three Different Substrates.....94

17. Inhibition of Low and High Uptake Forms of Human α-L-Iduronidase by Glycosaminoglycans.....95

Page

18. Thermal Stabilities of Low and High Uptake Forms of Human α-L-Iduronidase.....101

19. Effect of Protein on Low and High Uptake Forms of Human α-L-Iduronidase.....102

20. Amino Acid Composition of Low and High Uptake Forms of Human α-L-Iduronidase.....103

21. Segregation Analysis of Human α-L-Iduronidase and Human Chromosomes in 14 Mouse-Human Somatic Cell Hybrids.....115

22. Segregation Analysis of Human α-L-Iduronidase and Human Chromosomes in Subclones of Mouse-Human Somatic Cell Hybrids....116

23. α-L-Iduronidase Activities in Human Cell Lines Containing Structural Rearrangements of Chromosome 22.....124

24. Segregation Analysis of Feline α-L-Iduronidase and Feline Chromosomes in 13 Hamster-Feline Somatic Cell Hybrids.....130

LIST OF FIGURES

Page

1. The Metabolic Defect in Human and Feline Mucopolysaccharidoses I.....4

2. Current Concept of Lysosomal Enzyme Processing and Transport.....13

3. Electrophoresis of Standard Glycosaminoglycans in EDTA Tetrasodium Salt and LiCl Systems.....47

4. Electrophoresis of Standard Glycosaminoglycans in the EDTA Tetrasodium Salt/LiCl Combined System.....53

5. Electrophoresis of Glycosaminoglycans from Normal and MPS I-H Human Livers in the EDTA Tetrasodium Salt/LiCl Combined System.....58

6 DEAE-Cellulose Chromatographic Profile of Human α-L-Iduronidase.....65

7. DEAE-Cellulose Chromatographic Profile of Separated Soluble and Membrane-Associated Forms of Human α-L-Iduronidase.....67

8. Isoelectric Focusing Profile of Human α-L-Iduronidase.....69

9. Enzyme Uptake Profiles of Soluble and Membrane-Associated Forms of Human α-L-Iduronidase.....71

10. Hydroxyapatite Chromatographic Profiles of Low and High Uptake Forms of Human α-L-Iduronidase.....75

11. Biogel P-100 Chromatographic Profiles of Low and High Uptake Forms of Human α-L-Iduronidase.....78

12. HPLC Profiles of Low and High Uptake Forms of Human α-L-Iduronidase.....81

13. Native Polyacrylamide Gel Electrophoresis of the Purified Low and High Uptake Forms of Human α-L-Iduronidase.....85

14. SDS Polyacrylamide Gel Electrophoresis of the Purified Low and High Uptake Forms of Human α-L-Iduronidase.....86

15. Apparent Molecular Weight Determination of Low and High Uptake Forms of Human α-L-Iduronidase by Gel Filtration.....90

16. Lineweaver-Burk Plots of Low and High Uptake Forms of Human α-L-Iduronidase Using Three Different Substrates.....93

17. Inhibition of Low and High Uptake Forms of Human α-L-Iduronidase by Dermatan Sulfate and Heparan Sulfate.....97

Page

18. pH Profiles of Low and High Uptake Forms of Human α-L-Iduronidase Using Three Different Substrates.....100

19. Immunoprecipitation of Low and High Uptake Forms of Human α-L-Iduronidase by Rabbit Anti-Human Antibodies.....106

20. Immunologic Cross-Reactivity of Rabbit Anti-Human Antibodies with α-L-Iduronidase from Different Sources.....109

21. Immunodiscrimination Assay of Human and Mouse α-L-Iduronidase Activities.....111

22. Artificial Mixing and Immunoprecipitation of Human and Mouse α-L-Iduronidase Activities.....113

23. Metaphase Chromosome Spread of Mouse-Human Hybrid R-G-21-J15 Stained with Trypsin-Giemsa.....118

24. Human α-L-Iduronidase Activities in Mouse-Human Somatic Cell Hybrids with Varying Chromosome 22 Content.....120

25. α-L-Iduronidase Enzyme Levels as a Function of Cell Growth in Human Fibroblasts, Mouse RAG Cells and a Mouse-Human Somatic Cell Hybrid.....123

26. Regional Assignment of the Human α-L-Iduronidase Gene on Chromosome 22.....126

27. Electrophoretic Separation of Human, Feline and Rodent α-L-Iduronidase on Cellulose Acetate.....129

28. Comparative Gene Assignments for the Human and Feline α-L-Iduronidase Structural Genes.....132

LIST OF ABBREVIATIONS

Anhydro[^{3}H]mannitol-iduronide	anhydro[^{3}H]man
Bovine serum albumin	BSA
Centimeter	cm
Chondroitin 4-sulfate	C4S
Chondroitin 6-sulfate	C6S
Concanavalin A-Sepharose	Con A-Sepharose
Dermatan sulfate	DS
Diethylaminoethyl-cellulose	DEAE-cellulose
Endo-β-n-acetylglucosaminidase H	Endo H
Ethylenediaminetetraacetic acid	EDTA
Feline mucopolysaccharidosis I disease	fMPS I
Glycosaminoglycans	GAGs
Grams	g
Heparan sulfate	HS
Heparin	HP
High performance liquid chromatography	HPLC
Human serum albumin	HSA
Hurler disease	MPS I-H
Hurler/Scheie compound disease	MPS I-H/S
Keratan sulfate	KS
Liter	l
4-Methylumbelliferyl-α-L-iduronide	4MU α-Id
Microgram	µg
Microliter	µl
Micromole	µmol

Milliampere	mA
Milligram	mg
Millimolar	mM
Minute	min
Molecular weight	MW
Nanogram	ng
Nanomole	nmol
Optical density	OD
Phenyl α-L-iduronide	Phenyl α-Id
Phenylmethylsulfonyl fluoride	PMSF
Physiologic buffered saline	PBS
Picomole	pmol
Relative migration	R_f
Revolution per minute	RPM
Scheie disease	MPS I-S
Second	s
Sodium dodecyl sulfate	SDS
Specific activity	SA

BACKGROUND AND RATIONALE

A. Brief Historical Perspective of the Human Type I Mucopolysaccharide Storage Diseases:

Hurler disease (MPS I-H) was first delineated by Dr. John Thompson at the Royal Infirmary, Edinburgh, in 1900 (1). However, it was not until 1919 when Gerrod Hurler, an assistant to Professor Meihhard von Ffaundler of Munich, described two unrelated boys with corneal clouding, gibbus deformity and severe mental retardation that the syndrome aroused serious medical interest (1). The major clinical features of Hurler individuals include severe growth retardation, a characteristic facial appearance, hepatosplenomegaly, dysostosis multiplex and severe mental retardation (2). The condition now known as Scheie disease was first described in 1962 by Scheie and his colleagues as a variant of the Hurler syndrome (3). MPS I-S is characterized by corneal clouding, milder dysostosis multiplex and mild aortic valve involvement; few other physical effects are evident and intelligence is usually normal (2). On the basis of electron microscopic studies, it had been assumed by Brante in 1952 that the storage materials in these diseases were glycosaminoglycans (GAGs) (4). Indeed, five years later Dorfman and Lorincz confirmed this observation biochemically (5). In the early 1960's Hers and de Duve developed the concept of lysosomal diseases and in the next few years Hers demonstrated that Hurler syndrome was a lysosomal storage disease (6).

In 1968 Fratantoni, Hall and Neufeld provided definitive proof of a GAG degradative defect in MPS I-H; cultured fibroblasts accumulated excessive amounts of $^{35}SO_4$-labeled GAGs when $^{35}SO_4$ was incubated in the

media and, furthermore, clearance of the radiolabeled GAGs was abnormally slow when the fibroblasts were subsequently chased with "cold" medium (7). Fratantoni, Hall and Neufeld also initiated experiments mixing fibroblasts from patients with different clinical types of GAG storage diseases and demonstrated cross-correction of the metabolic defects. Surprisingly, cells from Hurler and Scheie patients, although phenotypically distinct, failed to cross-correct one another; i.e, they had a deficiency of the same corrective factor (7). One early explanation for this observation which was subsequently confirmed by both biochemical and genetic analyses was allelism; the same gene is altered but the mutations occurred either at different sites in the coding region or, alternatively, a different base change occurred at the same site (8). Consequently, the same enzyme molecule may be altered in two different ways and the functional properties of the two mutant enzymes presumably may differ; hence the clinical manifestations also might differ. McKusick et al. have recently identified seven individuals who present with an autosomal recessively inherited phenotype intermediate between those of Hurler and Scheie (9); they have termed this disease the Hurler/Scheie compound (MPS I-H/S). These investigators have suggested that these patients had the allelic compound of one Hurler gene and one Scheie gene, however, it is also possible that this intermediate disease results from a third allele at the structural gene. In 1972 Bach et al. definitively identified the Hurler-Scheie corrective factor as the lysosomal enzyme, α-L-iduronidase (10) stimulating biochemical and genetic investigations of these phenotypically diverse syndromes (Figure 1).

Figure 1: The Metabolic Defect in Human and Feline Mucopolysaccharidoses I.

Schematic illustration of the enzymatic block which occurs in the autosomal recessively inherited human and feline mucopolysaccharidosis I diseases (α-L-iduronidase deficiency diseases).

FIGURE 1

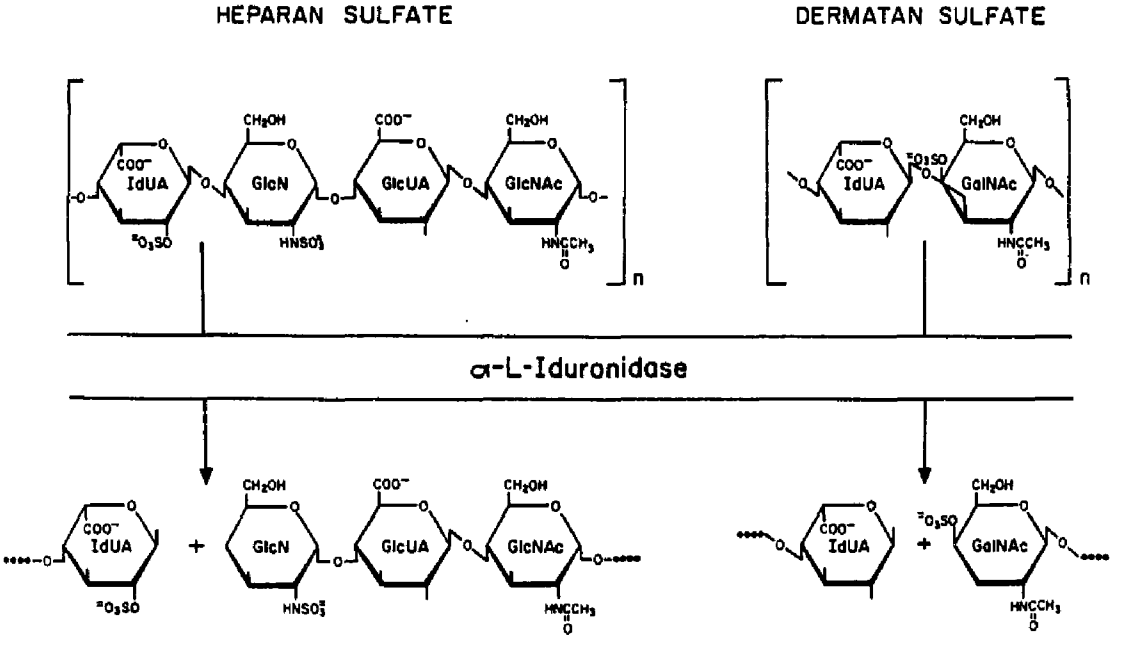
HEPARAN SULFATE
DERMATAN SULFATE
IdUA
GlcN
GlcUA
GlcNAc
GalNAc
α-L-Iduronidase

B. Analytical Studies of Glycosaminoglycans in Normal and Mucopolysaccharidosis I Homozygotes:

GAGs are ubiquitous, complex polysaccharides that are found in bacterial, plant and animal tissues, usually in covalent association with protein (11). Seven types are commonly recognized; six of these are structurally related with a carbohydrate backbone consisting of alternating uronic acid (L-iduronic acid and/or D-glucuronic acid) and hexosamine (D-glucosamine or D-galactosamine) residues. All except one, hyaluronate, are sulfated. Although the GAGs are widely distributed within the animal kingdom (12), their precise physiologic functions remain unknown. They appear to be essential for maintaining the structural integrity of many connective tissues and have, in addition, been assigned a number of functions related to their characteristic physicochemical properties. Table 1 (11) outlines the tissue distribution and properties of the major mammalian GAGs.

There is little information currently available on the levels of GAGs in patients with various mucopolysaccharidoses (13). Kobayashi was the first to demonstrate that granules of "acid mucopolysaccharides" (GAGs) were visible in the cells of three patients with Hurler disease (14). The granules had metachromatic properties and stained positively for mucopolysaccharides. Excessive urinary excretion of dermatan sulfate and heparan sulfate in patients with MPS I-H was first described by Dorfman and Matalon in 1957 (5). Since then, numerous reports have appeared on the biochemical nature of the storage materials excreted in the urine of MPS I-H, MPS I-S and MPS I-H/S individuals (15,16). However, efforts to separate and quantitate the individual GAGs in tissue, cellular or subcellular preparations have been hampered by the lack of

TABLE 1

CHEMICAL PROPERTIES AND TISSUE DISTRIBUTION OF THE SIX MAJOR MAMMALIAN GLYCOSAMINOGLYCANS

Polysaccharide	Mol. Wt. ($\times 10^{-3}$)	Repeating Monosaccharides	Other Sugar Components[a]	Examples of Occurrence in Mammalian Tissues
Hyaluronate	4-8000	D-glucuronic acid D-glucosamine	*[b]	Various connective tissues, skin, vitreous humor, synovial fluid, umbilical cord, cartilage
Chondroitin 4- and 6-sulfates	5-50	D-glucuronic acid D-galactosamine	D-galactose D-xylose	Cartilage, cornea, bone, skin, arterial wall
Dermatan sulfate	15-40	D-glucuronic acid L-iduronic acid D-galactosamine	D-galactose D-xylose	Skin, heart valve, tendon, arterial wall
Heparan sulfate	-	D-glucuronic acid L-iduronic acid D-glucosamine	D-galactose D-xylose	Lung, arterial wall, ubiquitous on cell surfaces
Heparin	6-25	D-glucuronic acid L-iduronic acid D-glucosamine	D-galactose D-xylose	Lung, liver, skin, intestinal mucosa (mast cells)
Keratan sulfate	4-19	D-galactose D-glucosamine	D-galactosamine D-mannose L-fucose sialic acid	Cartilage, cornea, intervertebral disc

[a] Including the sugar components of the polysaccharide-protein linkage region.

[b] The occurrence in hyaluronate of arabinose has been suggested but not conclusively verified.

reproducible and sensitive techniques for the resolution of these diverse molecules. To date, electrophoretic systems using cellulose acetate (17) or agarose (18) have proven useful, but have been limited by their inability to separate all the major mammalian GAGs in a simple, continuous monodimensional system. Current electrophoretic methods require a combination of discontinuous (different buffer systems or sequential ethanol precipitations) and/or two dimensional electrophoretic techniques (19,20).

The binding of GAGs to amino groups was initially observed by Nader et al. (21), who used an ampholine gradient and electrofocusing to separate mixtures of these molecules. The assumption that the GAGs were separated on the basis of specific complex formation with amino groups of the ampholine mixtures was supported by the demonstration that various diamineacetate buffers, containing simple amines, also partially separated GAGs in an agarose electrophoretic system (22). These findings suggested that amino groups of compounds such as EDTA salts, in combination with metal ions such as barium and lithium, might provide enhanced electrophoretic resolution of individual GAGs.

Therefore, in order to better evaluate the abnormal GAG patterns in individuals with the MPS I diseases, an investigation was undertaken to evaluate the ability of various EDTA salts and different metal ions, both singly and in combination, to separate individual GAGS in a cellulose acetate electrophoretic system. It was reasoned that the development of this new analytical tool would facilitate the comprehensive characterization of the stored GAGs in the human and feline MPS I disorders and, futhermore, help understand the substrate specificities of both normal and mutant α-L-iduronidase.

C. Studies of Lysosomal Enzyme Processing and Transport:

During the past decade, α-L-iduronidase has served as a prototypic model for studies of lysosomal enzyme processing and transport. Early studies by several laboratories provided evidence for a receptor mediated, active transport process which was necessary for the internalization of acid hydrolases by cultured fibroblasts (23,24). Intriguingly, only certain fractions of these acid hydrolases, termed "high uptake" forms, were taken up at rates exceeding that expected from nonspecific endocytosis (25). Studies by Kaplan et al. (26) with human platelet β-glucuronidase provided the first evidence that high uptake acid hydrolases were phosphoproteins. Alkaline phosphatase treatment of high uptake β-glucuronidase destroyed its uptake activity and converted the enzyme to less acidic, but catalytically active forms. Similar findings with α-L-iduronidase from human urine (27) and β-galactosidase and β-hexosaminidase from human platelets (28,29) indicated that this type of phosphohexosyl recognition system was a generalized mechanism for the receptor-mediated endocytosis of acid hydrolases by cultured skin fibroblasts. Soon after, in 1979, von Figura and Klein (30) demonstrated a release of alkaline phosphatase sensitive oligosaccharides following endoglycosidase (Endo) H treatment of high uptake α-N-acetylglucosaminidase. Other direct evidence for the involvement of mannose 6-phosphate residues in this receptor-mediated process included work by Natowicz et al. (31), who showed that acid hydrolysis of high uptake human spleen β-glucuronidase released mannose 6-phosphate and that the mannose 6-phosphate content of this enzyme varied directly with its ability to be pinocytosed by fibroblasts. Furthermore, studies by Kaplan et al. (32) demonstrated competitive inhibition of acid hydrolase

pinocytosis by certain phosphomannans from Saccharomyces cerevisiae.

Further insight into the mechanism of acid hydrolase pinocytosis has come from work with lysosomotropic amines (34). Several laboratories have found that chloroquine inhibited pinocytosis of exogenous enzymes and, furthermore, caused normal fibroblasts to secrete large amounts of acid hydrolases (35,36). Although amine treatment of normal cells mimicked the phenotype observed in I-cell disease, an autosomal recessively inherited deficiency of UDP-N-acetylglucosamine:glycoprotein N-acetylglucosamine transferase activity (37), the enzymes secreted by these cells were not recognition defective; in fact, they were greatly enriched for the high uptake enzyme forms (38). These observations suggested that amines block the normal segregation of newly synthesized lysosomal enzymes and disrupt their intracellular traffic pathway. Gonzalez-Noriega et al. (39) have suggested that the delivery system for lysosomal enzymes may rely on the pH dependent release of enzyme from receptors in lysosomes to permit free receptors to be reutilized. An alternative possibility for the observed action of these amines was suggested by Helenius et al. (40), who showed that certain enveloped virus-vesicle fusion processes which normally take place in the lysosomes were pH dependent and blocked by amines. These results inferred that amines might disrupt the trafficking of lysosomal enzymes by interfering with some pH dependent vesicle-vesicle fusion process on which enzyme delivery and receptor reutilization were dependent. The intriguing finding that ~80% of phosphomannosyl enzyme receptors in fibroblasts were present on intracellular membranes (41) was consistent with the hypothesis that these receptors play a role in regulating the intracellular transport of newly synthesized acid hydrolases, segregating

these enzymes from other products of the endoplasmic reticulum and directing them to lysosomes. Although it is now well-established that mannose 6-phosphate residues present on acid hydrolases are important recognition markers for their receptor-mediated endocytosis, it is not clear what other common structural features are present on these enzymes. In other words, what physical properties classify acid hydrolases as high uptake? Early kinetic studies by Kaplan et al. (32) with β-glucuronidase and Sando and Neufeld (33) working with α-L-iduronidase provided initial indications that there were indeed important structural features recognized by the fibroblast endocytosis receptor in addition to phosphomannose residues. Recent work has shown that lysosomal enzymes are synthesized as larger precursors and are subsequently trimmed to mature forms. The enzymes now known to undergo such processing include β-galactosidase (42), cathepsin D (43), β-hexosaminidase (44), α-glucosidase (45) and α-L-iduronidase (46). The precise nature of these multiple processing events is unclear, however, it has been generally assumed that the mechanism must include a complex sequence of proteolytic and carbohydrate modification events. Erickson et al. (43) have demonstrated the existence of a lysosomal enzyme signal sequence present on cathepsin D that is indistinguishable from those of secretory proteins (47) and raised the possibility of a common lysosomal "sorting sequence" that mediates sorting of lysosomal proteins from secretory proteins in the endoplasmic reticulum by a receptor-mediated process. Myerowitz and Neufeld (46) have immunoprecipitated four species of α-L-iduronidase from cultured fibroblasts; these species were absent in the fibroblasts obtained from individuals with Hurler disease. The 66,000 molecular weight species appeared to be of the low uptake form; in con-

trast, the 76,000 secreted form was readily taken up by the receptor-mediated endocytosis pathway. Interestingly, all species of α-L-iduronidase were phosphorylated, as shown by ^{33}P incorporation studies; in addition, the phosphate label could be removed by treatment with Endo-H.

To date, the primary limitation to performing comprehensive protein and carbohydrate structural studies on the various lysosomal enzyme biosynthetic intermediates (i.e., high and low uptake fractions) has been the inability to isolate large quantities of each purified form. α-L-Iduronidase, because of its exceptionally long half-life as compared to other lysosomal enzymes [4 to 5 days (46) versus 5 to 20 h for β-hexosaminidase (44), α-glucosidase (45) and cathepsin D (43)], provides a unique opportunity to extend these stimulating findings further. A summary of the current concept of lysosomal enzyme processing and transport appears in Figure 2.

D. Studies of Human α-L-Iduronidase Purification and Characterization:

As mentioned earlier, α-L-iduronidase is one of the enzymes needed for the degradation of dermatan sulfate and heparan sulfate, the two predominant GAGs excreted in the urine of human and feline individuals with the MPS I diseases (7). Shapiro et al. (48) first described the existence of two active forms of the enzyme in human urine, termed high uptake and low uptake according to the criteria of Brot et al. (49). These two forms differed in the rate at which they were endocytosed by cultured fibroblasts. Sando and Neufeld (33) subsequently showed that endocytosis of the high uptake form of the enzyme was competitively inhibited by mannose 6-phosphate, providing preliminary evidence for the role of phosphorylated carbohydrate residues in the receptor-mediated

Figure 2: Current Concept of Lysosomal Enzyme Processing and Transport.

Schematic summary of our current concept of lysosomal enzyme processing and transport adapted with permission from the thesis of Dr. Alessandra d'Azzo, University of Rotterdam.

FIGURE 2

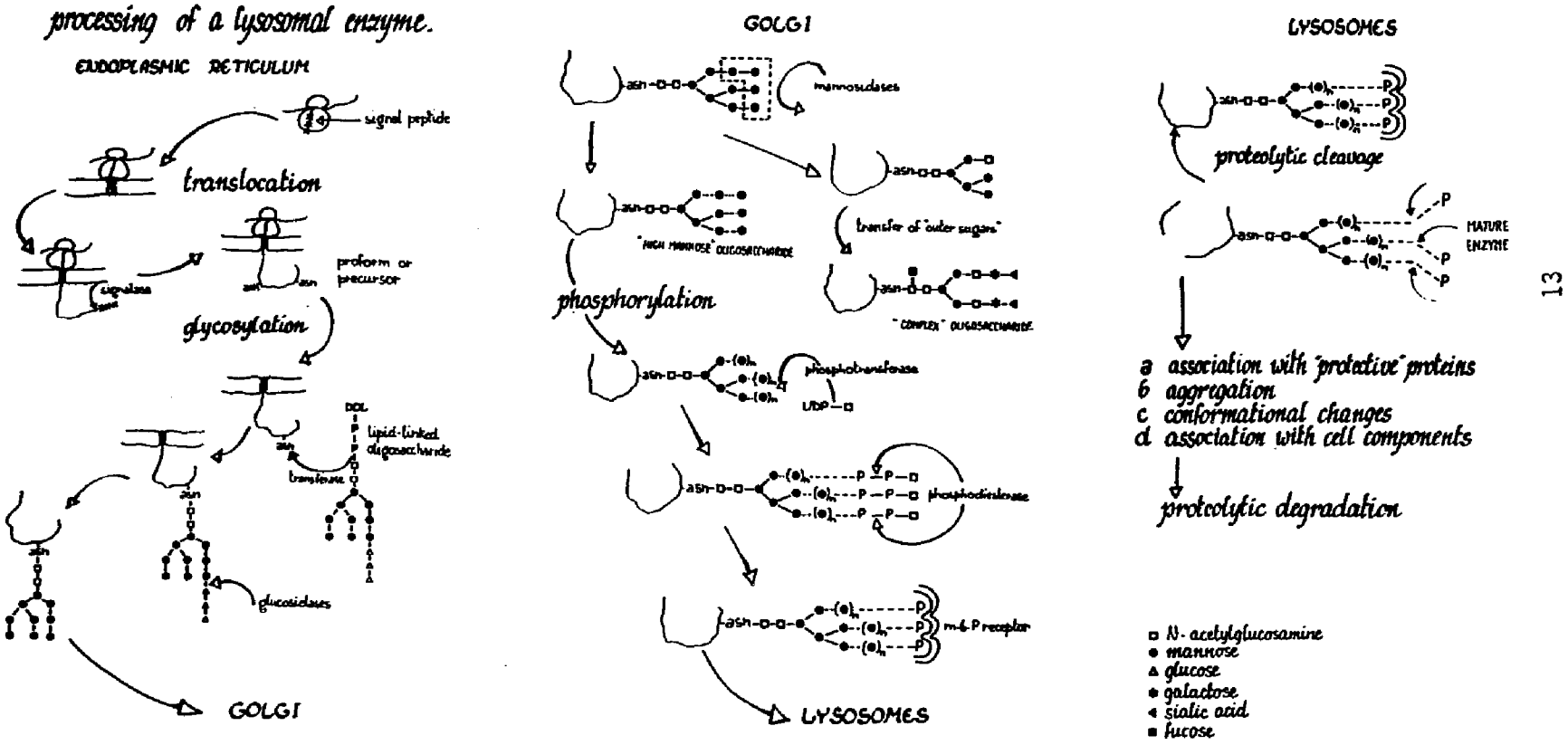
processing of a lysosomal enzyme.
ENDOPLASMIC RETICULUM
signal peptide
translocation
signalase
proform or precursor
glycosylation
DOL
lipid-linked oligosaccharide
transferase
glucosidases
GOLGI
GOLGI
mannosidases
"HIGH MANNOSE" OLIGOSACCHARIDE
transfer of "outer sugars"
"COMPLEX" OLIGOSACCHARIDE
phosphorylation
phosphotransferase
UDP
phosphodiesterase
m-6-P receptor
LYSOSOMES
LYSOSOMES
proteolytic cleavage
MATURE ENZYME
a association with "protective" proteins
b aggregation
c conformational changes
d association with cell components
proteolytic degradation
N-acetylglucosamine
mannose
glucose
galactose
sialic acid
fucose

endocytosis of lysosomal enzymes; this observation has been strongly supported by current work establishing the role of carbohydrate moieties in both intra- and intercellular lysosomal enzyme trafficking (50). As mentioned in the previous section, Myerowitz and Neufeld have recently immunoprecipitated and functionally characterized two distinct catalytically active α-L-iduronidase polypeptides (76,000 and 66,000 daltons) from human fibroblasts which corresponded to the high and low uptake forms of the enzyme, respectively (46). This hydrolase continues to serve as a prototype for studies of lysosomal enzyme processing and transport.

Chemical synthesis of artificial (51) and natural (52) substrates specific for α-L-iduronidase has helped stimulate structural investigations of the partially purified normal human enzyme from urine (53) and kidney (54); however, low starting activities, poor recoveries and insufficient purity have prohibited complete biochemical characterization. Rome et al. purified α-L-iduronidase from human kidney to a specific activity of 250 U/mg protein (1 unit is defined as the amount of enzyme which catalyzes the hydrolysis of 1 μmole of phenyl α-Id/h at 37°C) (54). This preparation was estimated to be 50-70% pure on the basis of SDS polyacrylamide gel electrophoresis. The native molecular weight of the enzyme was 65,000 ± 7,000 and it consisted of two subunits with molecular weights of 31,500 ± 4,500. Recently, the same group has reported that human fibroblast α-L-iduronidase was a monomer (46). This unusual observation, that the same enzyme from two different human sources had such different structural features, raises questions as to the correct subunit structure of this enzyme.

Rome et al. found that the enzyme was unstable at neutral or alkaline pH and at low ionic strength (54). It also became extremely sensitive to freeze-thawing and, therefore, was stored at 4°C. In spite of these precautions, the partially purified enzyme was not stable and large losses occurred in the final purification steps. In addition, 50% of the initial enzyme activity in the kidney crude homogenate was not recovered from the membranes; the final purified enzyme was shown to be of only one type, the low uptake form. One of the possible reasons for this initial poor recovery was the lack of detergents in the homogenization buffer.

Biochemical analysis of the Hurler and Scheie mutant enzymes has been limited to studies in crude leukocytes or cultured fibroblasts obtained from patients with these diseases; variable accounts of the residual activities are available. Estimates range from 0-12% for Hurler (55), Scheie (55) and Hurler/Scheie patients (57). Most of these studies have been conducted using different preparations of a colorimetric phenyl α-Id substrate; recently, a much more sensitive fluorometric substrate, 4MU α-Id, has been synthesized (51). However, it is not commercially available. Hopwood et al. have proposed that the Hurler defect was a K_m mutation based on kinetic data they obtained in cultured fibroblasts using a fluorescent substrate which was synthesized in their laboratory (58); no other studies of the Hurler or Scheie mutations have been reported. Unfortunately, the inconsistencies of substrate and assay procedures, as well as the lack of adequate biochemical characterization information on the normal human enzyme, makes comparative evaluation of different groups' data virtually impossible.

E. Comparative Gene Mapping and Studies of Lysosomal Enzyme Gene Regulation:

Since the work of Thomas Hunt Morgan and his students near the turn of the century it has been known that genes are arranged linearly along chromosomes (59); the experimental proof of residence of genes on chromosomes was provided independently by Bridges, using Drosophila melanogaster (60) and by Creighton and McClintock studying maize (61). In the last 10 years, remarkable advances in chromosomal staining methods have revealed distinct landmarks permitting the unique identification of each chromosome and, furthermore, making the assignment of specific genes to unique chromosomes a feasible task (62). More recently, somatic cell hybridization techniques have provided a highly productive approach to chromosome mapping (62). The first step in this method is fusion of human somatic cells with those from another species, a process facilitated by either inactivated viruses such as Sendai (63) or by certain chemical agents (i.e., ethylene glycol) (64). The nuclei of hybrid cells contain chromosomes of both parent cells. In subsequent cell divisions there is a progressive and preferential loss of human chromosomes from these inter-species hybrids. In the synteny test, the localization of gene loci on the same chromosome in man is demonstrated by the consistent concordant presence or absence of human phenotypes with specific chromosomes in a clone panel derived from inter-species hybridization. Alternatively, in the assignment test, the location of a specific gene locus to a chromosome is demonstrated by concordance between the presence and absence of the chromosome with the specific phenotype in the hybrid clones. To date, more than 250 human genes have been assigned to specific chromosomes and/or chromosomal regions by these methods (65).

The lysosomal gene family (i.e., structural and regulatory genes necessary for the proper expression of the lysosomal enzyme proteins) provides a unique opportunity to study the genomic distribution of a complex family of biochemically related proteins. Our current understanding of the genetic regulation of lysosomal enzymes comes primarily from studies conducted in the mouse, Mus muscalis, by Paigen's group currently at Berkley (66). A genetically determined developmental program exists for each enzyme, specifying the changes in enzyme concentration that accompany differentiation in each tissue (67). As first demonstrated for β-glucuronidase (68), genetic controls of developmental programming are seen for lysosomal enzymes. Several different types of classical genetic breeding approaches have characterized mutants of a single locus, Gus-t, which is closely linked to the enzyme structural gene and controls the postnatal expression of this enzyme. Genetic differences in developmental programming have been found for other lysosomal enzymes, including α-galactosidase (69), β-galactosidase (70), and arylsulfatase (71,72). Work with β-glucuronidase suggests that correct developmental expression of this enzyme relied on an interaction between "temporal genes" adjacent to each structural gene, such as the Gus-t locus, and one or more distant genes that code for specific developmental signals (73). Furthermore, a number of these distant regulatory genes may control the expression of different unlinked lysosomal structural genes (67). The nature of these mutations is unclear. It is possible that the regulatory mutants proximal to the structural genes represent alterations in the adjacent promotor sequences necessary for faithful transcription of eukaryotic genes. The existence of distal, trans-active regulatory sequences which may act on a number of different

unlinked structural genes implies that the products of these loci recognize common entities, either at the DNA, RNA or protein level among the lysosomal family. Structural similarities among lysosomal enzymes (i.e., glycosylation, signal peptides) have been extensively characterized (74,75), however, no data is currently available on the individual gene structure or genomic organization of this intriguing enzyme family; undoubtedly, further studies must await the employment of recently developed recombinant DNA technologies.

To date, fourteen structural genes encoding human lysosomal enzymes have been localized to specific chromosomes and/or chromosomal regions (Table 2); they are dispersed among eight different autosomes and the X chromosome. No obvious clustering of these loci may be observed, however, it is interesting to note that three have been mapped to chromosome 22, the smallest human autosome.

Because of the unique structural similarities of the lysosomal enzyme proteins, it is intriguing to speculate on the evolutionary relationship of their respective genes. Did these loci all arise from a common progenitor sequence? Do the genes contain common DNA sequences which encode common functional domains? Do they undergo fluidity throughout the mammalian genome? One approach to answering these speculative questions is via comparative gene mapping. The growth of linkage maps in many prokaryotic and eukaryotic species over the past fifty years has provided insight into comparative gene mapping (76). During the evolutionary divergence of the mammalian order considerable numbers and types of chromosome duplications, translocations, inversions and other rearrangements have become fixed in the genomes of different species (77,78). The occurrence of homologous gene-enzyme systems in

TABLE 2

CHROMOSOME ASSIGNMENTS OF THE STRUCTURAL GENES
FOR HUMAN LYSOSOMAL ENZYMES

Enzyme	Regional Assignment	Chromosome
β-Glucosidase	1p11-1qter	1
α-L-Fucosidase	1p32-1p34	1
β-Galactosidase	3q21-3qter	3
β-Hexosaminidase, β-subunit	5cen-5q13	5
Arylsulfatase B	5q15-5qter	5
β-Glucuronidase	7pter-7q22	7
Acid Phosphatase-2	11p12-11cen	11
β-Hexosaminidase, α-subunit	15q12-15qter	15
α-D-Mannosidase	19pter-19q13	19
β-Galactosidase	22q13-22qter	22
Arylsulfatase A	22q12	22
α-N-Acetyl-Galactosaminidase	-	22
α-Galactosidase A	Xq22-Xq24	X
Sulfo-Iduronidase Sulfatase	-	X

mammals and similar chromosome banding patterns in primates has permitted the study of both conserved and non-conserved linkage groups between man and other primates, man and mouse and, to a limited extent, between other mammalian species (79). The domestic cat, Felis catus, has served as an important animal model in studies of physiology, oncology, neurochemistry, and genetics (80,81), and, as detailed in the next section, a feline model of the human mucopolysaccharidosis I-H disorder has been recently described (82). O'Brien and coworkers (76) have derived a genetic map of 17 feline linkage groups which include 33 independent loci; thirty-one of these loci are homologous to genes previously mapped in man, primates and the mouse. Intriguingly, there is extensive conservation of human and feline linkage associations (76), in contrast to those of human vs. rodent (78,79) and feline vs. mouse (76) comparative linkage maps. Currently, the only human autosomes for which no comparative feline mapping data is available are chromosomes 5 and 22. Comparative analyses of the chromosome banding homologies and gene assignments have already, and will continue, to provide insight into the distant relationships of mammalian chromosomes and further the understanding of their continuing evolution.

F. Animal Models of Human Lysosomal Storage Diseases:

To date, over 30 human inborn errors of the lysosomal apparatus have been identified (83). Each is inherited as an autosomal or X-linked recessive trait and has been shown to result from the deficient activity of a specific enzyme. At the metabolic level, the enzymatic deficiency causes a block resulting in either the accumulation of the substrate(s) [and precursor(s)] and/or the absence of a critical meta-

bolic product. The metabolic abnormalities lead to the physiologic and phenotypic manifestations characteristic of the specific enzymatic defect.

Table 3 lists the animal models of human lysosomal storage diseases; the disorders are classified as glycogenoses, glycoproteinoses, glycosphingolipidoses or mucopolysaccharidoses on the basis of the primary accumulated substrate. Although other models of human lysosomal storage diseases have been described (84,85), the criteria for inclusion in Table 3 was the actual demonstration of the same enzyme deficiency as in the analogous human disorder. Each of these models is inherited as an autosomal recessive trait.

Recognition of the affected proband and/or identification of the proband's parents or heterozygous relatives has permitted the establishment of active breeding colonies for cows with Pompe disease (86) and α-mannosidosis (87); goats with β-mannosidosis (88); cats with G_{M1}-gangliosidosis type 2 (89) G_{M2}-gangliosidosis type 2 (90,91), mucopolysaccharidosis Type I-H (82) and mucopolysaccharidosis Type VI (92, 93); dogs with Niemann-Pick disease (94); as well as dogs (95) and mice (96) with Krabbe disease. These models are the best characterized with respect to the clinical manifestations, natural history of the disease, morphologic pathology, and the nature of the metabolic defect [i.e., accumulated substrate(s) and deficient enzyme].

Two new glycoprotein/oligosaccharide storage diseases have been described in animals. Nubian goats with a severe neurovisceral oligosaccharide storage disease have been recently shown to have deficient β-mannosidase activity (88) and the subsequent lysosomal accumulation of a β-mannosyl-containing trisaccharide (97). This animal model is of

TABLE 3

ANIMAL MODELS OF HUMAN LYSOSOMAL STORAGE DISEASES[a]

Disease	Enzymatic Defect	Species
Glycogenosis:		
Glycogenosis Type II (Pompe)	Acid α-Glucosidase	Shorthorn Cow
Glycoproteinoses:		
α-Mannosidosis	Acid α-Mannosidase	Angus Cow Domestic Cat
β-Mannosidosis	Acid β-Mannosidase	Nubian Goat
Glycosphingolipidoses:		
G_{M1}-Gangliosidosis Type 2	Acid β-Galactosidase	Siamese Cat Friesian Calf Mixed Breed Dog
G_{M2}-Gangliosidosis Type 2	β-Hexosaminidase A & B	Domestic Cat
Type 3	β-Hexosaminidase A, Partial Activity	Yorkshire Swine
Gaucher Type 2	Acid β-Glucosidase	Silky Hair Terrier Dog
Krabbe	Galactosyl ceramide: β-Galactosidase	West Highland/ Cairn Terriers Twitcher Mouse
Niemann-Pick Type A	Sphingomyelinase	Poodles Siamese Cat
Mucopolysaccharidoses:		
MPS I-H (Hurler)	α-L-Iduronidase	Domestic Cat
MPS VI (Maroteaux-Lamy)	Arylsulfatase B	Siamese Cat

[a] Includes only enzymatically confirmed models.

particular interest since the analogous human disorder has not been identified to date. In addition to the well characterized bovine model of α-mannosidosis (87,98), a second model has been identified in a domestic kitten which presented with neurologic manifestations, dysmorphic features and growth retardation (99). Characterization of the residual acid α-mannosidase activity and urinary mannose-rich oligosaccharides suggested that the feline disease was similar to the severe form of human mannosidosis (100), whereas the bovine model was more analogous to the milder human variant (101). Hopefully, a breeding colony for the feline disease can be established since this model would be more convenient for therapeutic and other studies than the bovine analogue.

Three new models of human glycosphingolipidoses have been identified. Canine Gaucher type 2 disease has been described in several affected dogs in Australia. The deficiency of acid β-glucosidase and the accumulation of glucosyl ceramide and glucosyl psychosine have been demonstrated (102,103). A second model of human Krabbe disease (galactosyl ceramide: β-galactosidase deficiency) has been identified in mice with the "twitcher" mutation (96). The availability of this model should permit intensive study of the globoid cell reaction which is the characteristic neuropathologic finding in the human disease. Analogues of the human neurodegenerative disorder, Niemann-Pick Type A disease, have been reported in Siamese cats (104) and poodles (94). These animals should provide insight into the interrelationships among the sphingomyelinase isozymes.

Finally, as mentioned earlier, a feline model of human mucopolysaccharidosis I-H (Hurler disease) due to deficient α-L-iduronidase activ-

ity has been identified and a breeding colony has been established (82). This is the second recognized analogue of a human mucopolysaccharidoses, the other being Type VI (Maroteaux-Lamy disease). The availability of these two models, one characterized by neurologic involvement (MPS I-H) and the other only by visceral manifestations (MPS VI), should permit assessment of mucopolysaccharide metabolism in visceral and neural tissues as well as provide systems for the evaluation of various therapeutic endeavors.

Requisite to the use of animal models for the study of human disease is the necessity to establish the degree of homology between the human and animal counterparts. Obviously, an animal disease which has an identical molecular etiology to that of the corresponding human disorder will provide the ideal model for investigation of disease pathogenesis and treatment. For inborn errors of metabolism, an animal homologue would be one with the identical molecular defect at the genic level (i.e., the same or equivalent base substitution in the mutant gene). However, it is unlikely that any given animal model will share the precise gene mutation which occurs in the human disease. In fact, it is known that multiple mutations in the structural gene for any given protein can cause defective catalysis or function, as has been so well-demonstrated for the over 140 and 250 different mutations in the human molecules, glucose 6-phosphate dehydrogenase (105-107) and hemoglobin (108), respectively.

Finally, it must be emphasized that prior to characterizing the molecular pathology of a specific human disease or its respective animal model, such as the human and feline MPS I diseases, a firm understanding of the basic biochemistry of the normal condition(s) must be available.

It is the purpose of the experiments outlined in this thesis to facilitate future investigations into the biochemical abnormalities which result in both the human and feline MPS I diseases.

OBJECTIVES

Biochemical and somatic cell genetic studies have been undertaken to 1) quantitatively analyze the tissue distribution of the stored glycosaminoglycans in individuals with the autosomal recessively inherited human and feline mucopolysaccharidosis I diseases (α-L-iduronidase deficiency diseases), 2) purify milligram quantities of homogeneous normal human α-L-iduronidase in order to characterize the physicochemical properties and complex processing pathways of this prototypic lysosomal enzyme, and 3) localize the structural genes for human and feline α-L-iduronidase and study their regulated expression in mammalian-rodent somatic cell hybrids. The specific objectives of this research were:

a. To develop new analytical tools for the identification and quantitation of glycosaminoglycans.

b. To use these new analytical tools for the identification and quantitation of glycosaminoglycans in tissues of individuals with human and feline mucopolysaccharidoses I.

c. To develop novel purification methods for the rapid, high-yield isolation of homogeneous low and high uptake forms of α-L-iduronidase from human sources.

d. To characterize the physicochemical and immunologic properties of the homogeneous human enzyme forms.

e. To regionally localize the human α-iduronidase structural gene to a narrow chromosomal region using human-rodent somatic cell hybrids, immunologic and electrophoretic methods.

f. To comparatively map the feline α-L-iduronidase structural gene using feline-rodent somatic cell hybrids and electrophoretic methods.

MATERIALS

A. Glycosaminoglycan Analyses:

Keratan sulfate (KS), dermatan sulfate (DS), heparan sulfate (HS), heparin (HP), chondroitin 4-sulfate (C4S), chondroitin 6-sulfate (C6S) and hyaluronic acid (HA) were supplied by Drs. M.B. Mathews and J.A. Cifonelli who prepared these standards under a contract (#NO1-AM-5-2205) from the National Institutes of Health. In addition, purified dermatan sulfate was generously provided by Dr. R. Matalon. For comparison, chondroitin sulfate and heparin were purchased from Sigma Chemical Company, St. Louis, MO. Lithium chloride was obtained from Mallinckrodt Inc., Paris, KT. Alcian Blue 8GN was purchased from MCB Manufacturing Chemists Inc., Cinncinatti, OH. Pronase (from Streptomyces griseus) was supplied by Boehringer Mannheim, Indianapolis, IN. Cetylpyridinium chloride was purchased from Aldrich Chemical Company Inc., Milwaukee, WI. All other reagents and solvents were the highest grade available from the Fisher Scientific Company, Fairlawn, NJ. The microzone electrophoretic cell (Model R-101) and Duostat power supply were obtained from Beckman Instruments Inc., Anaheim, CA. Cellulose acetate electrophoretic strips (14.5 x 5.5 cm and 17 x 17 cm, 250 μm thickness) and a Chemitron electrophoresis tank (model 3000) were purchased from Kalex Inc., Manhasset, NY.

B. Purification and Characterization of Low and High Uptake Forms of Human α-L-Iduronidase:

Con A-Sepharose and SDS molecular weight standards were obtained from Pharmacia Fine Chemicals, Piscataway, NJ. DEAE-cellulose was pur-

chased from Whatman Laboratory Products, Clifton, NJ. Hydroxyapatite was from the Sigma Chemical Co., St. Louis, MO. Biogel P-100 was from Bio-Rad Laboratories, Richmond, CA. 4MU α-Id was kindly supplied by Dr. Bernard Weissman, University of Illinois, Chicago, Illinois. Anhydro [^{3}H]mannitol-iduronide was a gift from Dr. Irwin Leder, National Institutes of Health, Bethesda, MD. Phenyl α-Id was purchased from Calbiochem-Behring Co., San Diego, CA. Ampholytes and the multiphor isoelectric focusing apparatus (Model 2117) were from LKB Products, Stockholm, Sweden. Bovine serum albumin was obtained from Schwartz-Mann Research Laboratories, Orangeburg, NY. High purity acetonitrile was purchased from Burdick and Jackson Laboratories, Muskegon, MI. Fluorescamine was obtained from Pierce Chemical Co., Rockford, IL. Amicon ultrafilters and concentration chambers were purchased from Amicon Corp., Lexington, MA. High performace liquid chromatography (HPLC) unit and protein columns were purchased from Waters Associates, Milford, MA.

C. Comparative Gene Mapping of Human and Feline α-L-Iduronidase:

Human and mouse parental lines were routinely maintained using RPMI 1640 medium containing 10% fetal calf serum. Three human fibroblast lines (fetal lung, fetal liver, and fetal kidney) were obtained from different individuals and subsequently hybridized to the HPRT$^-$ mouse RAG cell line. Feline parental cells, as well as feline-hamster somatic cell hybrids, were obtained from Dr. Stephen O'Brien of the National Cancer Institute, Rockville, MD. Three feline parental lines were used: FGF, a feline lymphoblastoid cell line infected with feline leukemia virus; FL-74, obtained from the Crandel feline kidney cell and CRFK, a feline lymphoblastoid line also isolated from the kidney. Chinese

hamster parental cell line E36, used for the preparation of the feline-hamster somatic cell hybrids, was isolated from early embryo fibroblasts. Hamster cell line YH21, used for the preparation of the human-hamster somatic cell hybrids, was kindly supplied by Dr. Marcello Siniscalco of the Memorial Sloan Kettering Cancer Institute, New York, NY.

METHODS

A. Glycosaminoglycan Analyses:

1. Glycosaminoglycan Electrophoresis:

a. Gel Preparation and Sample Application. Cellulose acetate microzone electrophoretic strips were stored at 4°C in a 30% methanol solution. For the standard procedure strips were removed, thoroughly blotted on Whatman #1 filter paper and immersed in 10 mM EDTA (tetrasodium salt)/50 mM LiCl, pH 8.4, up to 6.0 cm from the top of the gel for 10-15 min. Strips were rapidly blotted again and mounted on the Beckman microzone apparatus. Samples (1 µl containing about 1-5 µg GAG) were applied in a 0.75 cm band at 3.0 cm from the cathodal portion of the gel which was not previously equilibrated in the electrophoresis solution. For the 17 cm x 17 cm cellulose acetate sheets, the Chemitron electrophoretic tank was used. The gel preparation was performed essentially as described above, but the larger sheets were submerged to 4.0 cm from the cathodal end and the samples applied as 1.25 cm bands.

b. Electrophoresis and Staining. Electrophoresis was carried out for 45 min at 4°C with a constant current (2.5 mA/cm gel width; 15 volts/cm gel length) unless otherwise noted. Samples were applied for migration from cathode to anode. After electrophoresis, the gels were stained for 1.0 min in 0.1% Alcian Blue 8GN at 25°C. Gels were destained by two serial submersions in 100 ml of 2% glacial acetic acid for five min each.

c. Quantitation. Individual GAGs were quantitated by a modification of the procedure described by Kimura et al. (109). After electrophoresis, each band was cut out and immersed in 2.0 ml of chloro-

form/methanol 9:1(v/v) which dissolved the cellulose acetate. The absorbance of the dissolved stain was spectrophotometrically determined at 625 nm. For blanks, gel slices of exactly the same size were dissolved and their absorbance determined. Blanks consistently had less than 0.5% of the values obtained for the corresponding GAG sample. Standard curves for each GAG were prepared with Alcian Blue and found linear over the amounts employed (1.0-5.0 μg).

d. Recovery of GAGs. For recovery determinations, electrophoresis was performed with and without ethanol precipitation (19). In the former experiments, samples (5 μg) were electrophoresed for 15 min (2.5 mA/cm gel width), removed and then immersed for 2 min in the standard solution (10 mM EDTA tetrasodium salt/50 mM LiCL, pH 8.4) containing 15% ethanol. These same cellulose acetate sheets were then subjected to electrophoresis for an additional 15 min (2.5 mA/cm gel width) and again immersed for 2 min in the standard solution, this time containing 50% ethanol. After a final 15 min of electrophoresis (2.5 mA/cm gel width) samples were stained and quantitated as described above.

2. Evaluation of Optimal Glycosaminoglycan Separation:

Optimal separation of GAGs was determined in two sets of experiments. First, the effects of varying the 1) EDTA salt (disodium, trisodium, tetrasodium, tetrasodium dihydrate and ferric-sodium), 2) EDTA salt concentration (25 mM-1.0 M), 3) pH (3.5-11.5) and 4) current (0.5-5.0 mA/cm gel width) on the electrophoretic migration of the individual GAGs were determined. Each condition was systematically varied while the others were maintained constant. In the second set of

experiments, the electrophoretic migration of each GAG was determined in solvent systems containing different cations (LiCl, $Ba(Ac)_2$, $Cd(Ac)_2$, $ZnSO_4$ and $ZnCl_2$) in combination with the EDTA tetrasodium salt. The concentration of the cation (10-50 mM), EDTA tetrasodium salt concentration (10-50 mM) and pH (3.5-11.5) were varied systematically. For both sets of experiments the mean R_f (mid-band distance from point of application/total gel length) of each GAG was determined after three independent runs. Migration distance was measured within ± 1.0 mm; therefore, the error in each R_f value was less than 0.002 units.

3. Tissue Isolation of Glycosaminoglycans:

Tissues from human and feline individuals with mucopolysaccharidoses I and age-matched normal controls were obtained at autopsy within 2 h of death and immediately frozen at -70°C. The frozen tissue samples (1.0-5.0 g) were thawed, thoroughly minced and extracted three times in 50 ml of chloroform/methanol 2:1 (v/v). This defatted material was then lyophilized and dissolved in 5 volumes of 0.5 M acetate buffer, pH 7.5, and pronase treated (final concentration, 50 mM) for 24 h at 60°C. The proteolytic digests were centrifuged (12,000 x g; 20 min) and the GAGs isolated from the supernatant by addition of cetylpyridinium chloride to a final concentration of 10%. Salt complexes were subsequently collected by centrifugation (25,000 x g; 30 min), redissolved in 5 volumes of 98% ethanol and stirred overnight at 4°C. Precipitates were collected by filtration and resuspended in 200 µl of distilled water; 2.0 µl aliquots were applied for the electrophoretic analyses.

B. Purification and Characterization of Low and High Uptake Forms of Human α-L-Iduronidase:

1. Standard Enzyme and Protein Assays:

While monitoring the purification, enzyme activity was routinely measured using 4MU α-Id (110). For the standard assay procedure, a stock solution of 25 μM 4MU α-Id in 0.4 M sodium formate buffer containing 0.2% Triton X-100, pH 3.5, was prepared. The assay mixture, containing 25 μl each of substrate solution and enzyme source, was incubated for 1 h at 37°C; the reaction was terminated with 2.3 ml of 0.1 M ethylenediamine and fluorescence was read on a Turner Model 111 fluorometer. One unit of activity represents the amount of enzyme which hydrolyzes 1 nanomole of substrate/h unless otherwise noted.

Colorimetric assays using phenyl α-Id were performed according to the procedure of Hall et al. (111). For these assays, a unit of catalytic activity is defined as the amount of enzyme catalyzing the hydrolysis of 1 micromole of substrate/h.

Protein was routinely measured by a modified fluorescamine assay (112). Lowry protein determinations were performed as previously described (113) wherever noted.

2. Apparent Molecular Weight Determinations:

The apparent molecular weight of native α-L-iduronidase was determined by gel filtration on Sephadex G-200. The resin was swollen in 10 mM citrate phosphate buffer, pH 4.0, containing 0.5 M NaCl and 0.02% sodium azide and packed in a 5.0 X 100 cm Pharmacia column. The flow rate was 5 ml/h. The column was calibrated using 250 μg of bovine serum albumin (M_r 64,000), chick ovalbumin (M_r 44,000), chymotrypsin

(M_r 25,700) and ribonuclease (M_r 13,700) as molecular weight standards. Enzyme samples contained 5,000 units of post-Biogel P-100 purified α-L-iduronidase (SA ∿ 105,000 U/mg Lowry). Fractions of 3 ml were collected and assayed for α-L-iduronidase activity (4MU) and protein (fluorescamine) content. Molecular weights were estimated from the elution volume.

3. Flat-Bed Isoelectric Focusing:

Flat-bed isoelectric focusing was performed on an LKB multiphor apparatus using a pH 3.5-9.5 gradient which was established in polyacrylamide gels according to the manufacturer's instructions. The gels were prefocused for 1 h until a final voltage of 800 V was obtained. Samples (100 µl containing 1,000 4MU units) were applied using 0.7 x 1.5 cm Whatman No. 17 filter paper strips. Focusing was carried out for 3 h at 800 V (constant voltage) at 4°C; after 2 h the application strips were removed. Following electrophoresis, 1 cm pieces were removed from the gel and soaked at 4°C in glass distilled H_2O overnight and the pH of the leached ampholines was determined.

For activity staining, the lanes containing enzyme sample were overlaid with Whatman No. 3 filter paper saturated with 0.2 ml of 50 µM 4MU α-Id in 0.4 M sodium formate buffer, pH 3.5, placed in a covered moist chamber and incubated at 37°C for 2 h. The overlay was then removed, the gel placed in a saturated ammonia tank for 60 sec and subsequently visualized under a UV light.

4. Native Polyacrylamide Gel Electrophoresis:

Disc gel electrophoresis was used to routinely monitor the

progress of the enzyme purification. Samples containing 50 µg of protein (flourescamine) were electrophoresed at 4°C in 7% polyacrylamide gels using a constant current of 4 mA/gel in a pH 4.3 buffer system designed for the electrophoresis of basic proteins (114). Three solutions, A) containing 48 ml of 1 N KOH, 17.2 ml of glacial acetic acid and 40 ml of TEMED made up to 100 ml with glass distilled H_2O, B) containing 48 ml of 1 N KOH, 2.87 ml of glacial acetic acid and 0.46 ml TEMED made up to 100 ml, and C) containing 28 g of acrylamide and 0.735 g of BIS made up to 100 ml were mixed in a ratio of 1 part A:2 parts C:1 part H_2O and combined 1:1 with 0.15% ammonium persulfate catalyst to form the separating gel; solution B was subsequently mixed with acrylamide, riboflavin and H_2O (1:1:1:5) to form the stacking gel. The final gel size was 6 mm X 6 cm. Protein was stained in a solution containing 0.25% Coomassie Brilliant Blue R in 20% trichloroacetic acid and the gels were destained overnight in a solution containing 7.5% acetic acid and 15% methanol. Alternatively, protein was stained with Coomassie Brilliant Blue G-250 in 10% methanol using the method of Blakesley and Boezi (115) which did not require destaining.

5. SDS Polyacrylamide Slab Gel Electrophoresis:

Samples containing 100-150 µg of protein (fluorescamine) were lyophilyzed, taken up in sample buffer containing 0.125 M Tris/HCl, pH 6.8, 2% SDS, 10% glycerol and 0.001% bromphenol blue and boiled for 5 min. Slab gel electrophoresis was performed at 23°C according to the method of King and Laemmli (116) as modified by Guzman et al. (117). The running buffer consisted of 0.05 M Tris, 0.384 M glycine and 0.1% SDS (final pH 8.8). The slab gels (1.55 mm thick, 13 cm wide and 17 cm

long) contained 10% polyacrylamide and were run at 70 mA until the bromphenol blue dye front moved approximately 15 cm. The gels were stained with Coomassie Brilliant Blue R as described above.

6. Enzyme Uptake Studies:

Skin fibroblasts obtained from a homozygote with MPS I-H were grown to late confluency in 75 mm^2 Falcon flasks with RPMI 1640 medium containing 10% fetal calf serum; this serum-containing medium was subsequently replaced with serum-free medium 24 h before uptake experiments were performed. Samples containing post Con A-Sepharose purified enzyme were prepared in 10 mM sodium phosphate buffer, pH 6.0 containing 0.1 M NaCl and 1 mg/ml BSA. 1 ml of enzyme solution was mixed with 9 ml of serum-free media (final enzyme concentration of approximately 20 U/ml media) and added to the cultured cells. After gassing with CO_2, the cells were incubated for various times at 37°C. Cells were harvested by trypsinization; pellets and media were assayed for α-L-iduronidase activity as previously described (110).

7. Antibody Production and Characterization:

Antibody was produced against highly purified low uptake α-L-iduronidase (105,000 U/mg Lowry) in New Zealand white rabbits. Initial injections containing 150 µg protein (suspended in a 1:1 emulsion with Freunds complete adjuvant) were both intramuscularly and subcutaneously administered. After 3 weeks, the rabbits were boosted with 50-75 µg protein and bled from the ear 1 week later. Titration curves were either prepared on the sera directly or, alternatively, on IgG fractions which had been isolated by DEAE-cellulose chromatography. The immunoti-

tration mixtures contained approximately 20 U of α-L-iduronidase and 50-50,000 µg of rabbit anti-human α-L-iduronidase in 10 mM sodium phosphate buffer, pH 6.0, with 1 mg/ml of human serum albumin (HSA); the final volume was adjusted to 90 µl in 1.0 ml conical centrifuge tubes. For titration curves using DEAE-cellulose purified IgG, 160 µg whole rabbit serum was added to the incubation mixture. After 30 min at 37°C, 250 µg of goat anti-rabbit IgG (10 µl) was added, incubated for an additional 30 min at 37°C and then stored overnight at 4°C. The tubes were centrifuged for 20 min at 25,000 X g and aliquots (25 µl) of the supernatant and/or resuspended immunoprecipitates were assayed for 4MU α-Id activity as previously described (82).

8. Amino Acid Composition Analyses:

Amino acid analyses were performed on post HPLC samples of both forms of α-L-iduronidase by Dr. Al Smith (University of California, Davis, CA). Acid hydrolyses (50 µg Lowry protein/hydrolysis) were performed for 24, 48 and 72 h at 110°C in 6N HCl. Amino acid concentrations were then determined in a Durram B-500 amino acid analyzer. Tryptophan levels were determined spectroscopically by the method of Edelhoch (118).

9. Purification Procedure:

All purification steps were carried out at 4°C unless otherwise noted and all buffers used throughout the purification contained 0.02% NaN_3 and 0.01 mM PMSF. Frozen human lungs (8,000-10,000 g) which had been stored at -20°C within 4 h after death were thawed, trimmed of connective tissue and finely minced. This tissue was then transferred

in 10 mM Tris/HCl buffer, pH 7.3, containing 0.1 M NaCl (1:1.5 tissue:buffer) to a Waring blender model CB-6 and homogenized for 60 sec at low speed and then for 30 sec at high speed. This material was subsequently centrifuged at 20,000 X g for 1 h and the supernatants (crude homogenate) removed for further purification. In order to accurately compare protein and enzyme assays throughout the purification, 1 ml aliquots were removed at each step and dialyzed against 4 changes (16 L total volume) of 10 mM sodium citrate buffer, pH 4.0, containing 0.1 M D(+) mannose and 0.5 M NaCl.

a. DEAE-Cellulose Chromatography. A column (5 X 40 cm) containing DEAE-cellulose was thoroughly equilibrated with the homogenization buffer by washing with 5-10 bed volumes. The crude homogenate was pumped onto the column at a constant flow rate of 10 ml/min and washed with 5 bed volumes of the homogenization buffer. The column flow through and wash fractions were pooled and prepared for Con A-Sepharose chromatography. After washing the column extensively until the absorbance OD 280 was less than 0.100, the remaining "bound" enzyme was eluted with 10 mM Tris/HCl buffer, pH 7.3 containing 0.6 M NaCl. The peak fractions from this eluant were also pooled and prepared for Con A-Sepharose chromatography.

b. Concanavalin A-Sepharose Chromatography. Magnesium chloride (10 mM final concentration), manganese chloride (1 mM final concentration) and sodium chloride (0.5 M final concentration) were added directly to the pooled fractions obtained after DEAE-cellulose chromatography. Con A-Sepharose (a minimum of 50 ml, settled bed volume) was added to each solution and gently mixed by an overhead stirrer for 18 h at 4°C. The slurry was filtered on a 60 ml Buchner sintered glass

(coarse) funnel and washed with 8-10 bed volumes of Con A binding buffer (see above). The Con A-Sepharose was then packed in a column (3 x 20 cm) and eluted at 23°C with buffer containing 1 M α-methylmannoside at a constant flow rate of 1.0 ml/min. 5 ml fractions were collected and assayed for enzymatic activity and protein. Fractions with nearly constant specific activities were pooled, concentrated by Amicon ultrafiltration in a Model 3 stirred cell using a YM-10 membrane and dialyzed overnight (16 L total volume) against 10 mM sodium phosphate buffer, pH 6.0, containing 0.1 M NaCl.

c. Hydroxyapatite Chromatography. Hydroxyapatite chromatography was performed essentially as described by Rome et al. (54). A column (2.5 X 40 cm) was packed with hydroxyapatite and washed with 5-10 bed volumes of the above buffer. The concentrated sample was pumped onto the resin at a constant rate of 10 ml/h. After sample application, the column was washed with a minimum of 3 bed volumes of buffer and the bound protein was subsequently eluted with a 500 ml linear gradient from 10 mM sodium phosphate, pH 6.0, containing 0.1 M NaCl to 100 mM sodium phosphate, pH 6.0, containing 0.5 M NaCl. The main activity peak was pooled, concentrated to less than 50 ml by Amicon ultrafiltration using a YM-10 membrane, dialyzed extensively against 10 mM citrate phosphate buffer, pH 4.0, containing 0.5 M NaCl and 0.1 M D(+)mannose, and stored at 4°C.

d. Gel Filtration. The concentrated post-hydroxyapatite enzyme was applied to a column (2.5 X 80 cm) of Biogel P-100 which had been previously equilibrated and washed with sample buffer. The preparation was eluted at a constant flow rate of 5 ml/h. Fractions (4 ml) were collected and assayed for enzymatic activity and protein and those

containing a nearly constant specific activity were pooled and concentrated in order to maintain a protein content greater than 0.1 mg/ml (fluorescamine).

10. High Performance Liquid Chromatography:

Chromatography was performed with modular components from Waters Associates. Solvent delivery was controlled by a Model 600A pump interfaced with a Model U6K sample injector, dual I-250 protein separation columns and a Model 440 absorbance detector equipped with a 214 nm filter. Graphic display of the detector signal was achieved with an Omniscribe servo-recorder and elution times were measured with an electronic memory digital timer.

The dual I-250 protein columns (7.8 mm X 30 cm, each) were packed with 10 µm silica based media to which a hydrophobic moiety was bound. Routinely, a guard precolumn dry packed with I-250 gel permeation media (60 µm) was employed during chromatographic procedures. Aqueous phases were filtered (0.45 µm, Millipore Corp.) and degassed before use. The mobile phase used was 10 mM Tris/HCl containing 0.2 M NaCl, pH 7.3. Chromatography was normally run at a flow rate of 1.0 ml/min with a chart speed of 0.5 cm/min and absorbance measured at 214 nm.

Samples injected were usually between 50 and 150 µl for filtered enzyme preparations or purified protein standards used for molecular weight calibration of the column. Elution volumes (Ve) for the resolved peaks were calculated by multiplying peak times (min) by the flow rate (ml/min). The void volume (Vo) of the column was taken as the elution volume of thyroglobulin. The mobile phase was pumped through the columns at an operating pressure of 1,200 psi. The HPLC system had a V_0 and a total included volume of 11.4 and 28.7 ml, respectively.

C. Comparative Gene Mapping of Human and Feline α-L-Iduronidase:

1. Preparation of Somatic Cell Hybrids:

Human-hamster somatic cell hybrids were prepared and supplied by Dr. Marcello Sinescalco of the Memorial Sloan Kettering Cancer Institute and the feline-hamster cell hybrids were from Dr. Stephen O'Brien of the National Cancer Institute. Human-mouse somatic cell hybrids were prepared by Dr. Moyra Smith. Parental cells were fused by centrifugation through a 7-50% polyethylene glycol gradient (119) and heterokaryons were cultured in hypoxanthine/aminopterin/thymidine selective medium (120). Hybrid clones were then obtained by the technique of Ham and Puck (121) and, after 10-20 passages, selected primary hybrid clones were recloned, giving rise to secondary clones, and for some hybrids, tertiary clones.

2. Determination of the Human and Feline Chromosome Constitution in Somatic Cell Hybrids:

Marker enzymes for specific human chromosomes were determined by Dr. Kenneth Astrin using established electrophoretic methods (122). Metaphase spreads were prepared (123) and the chromosomes were banded to distinguish mouse from human chromosomes with the Giemsa 11 technique (124) and subsequently destained and banded with quinacrine hydrochloride fluorescence (125). The human chromosomal constitution of individual hybrid clones was based on enzyme marker data and/or cytogenetic analyses; cell lines in which at least 30% of the metaphase spreads contained a specific chromosome were considered positive for that chromosome. Enzyme marker and cytogenetic analyses of the feline-hamster somatic cell hybrids were performed in the laboratory of Dr. Stephen

O'Brien as previously described (76). Human or feline α-L-iduronidase assays, marker enzyme electrophoreses and cytogenetic analyses were performed on individual cell hybrids harvested from the same passage.

3. Immunodiscrimination of Human and Murine α-L-Iduronidase:

Cell pellets from parental or hybrid lines were prepared from confluent cell cultures grown in T-75 mm^2 flasks by harvesting the cells with a rubber policeman into their media, centrifuging at 5,000 x g for 10 min and washing twice with a total of 10 ml of PBS. Cell extracts were prepared by resuspending these pellets in 100 µl of 0.4 M sodium formate buffer, pH 3.5, containing 0.2% Triton X-100 and sonicating for a total of 90s (3 bursts; 30 s each) at 4°C. The sonicates were then centrifuged at 20,000 x g for 30 min and the supernatants removed and assayed for α-L-iduronidase activity using 4MU α-Id as previously described (110). 75 U of activity (1 U is the amount of enzyme which cleaves 1 picomole of substrate/h) is removed and incubated for 30 min at 37°C with rabbit anti-human α-L-iduronidase antibodies (10 µl) in a total volume of 70 µl (adjusted with PBS). Goat anti-rabbit immunoglobulin was then added (10 µl), incubated for an additional 30 min at 37°C and stored overnight at 4°C. Blanks containing normal rabbit antisera instead of anti-human α-L-iduronidase were also prepared. Samples were then centrifuged in 1.0 ml conical polypropylene tubes at 20,000 x g for 30 min in a Sorvall RC-2B centrifuge, the supernatants were removed and the immunoprecipitates resuspended by gentle sonication and washed twice with PBS. The supernatants and pellets were subsequently assayed for α-L-iduronidase activity using a final substrate concentration of 100 µM 4MU α-Id as described (82). The ammonium

sulfate concentrated rabbit anti-human α-L-iduronidase antibodies used for these studies were prepared as described earlier.

4. Electrophoretic Separation of α-L-Iduronidase from Different Sources:

Cell extracts were prepared from confluent cell cultures as described in the previous section; a minimum of 1000 picomoles/h/ml of α-L-iduronidase was used per cell line for each experiment. Electrophoresis was performed on 350 micron cellulose acetate strips (17 cm x 17 cm) in 10 mM Tris/HCl, pH 7.1 (250 constant V) for 2 h at 4°C. After electrophoresis, the gel was sliced into 1.8 cm strips, homogenized in 300 µl of 0.4 M sodium formate buffer, pH 3.5, containing 0.2% Triton X-100 and incubated with 100 µl of 100 µM 4MU α-Id for 18 h at 37°C. Activity was determined as described above.

5. Regional Gene Mapping of Human α-L-Iduronidase:

Human cell lines containing known structural rearrangements of portions of chromosome 22 were obtained from the Mutant Cell Repository, Camden, NJ. These partial monosomic and trisomic lines, as well as normal diploid fibroblast lines, were grown in RPMI 1640 cell media containing 10% fetal calf serum. Normal control and rearranged cell lines were harvested at similar cell densities and assayed for α-L-iduronidase activity using 4MU α-Id.

RESULTS

A. Glycosaminoglycan Analyses:

1. Development of a Novel Electrophoretic System for the Analysis of Glycosaminoglycans:

a. Resolution of GAGs in EDTA Systems. Table 4 shows the effect of varying the EDTA tetrasodium salt concentration, current and pH on the relative R_f values for the six major GAGs. As shown in Fig. 3 on the left, four distinct bands composed of KS and HA, HS, C4S and DS, and HP were observed with the optimal electrophoretic conditions (50 mM EDTA tetrasodium salt, pH 9.0, and a constant current of 2.5 mA/cm gel width). The migration of the four bands was dependent on the EDTA tetrasodium salt concentration; the most rapid migration was achieved at 25 mM whereas the GAGs remained near the origin when electrophoresed in the presence of 1.0 M salt. Varying pH from 3.5 to 11.5 had little effect on the migration of the GAGs with the exception of HA as previously reported (11). Electrophoresis at higher amperages (> 3.0 mA/cm gel width) caused diffusion of the bands, while migration was markedly decreased at lower amperages (< 0.5 mA/cm gel width).

Table 5 shows the effect of using different EDTA salts on the electrophoretic migration of the six GAGs. Compared with the GAG migration pattern observed with the tetrasodium salt under optimal conditions (Fig. 3 on the left), the other EDTA salts gave different results when the same conditions were used. The trisodium salt resolved the GAGs into four bands, but the relative migration of HS was faster while that of co-migrating DS and C4S was slower. Use of the disodium salt resulted in only three bands with KS and HA, DS and HP, and HS and C4S co-migrating.

TABLE 4

EFFECT OF EDTA TETRASODIUM SALT CONCENTRATION, CURRENT AND pH ON THE RELATIVE MIGRATION OF INDIVIDUAL GAGS[a]

GAG	Optimal Conditions[b]	EDTA Tetrasodium Salt Concentrations (M)			Current (mA/cm gel width)			pH		
		0.025	0.10	1.0	0.50	1.0	5.0	3.5	7.0	11.5
KS	0.248	0.524	0.202	0.025	0.100	0.125	0.624	0.235	0.250	0.231
DS	0.261	*[c]	0.225	0.025	0.100	0.210	*	0.261	0.250	0.243
HS	0.255	*	0.220	0.025	0.108	0.205	0.660	0.260	0.253	0.245
HP	0.266	*	0.227	0.025	0.110	0.205	*	0.262	0.260	0.274
C4S	0.260	*	0.225	0.025	0.110	0.205	*	0.260	0.255	0.246
HA	0.247	0.520	0.200	0.025	0.110	0.185	0.620	0.222	0.250	0.350

[a] As individual conditions were varied, the others were maintained at their optima; values represent the average R_f value obtained from four independent electrophoretic experiments.

[b] Optimal conditions for GAG separation were 50 mM EDTA, pH 9.0, using 2.5 mA/cm gel width.

[c] Indicates conditions where GAG migrated off the end of the gel.

Figure 3. Electrophoresis of Standard Glycosaminoglycans in EDTA Tetrasodium Salt and LiCl Systems.

Electrophoresis of standard GAGs in EDTA tetrasodium salt (left panel). (1) standard mixture; (2) HA; (3) C4S; (4) HP; (5) HS; (6) DS; (7) KS. One µl of the standard mixture (0.5 µg of each GAG/µl; lane 1) and each purified GAG (2.0 µg/µl; lanes 2-7) was applied. Electrophoresis was carried out in 50 mM EDTA tetrasodium salt, pH 9.0, for 45 min at 4°C with a constant current of 2.5 mA/cm gel width. The gel was stained with Alcian Blue as described in the Methods section.

Electrophoresis of standard GAGs in LiCl (right panel). GAG standards, concentrations and order of application are the same as above. Electrophoresis was carried out in 50 mM LiCl, pH 3.0, for 1 h at 4°C with a constant current of 2.5 mA/cm gel width.

FIGURE 3

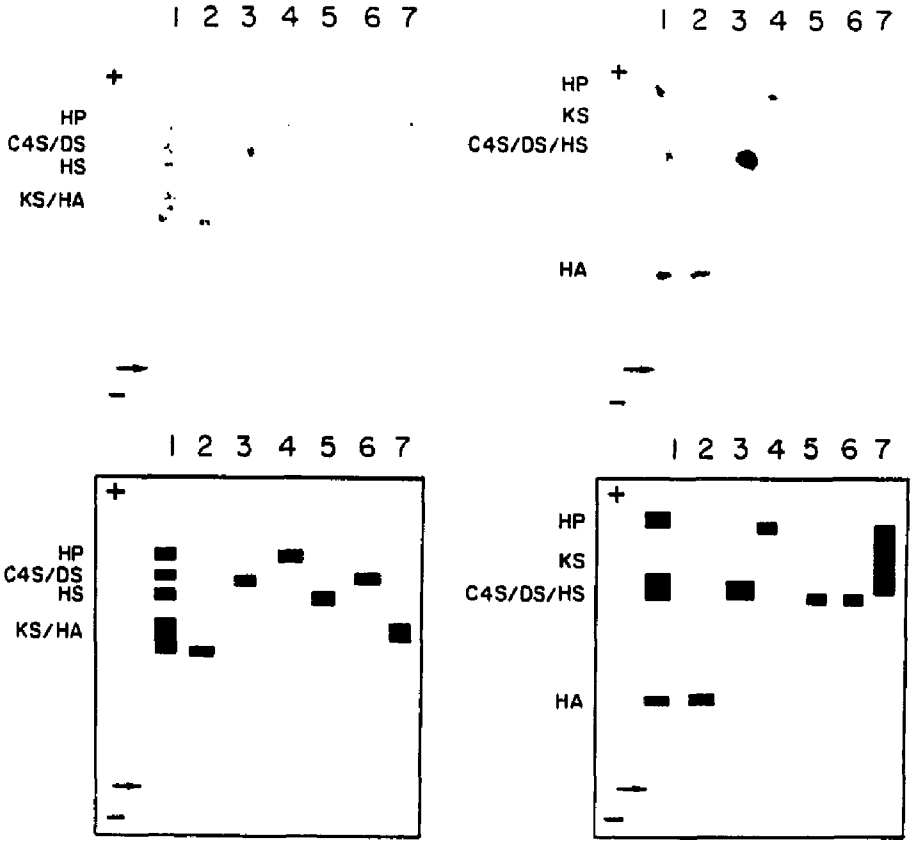
1 2 3 4 5 6 7
+
HP
C4S/DS
HS
KS/HA
1 2 3 4 5 6 7
+
HP
KS
C4S/DS/HS
HA
1 2 3 4 5 6 7
+
HP
C4S/DS
HS
KS/HA
1 2 3 4 5 6 7
+
HP
KS
C4S/DS/HS
HA

TABLE 5

EFFECT OF DIFFERENT EDTA SALTS ON THE RELATIVE MIGRATION OF INDIVIDUAL GLYCOSAMINOGLYCANS[a]

GAG	Disodium	Trisodium	Tetrasodium	Tetrasodium Dihydrate	Ferric-Sodium
KS	0.222	0.250	0.248	0.255	0.200
DS	0.245	0.255	0.261	0.260	0.213
HS	0.240	0.260	0.255	0.262	0.200
HP	0.245	0.264	0.266	0.260	0.215
C4S	0.240	0.254	0.260	0.259	0.200
HA	0.222	0.250	0.247	0.255	0.200

[a] All samples were electrophoresed in 50 mM of each EDTA salt, pH 9.0, using a constant current of 2.5 mA/cm gel width; values represent the average R_f obtained from four independent electrophoretic experiments.

With EDTA ferric-sodium salt KS, HP, C4S and HA all migrated to an R_f of 0.200 while DS and HP comigrated to a slightly more anodal position. Use of EDTA tetrasodium dihydrate was not satisfactory since there was poor resolution due to streaking.

b. Resolution of GAGs in EDTA/Cationic Systems. After electrophoresis in EDTA tetrasodium salt (50 mM, pH 9.0), the six GAGs were resolved into four comigrating bands (Fig. 3; left), whereas after electrophoresis in LiCl (50 mM, pH 3.0) three comigrating bands were observed (Fig. 3; right). Since the migration patterns of GAGs in these two systems appeared complementary, it was reasoned that EDTA/cationic mixtures might resolve all six GAGs. Therefore, the use of different EDTA/cationic combinations was investigated (Table 6). The combination of LiCl and EDTA tetrasodium salt provided the best solvent system for the separation of the six GAGs. The addition of barium acetate (10-50 mM) to this mixture did not improve the separation. Furthermore, the combination of EDTA and various concentrations (10-50 mM) of barium acetate alone gave poor GAG resolution. Table 7 shows the effect of EDTA concentration, LiCl concentration and pH on the relative migration of the individual GAGs in the combined system. Optimal resolution was achieved with 10 mM EDTA/50 mM LiCl, pH 8.4 at 2.5 mA/cm gel width (Fig. 4). As expected, pH variations had little effect in these systems.

c. Quantitation of Individual GAGs. When purified individual GAGs were electrophoresed, as little as 1 to 5 ng were easily visualized. However, at least 500 ng of each GAG were required for reproducible spectrophotometric quantitation by the modified method of Kimura et al. (109). Following visualization with Alcian Blue, the individual GAGs

TABLE 6

RESOLUTION OF GLYCOSAMINOGLYCANS IN EDTA/CATIONIC SYSTEMS[a]

GAG	Barium Acetate	Cadmium Acetate	Lithium Chloride	Zinc Sulfate	Zinc Chloride
KS	0.345	0.332	0.297	0.300	0.300
DS	0.360	0.355	0.379	0.320	0.320
HS	0.345	0.330	0.345	0.300	0.300
HP	0.345	0.351	0.428	0.300	0.300
C4S	0.360	0.350	0.358	0.300	0.300
HA	0.340	0.332	0.275	0.292	0.292

[a] Gels were run at 10 mM EDTA/50 mM cation, pH 8.4, using 2.5 mA/cm gel width; values represent the average R_f obtained from four independent electrophoretic experiments.

TABLE 7

EFFECT OF EDTA CONCENTRATION, LiCl CONCENTRATION AND pH ON THE RELATIVE MIGRATION OF INDIVIDUAL GLYCOSAMINOGLYCANS IN EDTA/LiCl SYSTEMS

GAG	Optimal Conditions[a]	EDTA Tetrasodium Salt Concentration (M)[b]			LiCl Concentration (M)			pH		
		0.025	0.050	0.100	0.010	0.025	0.100	3.5	7.0	11.5
KS	0.297	0.270	0.224	0.185	0.640	0.345	0.260	0.260	0.298	0.280
DS	0.379	0.290	0.235	0.185	*[c]	0.380	0.275	0.261	0.375	0.362
HS	0.345	0.282	0.235	0.185	*	0.370	0.275	0.260	0.375	0.360
HP	0.425	0.290	0.240	0.185	*	0.385	0.282	0.273	0.432	0.445
C4S	0.358	0.282	0.235	0.185	*	0.372	0.275	0.260	0.380	0.360
HA	0.276	0.272	0.224	0.185	0.635	0.343	0.260	0.264	0.275	0.302

[a] Optimal conditions for GAG separation were 10 mM EDTA/50 mM LiCl, pH 8.4, using 2.5 mA/cm gel width; values represent the average R_f obtained from four independent electrophoretic experiments.

[b] While EDTA concentration was varied, the LiCl concentration was maintained at its optimum, 50 mM. Similarly, while LiCl concentration was varied, EDTA was maintained at 10 mM.

[c] Indicates conditions where GAG migrated off the end of the gel.

Figure 4. Electrophoresis of Standard Glycosaminoglycans in EDTA Tetrasodium Salt/LiCl Combined System.

Electrophoresis of standard GAGs in EDTA tetrasodium salt/LiCl. GAG standards, concentrations and order of application are the same as those in Fig. 3. Electrophoresis was carried out in 10 mM EDTA tetrasodium salt/50 mM LiCl, pH 8.4, for 45 min at 4°C with a constant current of 2.5 mA/cm gel width.

FIGURE 4

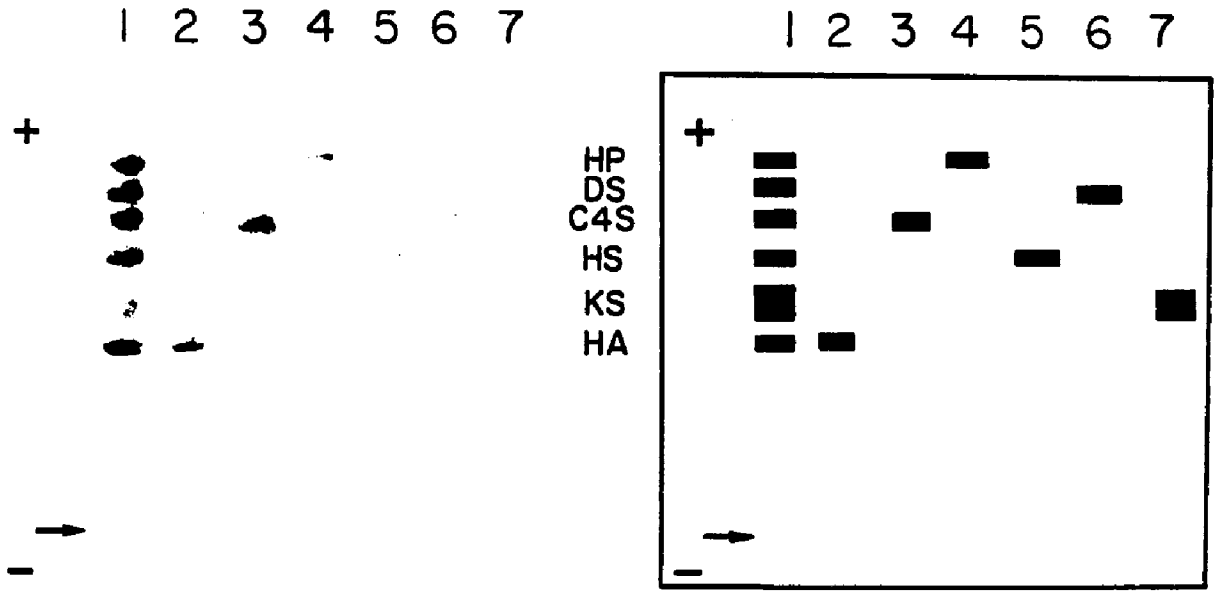

were quantitated with and without the ethanol precipitation procedure described by Cappelletti et al. (19). Table 8 compares the recovery of each GAG; the data presented represent the average of four separate experiments. When 5 µg of each purified GAG was electrophoresed, only 16 to 79% of that applied was recovered when the discontinous, ethanol precipitation method was employed. In contrast, the recoveries of individual GAGs separated by this continuous electrophoretic system ranged from 77 to 96% of the applied amounts.

2. Analysis of Stored Glycosaminoglycans in Homozygotes with Human and Feline Mucopolysaccharidoses I:

Table 9 summarizes the quantitative data that was obtained after surveying a variety of tissues from a human Hurler disease homozygote; the data for each tissue represents the mean values obtained from four independent electrophoretic analyses of the same individual and age-matched controls. Note that in each tissue examined, other than kidney, there was a significant increase in the amount of glycosaminoglycan present in affected individuals (> 2-fold), as compared to controls. Interestingly, this preliminary data suggests that the liver from one Hurler homozygote stored dermatan sulfate in substantial amounts, but not heparan sulfate (Fig. 5). For all analyses reported, the specific identification of a particular GAG was based on co-migration of this material with known standards in the new electrophoretic system described in the previous section. Furthermore, this identification was confirmed by electrophoretic co-migration with known standards using other cellulose acetate buffer conditions (21). Table 10 summarizes the preliminary data obtained when a similar analysis was

TABLE 8

EFFECT OF ETHANOL PRECIPITATION ON THE PERCENT RECOVERY OF INDIVIDUAL GLYCOSAMINOGLYCANS[a]

GAG	Without Ethanol Precipitation	With Ethanol Precipitation
KS	89.8 ± 4.25	65.5 ± 4.35
DS	82.0 ± 3.50	61.4 ± 3.50
HS	96.4 ± 2.15	63.1 ± 2.21
HP	77.2 ± 5.10	55.8 ± 5.15
C4S	94.5 ± 3.25	79.2 ± 3.25
HA	78.6 ± 12.4	16.4 ± 12.4

[a] Electrophoresis was performed as described in the Methods section. Values represent the percent recovery of the applied amount (5 µg) of the individual GAGs.

TABLE 9

ANALYSIS OF STORED GLYCOSAMINOGLYCANS IN THE HUMAN MUCOPOLYSACCHARIDOSIS I-H DISORDER[a]

Tissue/Fluid	Dermatan Sulfate		Heparan Sulfate	
	MPS I-H	Control	MPS I-H	Control
Bile	4.38	1.00	5.00	1.75
Brain	9.31	1.35	nd[b]	nd
Heart	47.30	nd	22.10	nd
Kidney	nd	nd	0.27[c]	nd
Liver	2.14	2.67	14.80	5.85
Lung	0.65	nd	0.14	nd
Urine	1.65	nd	3.97	nd

[a] Data expressed as the mean µg GAG/mg starting weight for all tissue samples and mean µg GAG/µl for fluid samples.

[b] Non-detectable; < 0.05 µg GAG present on gel.

[c] Storage material heterogeneous; runs as a diffuse band on gel.

Figure 5. Electrophoresis of Glycosaminoglycans from Normal and MPS 1-H Human Livers in the EDTA Tetrasodium salt/LiCl Combined System.

Electrophoresis of GAGs from normal and Hurler livers in EDTA tetrasodium salt/LiCl. (1) HA; (2) HS; (3) DS; (4) liver extract from a patient with Hurler disease; (5) liver extract from a normal control. Methods of tissue GAG isolation and electrophoretic conditions are described in the Methods section, except gels were run for 60 min. Two µl of normal and Hurler liver extracts were applied.

FIGURE 5

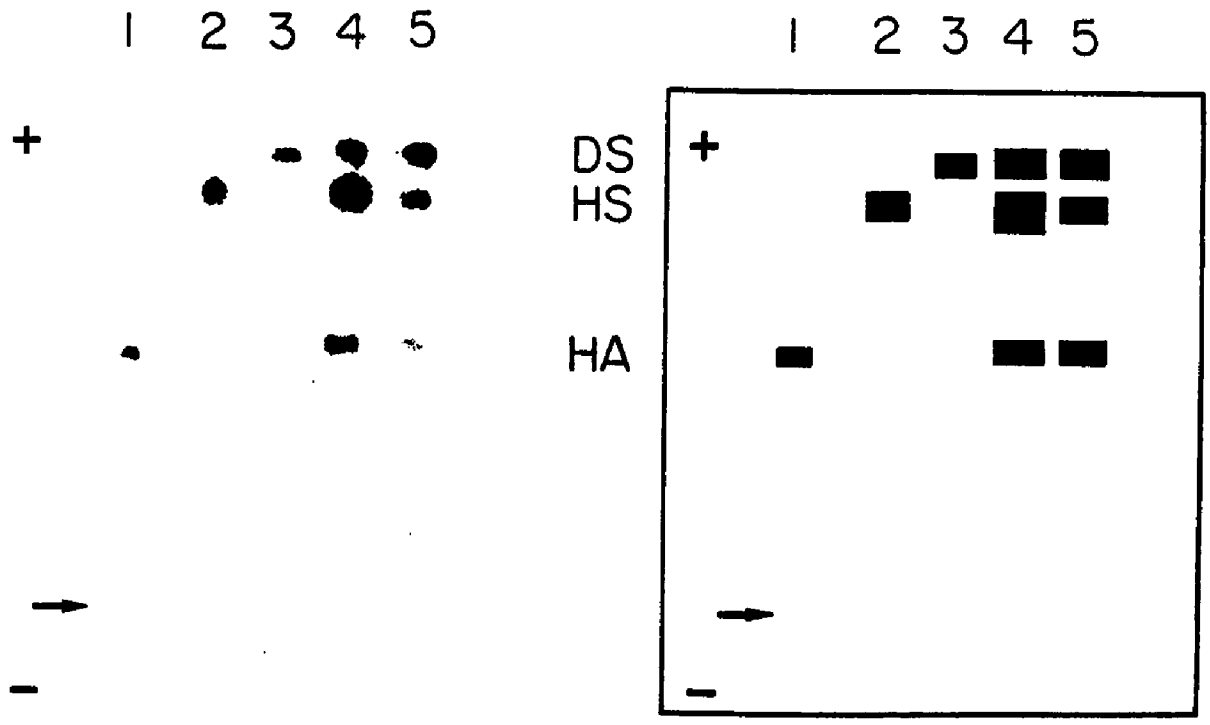

TABLE 10

ANALYSIS OF STORED GLYCOSAMINOGLYCANS IN THE FELINE MUCOPOLYSACCHARIDOSIS I DISEASE[a]

Tissue/Fluid	Dermatan Sulfate		Heparan Sulfate	
	fMPS I	Control	fMPS I	Control
Liver	12.75	3.71	4.85	4.57
Lung	4.85	nd[b]	nd	nd
Mixed Leukocytes	6.62	nd	nd	nd
Urine	2.05	nd	2.65	nd

[a] Data expressed as the mean µg GAG/mg starting weight for all tissue samples and mean µg GAG/µl fluid for urine samples.

[b] Non-detectable; < 0.05 µg GAG present on gel.

conducted on liver, lung, mixed leukocytes and urine samples from one affected homozygote with feline MPS I and two feline normal controls. Note the differential accumulation of dermatan sulfate and heparan sulfate in the different tissues and/or fluids.

B. Purification and Characterization of Low and High Uptake Forms of Human α-L-Iduronidase:

1. Optimization of Human Enzyme Source:

Table 11 shows data obtained in preliminary experiments which were designed to establish the optimum human source for the purification of α-L-iduronidase. Although cultured skin fibroblasts had the highest specific activity for this enzyme, lung was chosen on the basis of its total activity, which was at least 4 times greater than that in other tissues tested, and its availability. Table 12 summarizes experiments which were performed to optimize the homogenization procedure. Addition of either Triton X-100 or Nonidet P-40 detergents to the homogenization buffer increased the total amount of enzyme recovered by at least 2-fold, although the specific activity of α-L-iduronidase was not significantly changed. The use of a basic, pH 7.3, buffer did not reduce the total enzyme recovery at this stage of the procedure. Further homogenization of the pellets with 1% sodium taurocholate resulted in the recovery of $< 10\%$ additional α-L-iduronidase activity (data not shown).

2. Ion Exchange Chromatography:

Preliminary experiments were also performed to test the behavior of α-L-iduronidase on the anion exchange resin, DEAE-cellulose.

TABLE 11

α-L-IDURONIDASE ACTIVITY IN A VARIETY OF DIFFERENT HUMAN TISSUES[a]

Source	U/ml	U/mg[b]
Fibroblasts	122.0	28.00
Placenta	45.0	0.18
Lung	178.0	0.15
Kidney	37.2	0.10
Spleen	55.0	0.08
Liver	44.5	0.05

[a] Five g (wet weight) of each tissue were hand homogenized in 2 volumes of 10 mM sodium phosphate buffer, pH 6.0, containing 0.3% Nonidet P-40. For fibroblasts, data represents extracts of 1 confluent 75 mm^2 Falcon flask in 10 mM sodium phosphate buffer, pH 6.0, containing 0.3% Nonidet P-40. Cells were lysed by sonication (3 bursts; 30 s each) in a Branson, model 200 cup sonicator.

[b] Protein was measured by the fluorescamine assay.

TABLE 12

OPTIMIZATION OF α-L-IDURONIDASE EXTRACTION FROM HUMAN LUNG

Buffer[a]		U/ml	U/mg[b]
10 mM Tris/HCl, pH 7.3,	+ 0.1 M NaCl	39.5	0.12
	+ 0.1% Triton X-100	127.0	0.18
	+ 0.5% Triton X-100	132.0	0.09
	+ 0.5% Nonidet P-40	130.0	0.16
10 mM Sodium phosphate, pH 6.0,	+ 0.1 M NaCl	52.4	0.10
	+ 0.1% Triton X-100	143.0	0.17
	+ 0.5% Triton X-100	140.0	0.14
	+ 0.5% Nonidet P-40	145.0	0.15
10 mM Sodium citrate, pH 4.0,	+ 0.1 M NaCl	45.7	0.19
	+ 0.1% Triton X-100	138.0	0.20
	+ 0.5% Triton X-100	135.0	0.15
	+ 0.5% Nonidet P-40	145.0	0.15

[a] Five g (wet weight) of human lung was hand homogenized in 2 volumes of the appropriate buffer. Homogenates were centrifuged at 20,000 x g and the supernatants were assayed for α-L-iduronidase activity.

[b] Protein was measured by the fluorescamine assay.

Figure 6 illustrates that the total enzyme activity bound to the column at pH 7.3 could be eluted in two broad, distinct peaks when a linear salt gradient was applied. Similar experiments from a variety of other tissue homogenates also revealed the existence of two major peaks of enzymatic activity which were separable by DEAE-cellulose chromatography (data not shown). Figure 7A illustrates that if lung homogenates were made without detergent present in the buffer, the less electronegative fraction of the enzyme was predominately recovered (soluble form). If the pellets from this preparation were then re-homogenized in the presence of 0.3% Nonidet P-40, the majority of the additional enzyme activity eluted with the more electronegative fraction (membrane-associated form), as shown in Figure 7B.

3. Isoelectric Focusing:

Figure 8 reveals that when crude lung homogenates were isoelectrofocused in a pH gradient of 4.0 to 9.0 established with LKB ampholines and visualized using the flurogenic, 4MU α-Id substrate, a broad staining region was seen with a pI range of 5.85-7.35; two major, distinct bands of activity were identified. After cutting the gel into 1 cm slices and eluting the enzyme by overnight diffusion, the two major peaks of activity were observed at pH 6.00 and 6.85.

4. Enzyme Uptake Studies:

Figure 9 illustrates that the two fractions of human α-L-iduronidase which were separated by anion exchange chromatography differed in their degree of incorporation into cultured Hurler fibroblasts. The more electronegative, membrane-associated enzyme possessed

Figure 6. DEAE-Cellulose Chromatographic Profile of Human α-L-Iduronidase.

Tissue homogenization and DEAE-cellulose chromatography were performed as described in the Methods section. 100 g of frozen human lung was used as the starting material.

FIGURE 6

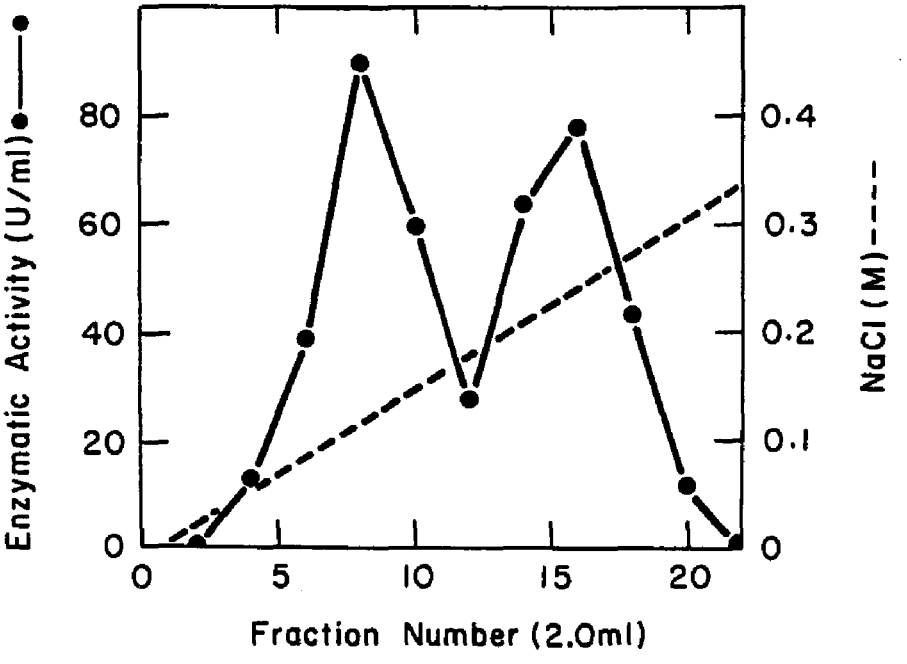
Enzymatic Activity (U/ml)
80
60
40
20
0
0
5
10
15
20
Fraction Number (2.0ml)
0.4
0.3
0.2
0.1
0
NaCl (M)

Figure 7. DEAE-Cellulose Chromatographic Profiles of Separated Soluble and Membrane-Associated Forms of Human α-L-Iduronidase.

DEAE-cellulose chromatography was performed as described in the Methods section. The procedures used for the isolation of the soluble (Panel A) and membrane-associated (Panel B) forms of human α-L-iduronidase are also described in the text.

FIGURE 7

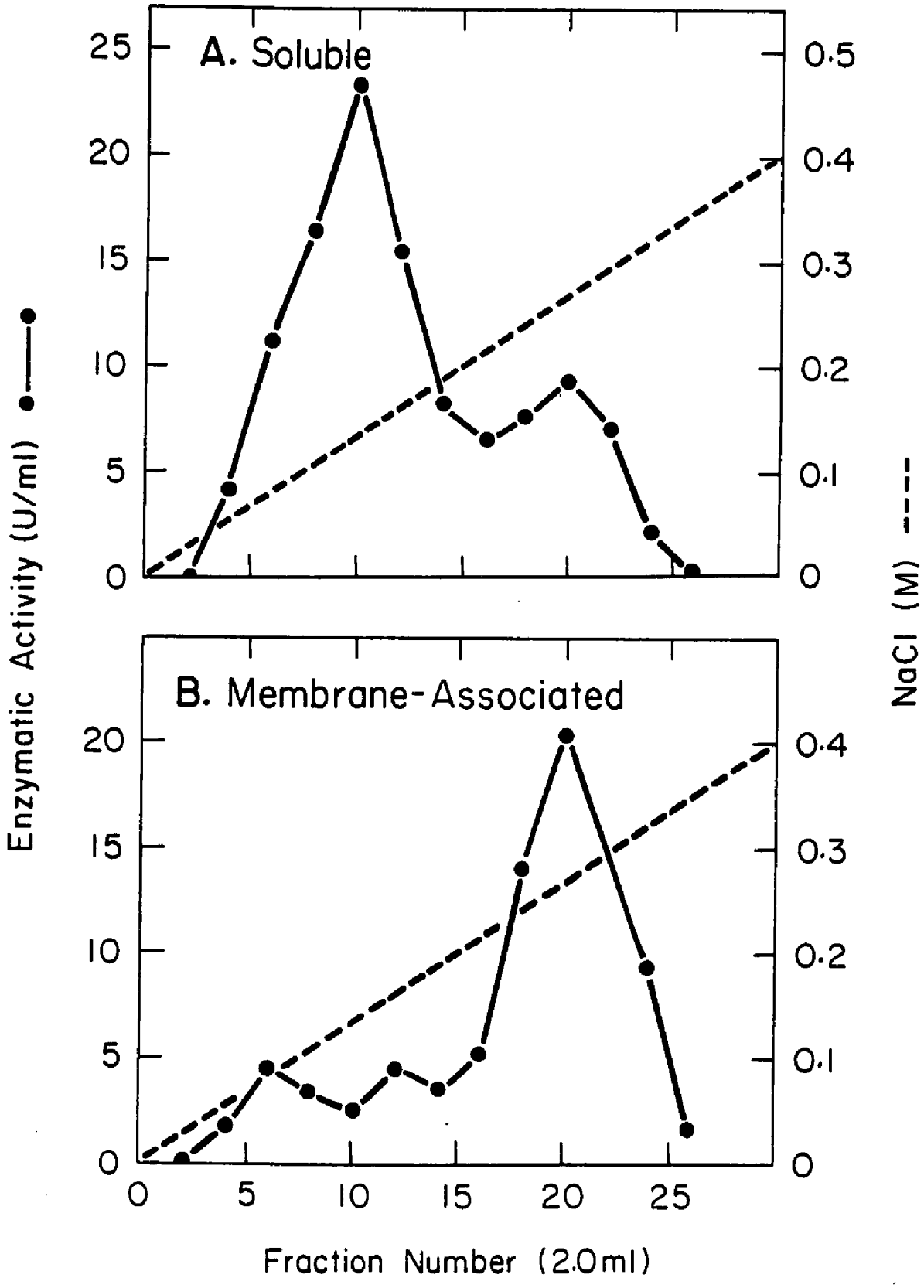
A. Soluble
B. Membrane-Associated
Enzymatic Activity (U/ml)
NaCl (M)
Fraction Number (2.0ml)
0
5
10
15
20
25
0.1
0.2
0.3
0.4
0.5

Figure 8. Isoelectric Focusing Profile of Human α-L-Iduronidase.

Isoelectric focusing, determination of enzymatic activity, and fluorescent staining with 4MU α-Id were performed as described in the Methods section. 1000 total U (250 µl) of α-L-iduronidase from crude human lung homogenates were applied to the gel.

FIGURE 8

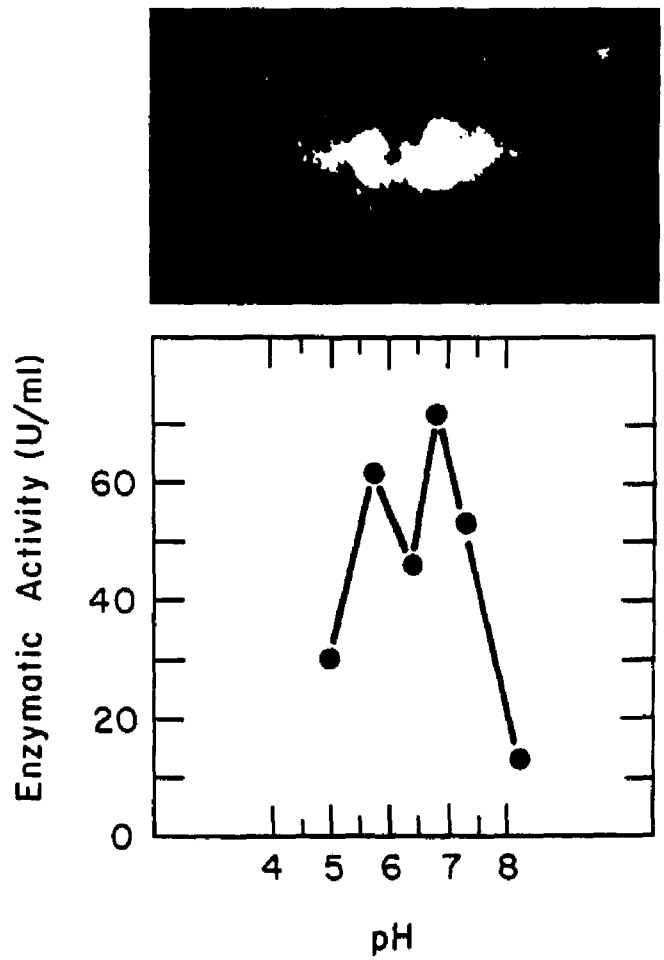

Figure 9. Enzyme Uptake Profiles of Soluble and Membrane-Associated Forms of Human α-L-Iduronidase.

Uptake characteristics of the partially purified (SA ∿ 20,000 U/mg Lowry) soluble and membrane-associated forms of human α-L-iduronidase were determined as described in the Methods section.

FIGURE 9

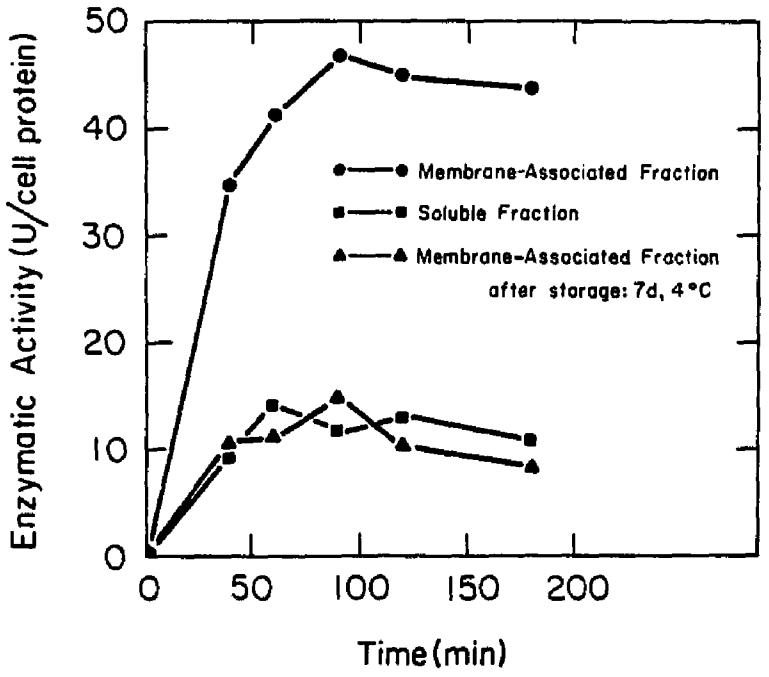
Enzymatic Activity (U/cell protein)
50
40
30
20
10
0
0
50
100
150
200
Time (min)
Membrane-Associated Fraction
Soluble Fraction
Membrane-Associated Fraction
after storage: 7d, 4°C

high uptake properties while the soluble form was taken up significantly less (low uptake). Upon storage of the partially purified high uptake enzyme (SA ∿ 20,000 U/mg Lowry) for one week at 4°C, all of the high uptake properties were lost.

5. Purification Procedure:

Table 13 summarizes a typical purification of α-L-iduronidase from 4,044 g of human lung. The 0.1 M NaCl enzyme fraction (low uptake) which appeared in the void and wash fractions of the DEAE-cellulose column was purified approximately 218,000-fold over the activity in the crude homogenate, while the 0.6 M NaCl eluant enzyme fraction (high uptake), which represented approximately 15-20% of the total enzymatic activity, was purified 175,000-fold over the crude. The majority of the hemoglobin present in the crude homogenate co-eluted with the low uptake enzyme fraction after DEAE-cellulose chromatography and therefore its specific activity at this step was significantly lower than the high uptake fraction. It should be noted that the yield after this first column step was greater than 100%; this observation was not due to quenching of the 4MU flouresence by pigments in the crude homogenate since assays that were stopped with trichloracetic acid in order to precipitate the proteins prior to fluorometric measurement gave similar results (data not shown). After the next step in the purification, Con A-Sepharose chromatography, the specific activities of the two enzyme forms were very similar (approximately 4,000-fold purified over the total crude homogenate activity); the total enzyme yield at this step was between 98-100%. The next step in the purification was hydroxyapatite chromatography. Figure 10 illustrates the elution profile obtained

TABLE 13

PURIFICATION OF LOW AND HIGH UPTAKE FORMS OF
α-L-IDURONIDASE FROM HUMAN LUNG[a]

Step	Volume	Total Activity	Specific Activity	Purification	Combined Yield
	(ml)	(units)	(U/mg)	(fold)	(%)
Crude extract	2,333	380,083	0.5	1	100
DEAE-Cellulose					
Low	2,000	365,000	3.65	7.3	100
High	725	97,050	42.50	85	
Con A-Sepharose					
Low	44	305,200	1,975	3,950	99
High	37	72,500	2,200	4,400	
Hydroxyapatite					
Low	52	137,500	22,400	44,800	45.9
High	64	37,250	19,075	38,150	
Biogel P-100					
Low	44	82,500	109,000	218,000	36.6
High	51	56,325	87,500	175,000	

[a] Enzyme assays were performed using 100 μM 4MU α-Id as described in the Methods section and protein was measured by the Lowry assay.

Figure 10. Hydroxyapatite Chromatographic Profiles of Low and High Uptake Forms of Human α-L-Iduronidase.

Hydroxyapatite chromatography of the separated low uptake (Panel A) and high uptake (Panel B) forms of human α-L-iduronidase was performed as described in the Methods section.

FIGURE 10

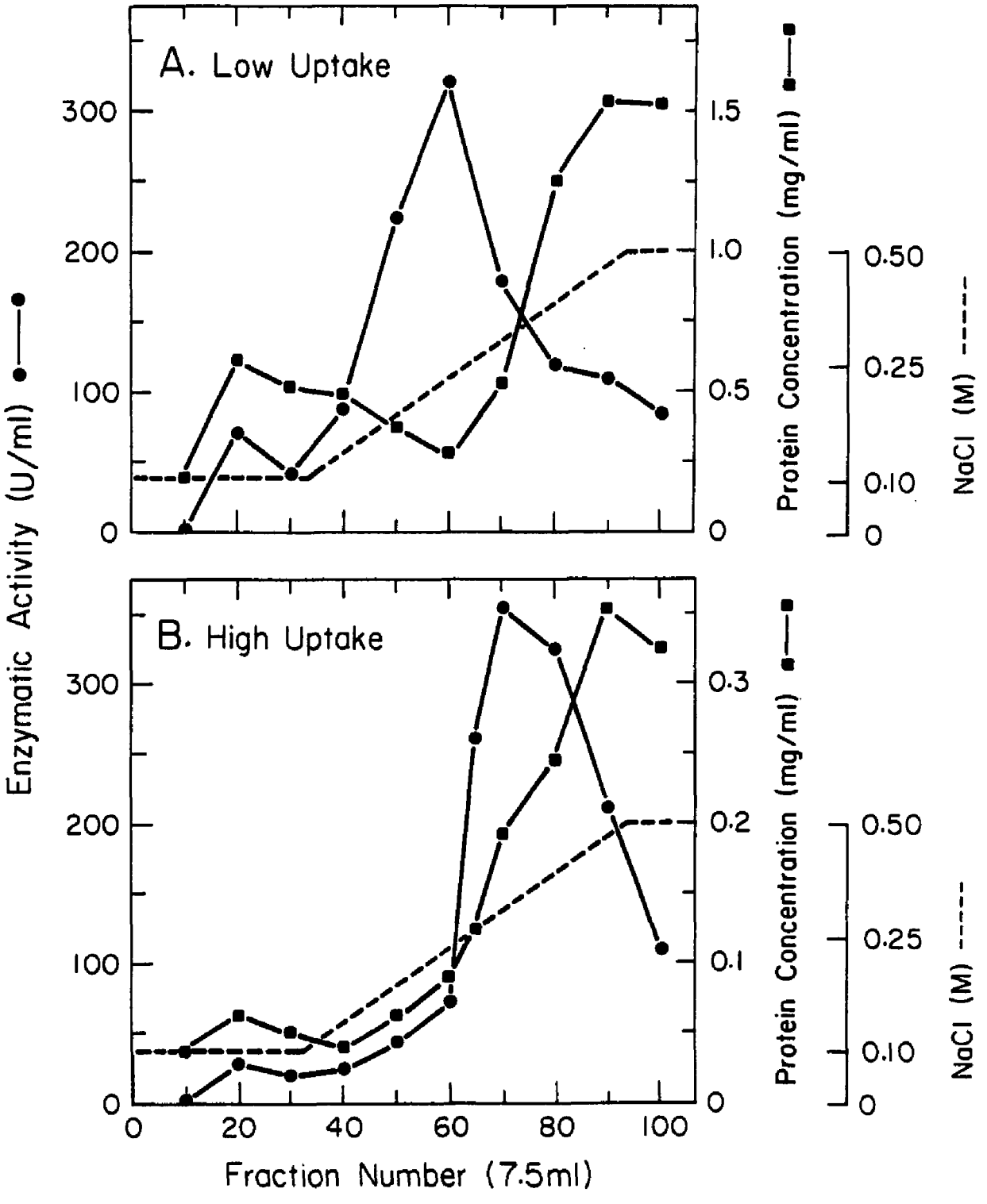
A. Low Uptake
B. High Uptake
Enzymatic Activity (U/ml)
Protein Concentration (mg/ml)
NaCl (M)
Fraction Number (7.5ml)
0
100
200
300
0.5
1.0
1.5
0.1
0.2
0.3
0.10
0.25
0.50
20
40
60
80

for the two enzyme fractions when they were chromatographed independently on this resin; note that the high uptake enzyme (Fig. 10B) elutes later in the gradient. For both enzymes there was trailing of the activity during the elution, and the final fold purification and % yield was dependent on where the collection cuts were taken; therefore, the results of this step were the most variable between different preparations. The final procedure in this stage of the purification was gel filtration on a Biogel P-100 column (Fig. 11); again the results were dependent on where the enzyme cuts were taken. Note that the initial peak of high uptake enzyme activity (Fig. 11B) eluted earlier than that of the low uptake enzyme (Fig. 11A), providing preliminary evidence for a molecular weight difference between the two fractions. The final yields at this stage of the purification were from 35-45%. Six glycosidases other than α-L-iduronidase were assayed for activity in each of the post Biogel P-100 enzyme preparations; their total activity was less than 0.5% of α-L-iduronidase (Table 14).

6. High Performance Liquid Chromatography:

In order to assure the use of homogeneous enzyme for comparative physiochemical studies, the proteins were further purified by high performance liquid chromatography. Figure 12 illustrates the profiles obtained for each enzyme after HPLC. When each protein peak was collected separately, concentrated and assayed for α-L-iduronidase activity, all were found to have significant amounts of catalytic activity. In addition, the specific activity in each protein peak was relatively constant.

Figure 11. Biogel P-100 Chromatographic Profiles of Low and High Uptake Forms of Human α-L-Iduronidase.

Biogel P-100 chromatography of the separated low uptake (Panel A) and high uptake (Panel B) forms of human α-L-iduronidase was performed as described in the Methods section.

FIGURE 11

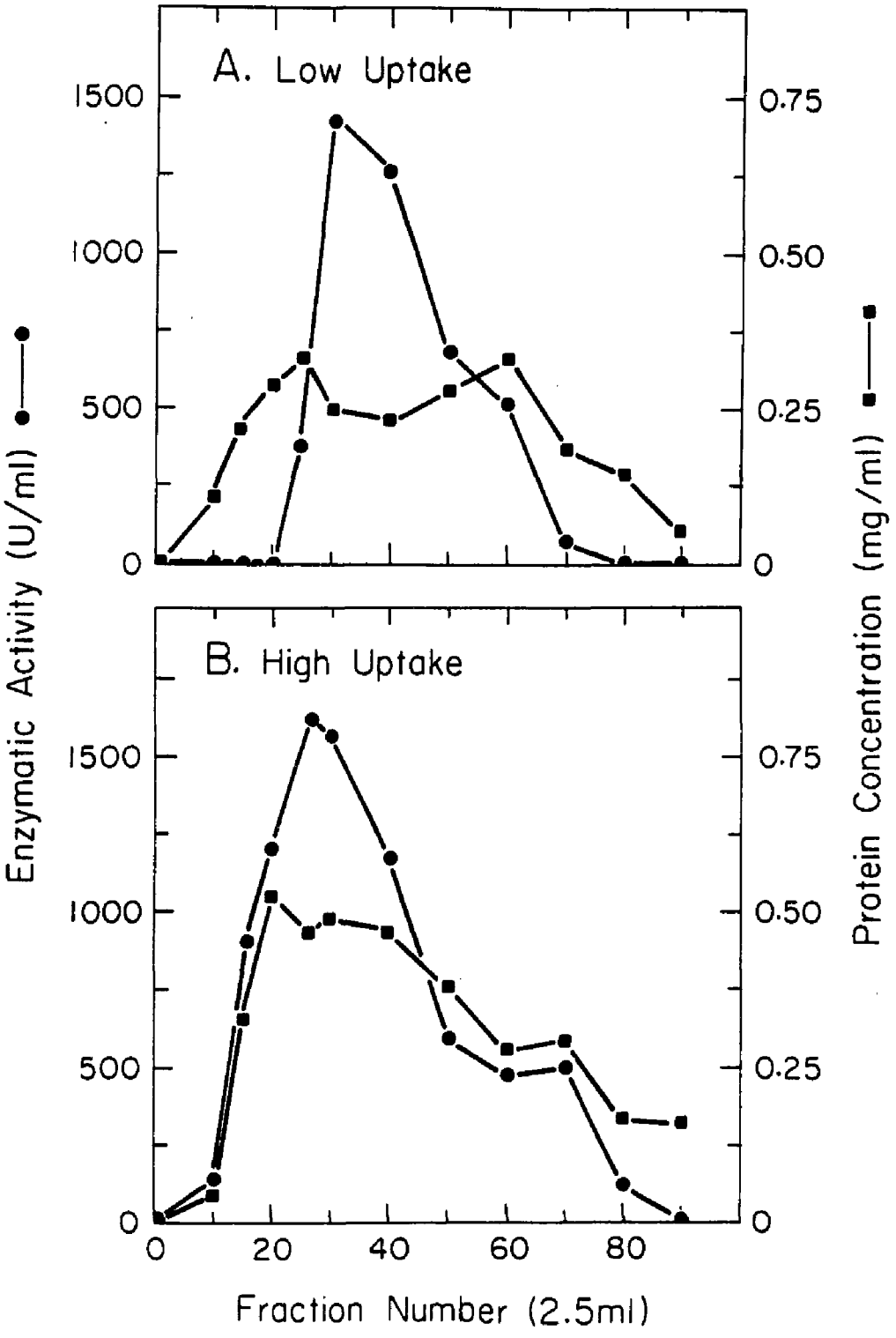
A. Low Uptake
B. High Uptake
1500
1000
500
0
0.75
0.50
0.25
0
0
20
40
60
80
Enzymatic Activity (U/ml)
Protein Concentration (mg/ml)
Fraction Number (2.5ml)

TABLE 14

CONTAMINATING GLYCOSIDASES IN THE PURIFIED LOW AND HIGH UPTAKE FORMS OF α-L-IDURONIDASE PRIOR TO HPLC[a]

Enzyme	Substrate Concentration (mM)	Buffer	pH	% Low Uptake α-L-Iduronidase	% High Uptake α-L-Iduronidase
β-D-Hexosaminidase A	4.00	0.04 M C-P	4.40	0.23	0.37
β-D-Glucosidase	5.00	0.05 M C-P	5.00	0.00	0.00
α-D-Galactosidase A	4.30	0.15 M C-P	4.60	0.00	0.00
α-D-Mannosidase	10.00	0.10 M C-P	4.20	0.05	0.18
α-L-Fucosidase	1.00	0.10 M C-P	5.80	0.18	0.00
β-D-Glucuronidase	10.00	0.10 M AC	4.85	0.00	0.00
α-L-Iduronidase	0.05	0.40 M NaF	3.50	100.00	100.00

[a] Purified low uptake (SA 109,000 U/mg Lowry) or high uptake (87,500 U/mg Lowry) were incubated for 1 h at 37°C under the conditions specified for each hydrolase. The resulting activities in nanomoles of product formed/h are expressed as the percentage of the 4-methylumbelliferyl α-L-iduronide activity; citrate phosphate (C-P), acetate (AC) and sodium formate (NaF).

Figure 12. HPLC Profiles of Low and High Uptake Forms of Human α-L-Iduronidase.

HPLC of the low uptake (Panel A) and high uptake (Panel B) forms of human α-L-iduronidase was performed as described in the Methods section.

FIGURE 12

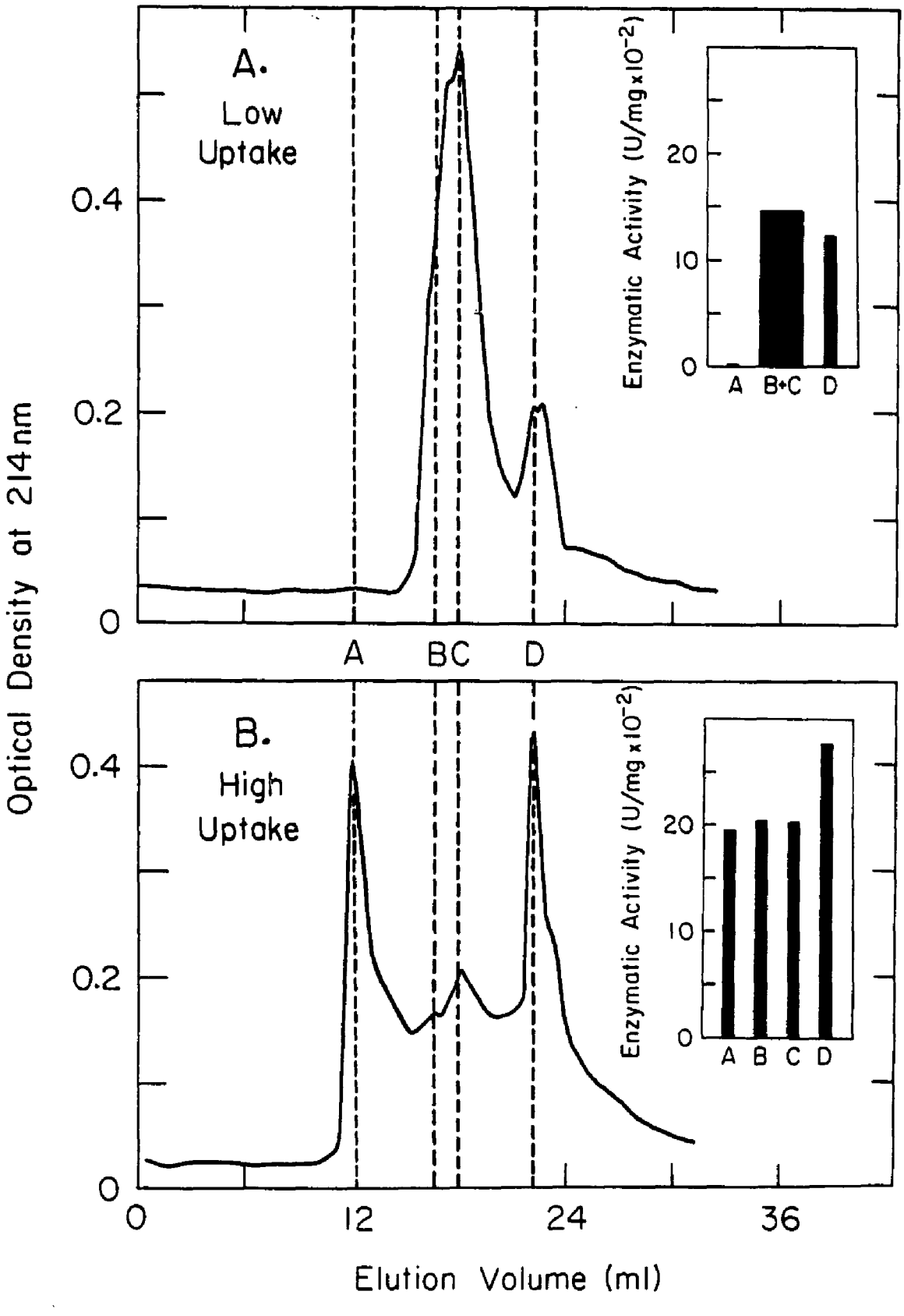
A.
Low
Uptake
B.
High
Uptake
Optical Density at 214 nm
0.4
0.2
0
A
BC
D
Enzymatic Activity (U/mg x10⁻²)
20
10
0
A B+C D
A B C D
0
12
24
36
Elution Volume (ml)

7. Stability of Human α-L-Iduronidase:

Both fractions of the enzyme became increasingly unstable with each purification step. After Con A-Sepharose chromatography, 3 cycles of freezing and thawing destroyed all of the enzymatic activity, although at this stage the enzyme was stable for up to 1 month at 4°C without significant loss of activity. Table 15 illustrates the instability of α-L-iduronidase at 4°C during the two final stages of the purification prior to HPLC. Addition of either glycerol or D(+)-mannose to the post-hydroxyapatite enzyme increased its $T_{1/2}$ at 4°C; at this stage the choice of buffers was not critical. However, after the final gel filtration chromatography the use of an acidic, pH 4.0 buffer increased the stability of the enzymatic activity although even with the addition of D(+)-mannose, the $T_{1/2}$ of the low uptake form at 4°C was only 72 h. On the basis of these results, the enzymes were stored at 4°C in 10 mM citrate phosphate buffer, pH 4.0, containing 0.5 M NaCl and 0.1 M D(+)-mannose as stabilizers. In addition, the final Biogel P-100 column was routinely run in the presence of this buffer.

8. Native Polyacrylamide Gel Electrophoresis:

Figure 13 illustrates that the post-Biogel P-100 purified low and high uptake forms of human α-L-iduronidase migrated as single Coomassie Blue staining bands on 7% polyacrylamide disc gels when 150 µg protein (Lowry) was applied of each. No significant differences in migration were noted.

9. SDS Polyacrylamide Gel Electrophoresis:

Figure 14 shows the patterns obtained on 10% SDS polyacryl-

TABLE 15

STABILITY OF THE LOW AND HIGH UPTAKE FORMS OF HUMAN α-L-IDURONIDASE DURING THE PURIFICATION PROCEDURE[a]

Stabilizing Conditions		$T_{1/2}$ 4°C; days Post-Hydroxyapatite		$T_{1/2}$ 4°C; h Post-Biogel P-100	
		Low	High	Low	High
10 mM Sodium Phosphate, pH 6.0,	+ 0.5 M NaCl	10.0	14.0	0.0	12.0
	+ 10% Glycerol	14.0	20.0	4.0	48.0
	+ 40% Glycerol	14.5	20.0	4.0	48.0
	+ 0.1 M D(+) Mannose	21.5	22.0	48.0	120.0
	+ 0.5 M D(+) Mannose	20.0	22.0	48.0	120.0
10 mM Sodium Citrate, pH 4.0,	+ 0.5 M NaCl	10.0	12.5	6.0	24.0
	+ 10% Glycerol	12.5	22.0	24.0	24.0
	+ 40% Glycerol	12.0	21.5	24.0	24.0
	+ 0.1 M D(+) Mannose	18.5	24.0	72.0	120.0
	+ 0.5 M D(+) Mannose	18.5	24.0	72.0	120.0

[a] 500 U of each enzyme were removed at the indicated stage of the purification procedure and stored at 4°C under each of the various conditions.

Figure 13. Native Polyacrylamide Gel Electrophoresis of the Purified Low and High Uptake Forms of Human α-L-Iduronidase.

7% native polyacrylamide gel electrophoresis of the purified (post-Biogel P-100; SA 105,000 U/mg Lowry) low uptake (150 µg Lowry; Lane A) and high uptake (150 µg Lowry; Lane B) forms of human α-L-iduronidase was performed as described in the Methods section. The arrow indicates the beginning of the separating gel; samples migrated from the anode towards the cathode.

FIGURE 13

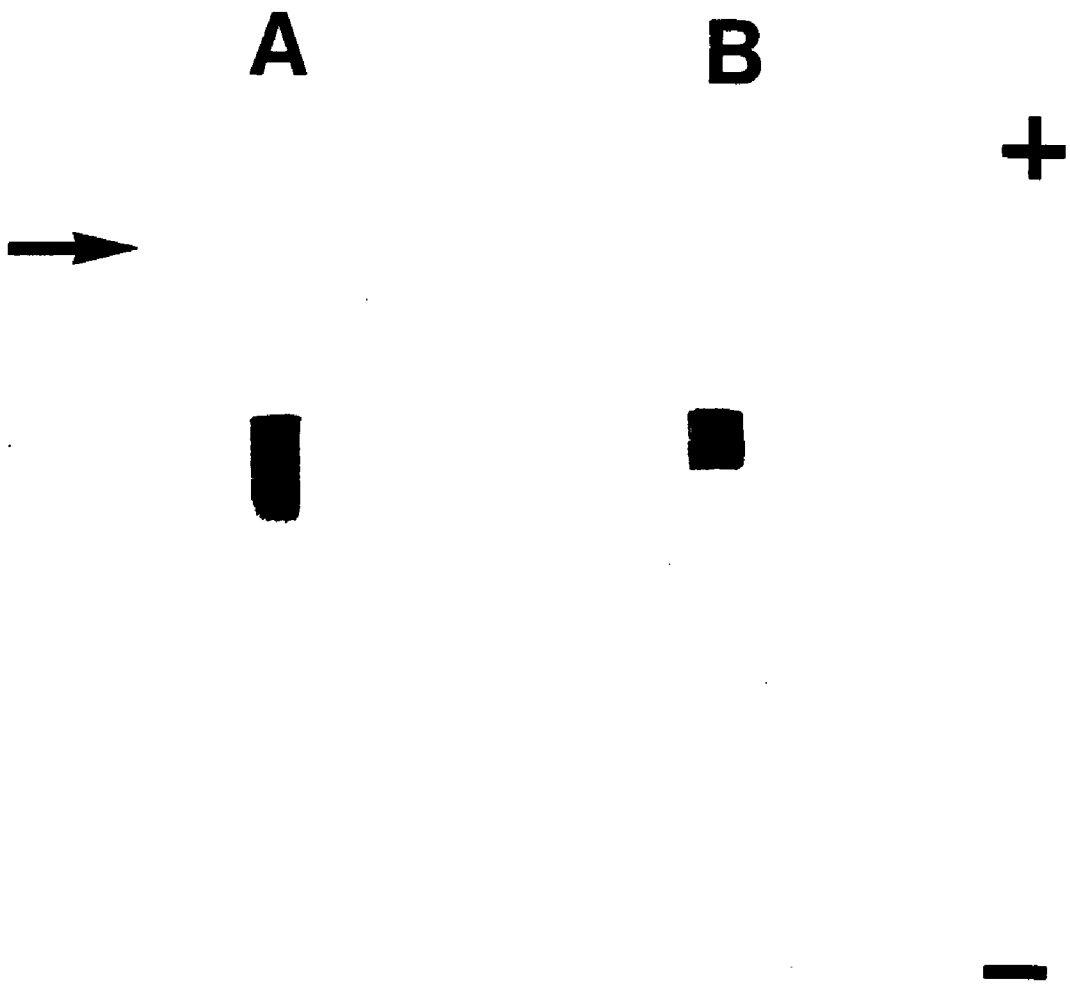

Figure 14. SDS Polyacrylamide Gel Electrophoresis of the Purified Low and High Uptake Forms of Human α-L-Iduronidase.

10% SDS polyacrylamide gel electrophoresis of the purified (post-Biogel P-100; 105,000 U/mg Lowry) low uptake (150 µg Lowry; Lane B) and high uptake (150 µg Lowry; Lane D) forms of human α-L-iduronidase was performed as described in the Methods section. Molecular weight standards are shown in Lanes A and D.

FIGURE 14

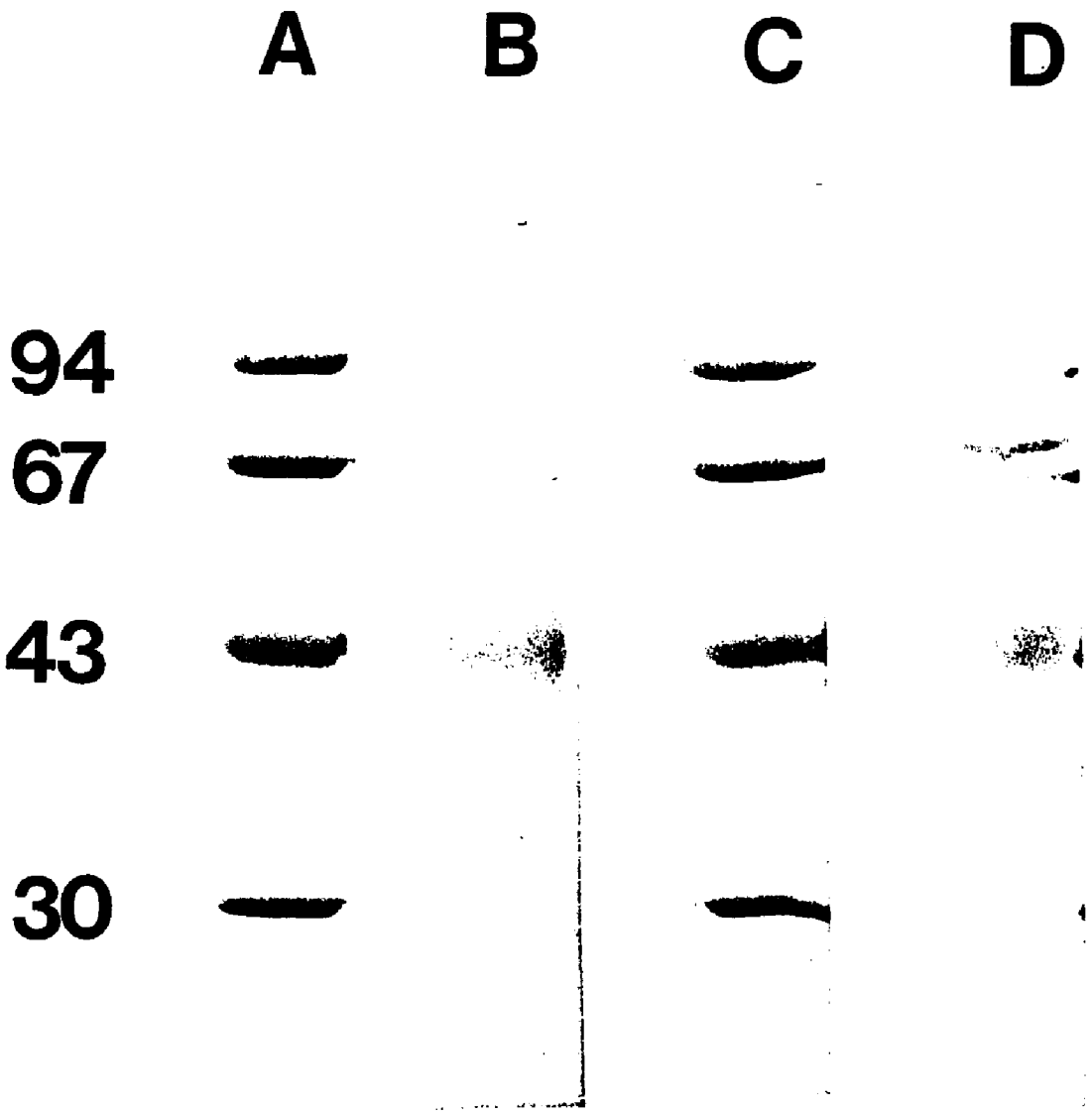

amide slab gels under reducing (10% β-mercaptoethanol; boiling for 10 min) conditions. Each sample contained 150 μg of post-Biogel P-100 protein (Lowry) which had been previously lyopholyzed and taken up in sample application buffer. Each form of the enzyme showed the same pattern under non-reducing conditions (data not shown). The low uptake enzyme fraction had two major diffuse Coomassie Blue staining bands which accounted for greater than 90% of the total protein; one migrated with a molecular weight of 72,000 and the other 42,000; the 72,000 band occassionally migrated as a tight doublet. Although in this gel the two bands appeared to be present in approximately equal amounts, the results of other gel experiments indicated that their ratio may vary; in some instances one or the other was entirely absent. The high uptake enzyme fraction routinely contained these two species and additional higher molecular weight components (90,000 and higher aggregates). Both enzyme samples that had been stored at 4°C for varying lengths of time at different stages of the purification often showed additional characteristic bands (55,000 and 28,000; photograph not shown).

10. Apparent Molecular Weight Determinations:

Figure 15 demonstrates the apparent native molecular weight of purified low uptake (SA ∿ 106,000 U/mg Lowry) and high uptake (SA ∿ 94,600 U/mg Lowry) α-L-iduronidase when determined by gel filtration on Sephadex G-200. The low uptake enzyme had an apparent molecular weight of 68,000, while the high uptake enzyme's apparent molecular weight was 85,000, based on the elution volume of the initial activity peaks. Note that in both instances the enzyme eluted from the column in broad peaks with similar specific activities (figure not shown).

Figure 15. Apparent Molecular Weight Determination of Low and High Uptake Forms of Human α-L-Iduronidase by Gel Filtration.

Apparent molecular weight determinations of the low and high uptake forms of human α-L-iduronidase were made by the procedure described in the Methods section using Sephedex G-200 chromatography. Apparent molecular weight estimates were based on the elution volumes.

FIGURE 15

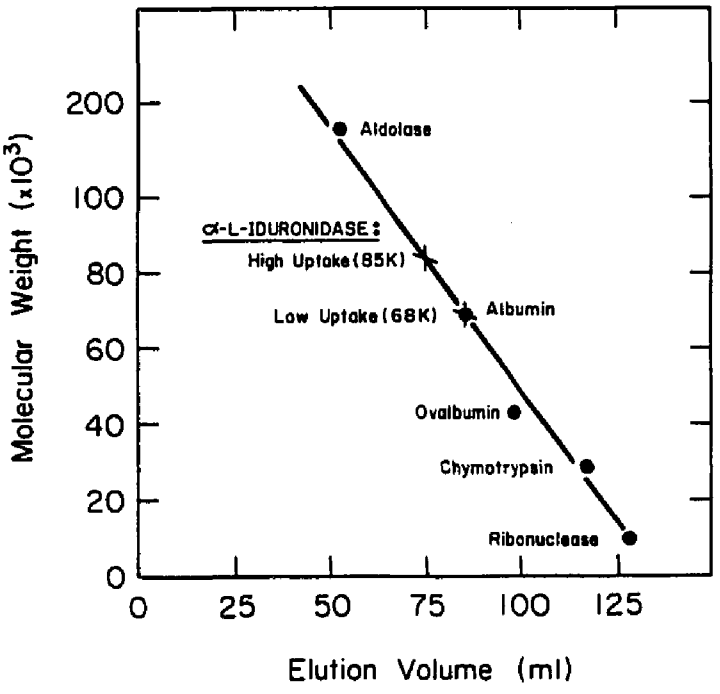
Molecular Weight (x10³)
200
100
80
60
40
20
0
0
25
50
75
100
125
Elution Volume (ml)
Aldolase
α-L-IDURONIDASE:
High Uptake (85K)
Low Uptake (68K)
Albumin
Ovalbumin
Chymotrypsin
Ribonuclease

11. Kinetic Properties:

Figure 16 illustrates the Lineweaver-Burk plots obtained for both forms of the purified (post-Biogel P-100) enzyme using two artificial substrates, 4MU α-Id and phenyl α-Id, and one natural substrate, anhydro[^{3}H]man; Table 16 summarizes the results. Note that the K_m and apparent V_{max} obtained for the low and high uptake forms of the enzyme were very similar using each of the three substrates. With each substrate, both enzymes exhibited normal Michaelis-Menten kinetics.

12. Effect of Glycosaminoglycans:

The effect of a number of purified GAGs on the 4MU α-Id activity was evaluated; Table 17 summarizes the results obtained at one concentration of GAG. Each of the GAGs exhibited an inhibitory effect on the enzymatic activity of the low and high uptake forms. Dixon plots (1/V vs. [I]), linear for each of the GAGs tested, indicated that the inhibition was non-competitive; K_i's were determined from these plots. Heparin was the most potent inhibitor of both enzymes (K_i's of 0.09 mg/ml and 0.13 mg/ml, respectively). Dermatan sulfate and Heparan sulfate, the presumed physiologic substrates, had K_i's of 0.19 mg/ml and 0.75 mg/ml for the low uptake enzyme fraction and 4.50 mg/ml and 3.30 mg/ml for the high uptake enzyme fraction. The inhibitory effect of each GAG was significantly less for the high uptake enzyme than the low uptake. In fact, Hyaluronic acid, a relatively potent inhibitor of the low uptake enzyme (K_i 0.13 mg/ml), had a very limited effect on the high uptake enzyme (K_i > 5.00 mg/ml). The Dixon plots obtained for DS and HS using a single substrate concentration (100 μM) are illustrated in Figure 17.

Figure 16. Lineweaver-Burk plots of Low and High Uptake Forms of Human α-L-Iduronidase Using Three Different Substrates.

K_m and apparent V_{max} determinations were made from the Lineweaver-Burke plots of the low uptake (SA 95,000 U/mg Lowry; ■——■) and high uptake (SA 76,000 U/mg Lowry; ●—●) forms of human α-L-iduronidase using the three indicated substrates: all enzyme assays were performed as described in the Methods section. 25 µl of each enzyme preparation was added to 25 µl of each substrate preparation in 0.4 M sodium formate buffer, pH 3.5, and incubated for 1 h at 37°C. The substrate concentrations represent the final concentrations in the assay mixture.

FIGURE 16

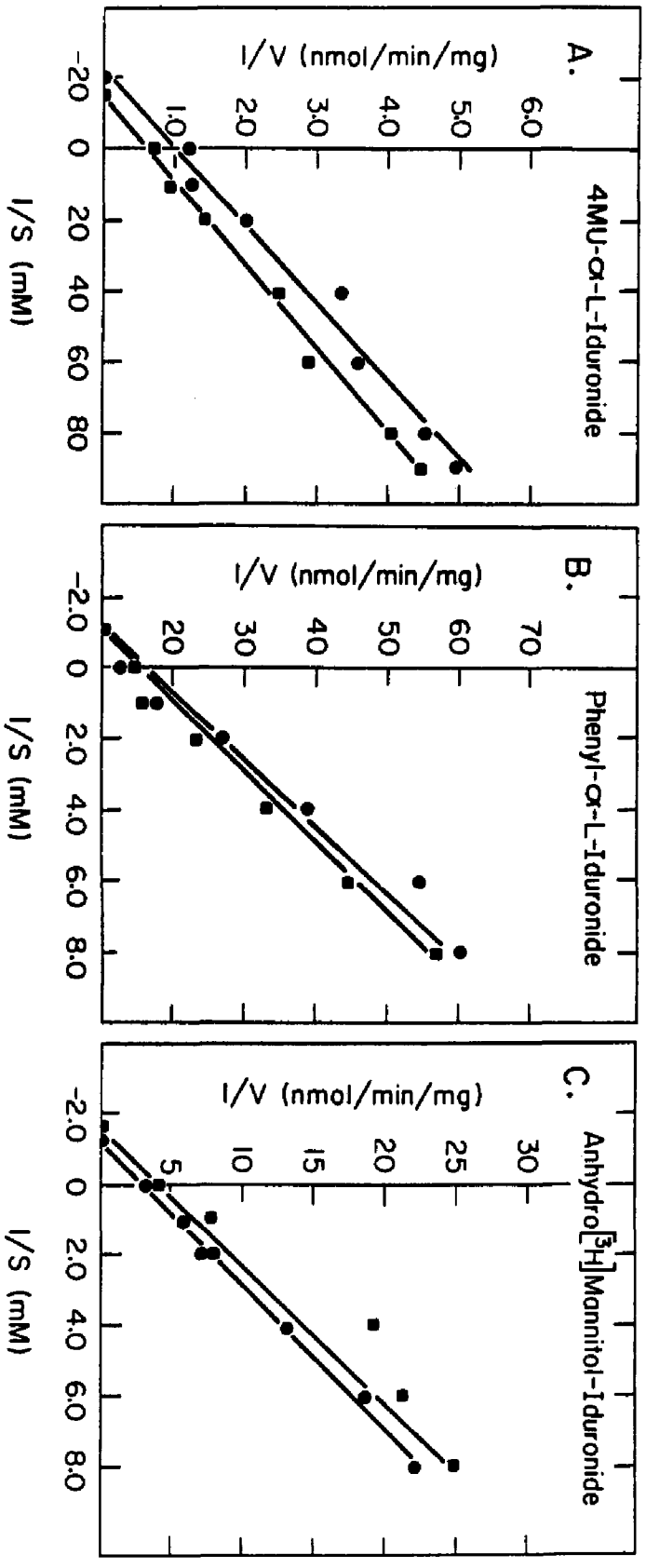
A.
4MU-α-L-Iduronide
I/V (nmol/min/mg)
1.0
2.0
3.0
4.0
5.0
6.0
-20
0
20
40
60
80
I/S (mM)
B.
Phenyl-α-L-Iduronide
I/V (nmol/min/mg)
20
30
40
50
60
70
-2.0
0
2.0
4.0
6.0
8.0
I/S (mM)
C.
Anhydro[3H]Mannitol-Iduronide
I/V (nmol/min/mg)
5
10
15
20
25
30
-2.0
0
2.0
4.0
6.0
8.0
I/S (mM)

TABLE 16

K_m AND V_{max} VALUES OBTAINED FOR PURIFIED LOW AND HIGH UPTAKE FORMS OF HUMAN α-L-IDURONIDASE USING THREE DIFFERENT SUBSTRATES[a]

Enzyme	Substrate	K_m	V_{max}
		mM	μmoles/mg/min
Low Uptake	4MU α-Id	0.07	1615
	Phenyl α-Id	1.42	83
	anhydro[^{3}H]man	0.86	250
High Uptake	4MU α-Id	0.06	1485
	Phenyl α-Id	1.66	105
	anhydro[^{3}H]man	1.04	279

[a] Experiments were performed on post-Biogel P-100 samples of each enzyme form.

TABLE 17

INHIBITION OF LOW AND HIGH UPTAKE FORMS OF HUMAN α-L-IDURONIDASE BY GLYCOSAMINOGLYCANS[a]

GAG	Low Uptake	High Uptake
C4S	0.51	2.89
C6S	0.55	3.15
DS	0.19	4.50
HA	0.13	5.00
HP	0.09	0.13
HS	0.75	3.30
KS	0.45	2.25

[a] K_i values are expressed in mg/ml and determined from Dixon plots as described in the text. All enzyme assays were performed using 4MU α-Id as described.

Figure 17. Inhibition of Low and High Uptake Forms of Human α-L-Iduronidase by Dermatan Sulfate and Heparan Sulfate.

K_i determinations for dermatan sulfate (Panel A) and heparan sulfate (Panel B) were made from the 1/V vs [I] plots (Dixon plots) of the low uptake (SA 105,000 U/mg Lowry) and high uptake (SA 91,000 U/mg Lowry) forms of human α-L-iduronidase assuming non-competitive inhibition. 4MU α-Id assays were performed as described in the Methods section using 100 μM substrate concentrations.

FIGURE 17

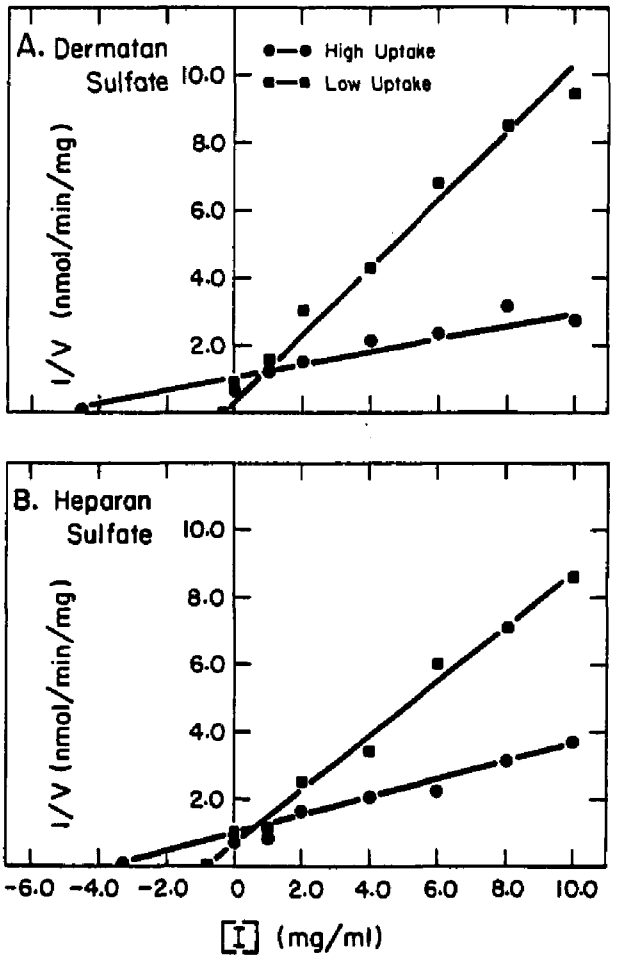
A. Dermatan Sulfate
High Uptake
Low Uptake
1/V (nmol/min/mg)
10.0
8.0
6.0
4.0
2.0
B. Heparan Sulfate
1/V (nmol/min/mg)
10.0
8.0
6.0
4.0
2.0
-6.0 -4.0 -2.0 0 2.0 4.0 6.0 8.0 10.0
[I] (mg/ml)

13. pH Optima and Thermal Stability:

pH optimization studies were performed for both enzymes using the three substrates discussed above (Fig. 18). In addition, the effects of two different buffers, sodium formate and citrate phosphate, on the pH optima were evaluated. Using sodium formate buffer, the pH optima for the low uptake enzyme were 3.55, 3.50 and 4.50 when using the 4MU α-Id, phenyl α-Id and anhydro[^{3}H]man substrates, respectively, and 3.50, 3.50 and 4.25 for the high uptake enzyme. For both enzyme forms, the use of citrate phosphate buffers shifted the optima approximately 0.50 pH units higher (data not shown).

Table 18 summarizes the thermal stabilities of the two enzyme forms at 45°C, 52°C and 60°C; the patterns obtained for each form were similar.

14. Effect of Protein:

Table 19 demonstrates that the post-Biogel P-100 purified low and high uptake forms of α-L-iduronidase (SA ∿ 90,000 U/mg Lowry) were not stable at 37°C for 1 h unless additional protein, in this case BSA, was added to the enzyme samples. These data also demonstrate that final protein concentrations of 0.1 mg/ml (Lowry) in the assay were suitable for stabilizing the 4MU α-Id activity; higher amounts of protein did not substantially increase the enzyme stability.

15. Amino Acid Composition Analyses:

Table 20 summarizes the amino acid composition data obtained for the post-HPLC forms of the enzyme. Protein peaks obtained after HPLC which had similar specific activities were pooled, and the amino

Figure 18. pH Profiles of Low and High Uptake Forms of Human α-L-Iduronidase Using Three Different Substrates.

Enzymatic activity of the low uptake (SA 105,000 U/mg Lowry; ■—■) and high uptake (SA 91,000 U/mg Lowry; ●—●) forms of human α-L-iduronidase was performed as described in the Methods section for each of the three indicated substrates. pH adjustments were made in 0.4 M sodium formate buffers.

FIGURE 18

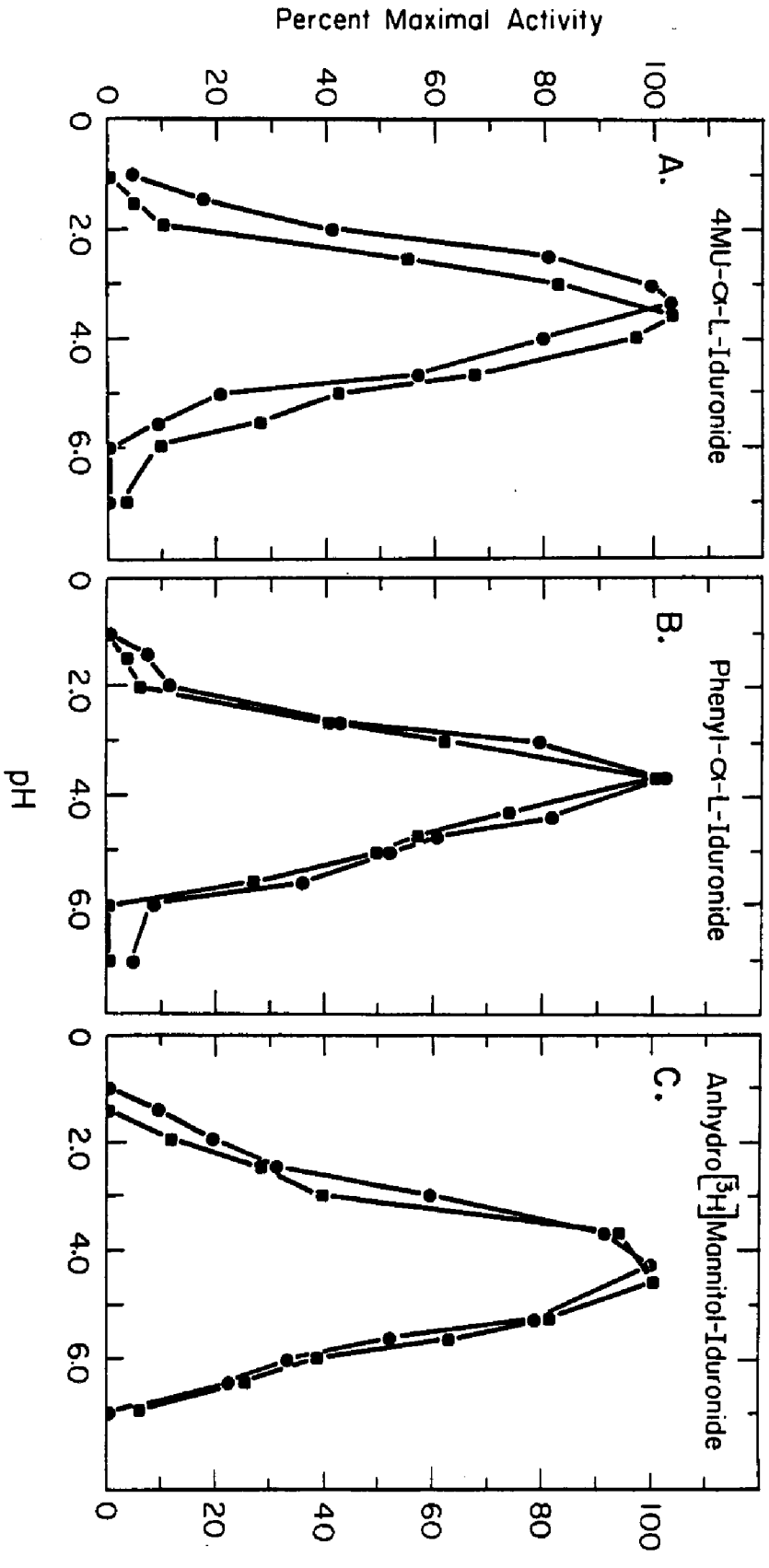
Percent Maximal Activity
0
20
40
60
80
100
A.
4MU-α-L-Iduronide
B.
Phenyl-α-L-Iduronide
C.
Anhydro[3H]Mannitol-Iduronide
pH
0
2.0
4.0
6.0

TABLE 18

THERMAL STABILITIES OF LOW AND HIGH UPTAKE FORMS OF HUMAN α-L-IDURONIDASE[a]

Temperature	Low Uptake	High Uptake
°C	$T_{1/2}$ (min)	$T_{1/2}$ (min)
45	34.5	42.5
52	23.0	25.0
60	11.0	12.5

[a] Protein concentrations were kept constant at 1 mg/ml in all assays by the addition of BSA.

TABLE 19

EFFECT OF PROTEIN ON LOW AND HIGH UPTAKE FORMS OF HUMAN α-L-IDURONIDASE

Protein Concentration[a]	Enzyme Activity[b]	
	High Uptake	Low Uptake
mg/ml	U/ml	U/ml
0.010	510	440
0.025	650	560
0.050	710	675
0.100	985	995
0.250	992	1010
0.500	1000	1008

[a] Final protein concentrations in the assay mixtures were adjusted with BSA and checked using the fluorescamine assay.

[b] Enzyme assayed with 50 μM 4MU α-Id for 1 h at 37°C as described in the Methods section.

TABLE 20

AMINO ACID COMPOSITION OF LOW AND HIGH UPTAKE FORMS OF HUMAN α-L-IDURONIDASE

Amino Acid	Residues/Molecule[a] Low Uptake	Residues/Molecule[b] High Uptake
ASX	56	55
GLX	54	66
Leucine	45	54
Serine	42	44
Glycine	35	50
Threonine	33	35
Alanine	36	47
Valine	35	32
Tyrosine	19	18
Proline	36	45
Phenylalanine	27	24
Isoleucine	19	21
Arginine	20	42
Lysine	22	25
Histidine	13	20
Methionine	7	9
1/2 Cystine	11	13
Tryptophan	15	17

[a] Based on a molecular weight of 72,000.

[b] Based on a molecular weight of 90,000.

acid composition was subsequently determined. The high uptake enzyme had significantly more glycine and arginine and, to a lesser extent, glutamate/glutamine, leucine, proline, alanine and histidine were also elevated. The data represents the average results obtained from the analysis of two independent preparations of each enzyme fraction.

16. Immunologic Findings:

Antibodies were raised in New Zealand white rabbits against the post-Biogel P-100 purified low uptake enzyme (SA ∿ 105,000 U/mg Lowry). Although efforts were made to perform all immunizations with active enzyme, due to the inherent instability of the purified protein a small percentage of the antigen was inactive. Figure 19 illustrates the immunotitration profiles for the low and high uptake post-Con A enzymes using ammonium sulfate concentrated antisera; note that the titer (final dilution of antisera which precipitated 50% of the initial activity) of this antisera with the high uptake enzyme was slightly lower than with the low uptake form. The Ochterlony immunodiffusion gel which is inserted in this figure demonstrates that the post-hydroxyapatite preparations of the low and high uptake enzyme (SA ∿ 18,000 U/mg Lowry) reacted equally well with the rabbit antisera under these conditions and each shows a single, visible precipitan bands. After Ochterlony immunodiffusion analysis of crude lung homogenates, the visible precipitan band also reacted when stained with the α-L-iduronidase specific substrate, 4MU α-Id, further indicating that the antibodies were recognizing this enzyme (photograph not shown).

Figure 19. Immunoprecipitation of Low and High Uptake Forms of Human α-L-Iduronidase by Rabbit Anti-Human Antibodies.

Enzymatic activity determinations and the procedures used for the preparation of the rabbit anti-low uptake α-L-iduronidase human antibodies are described in the Methods section. For the immunoprecipitation experiments, the initial amount of enzyme activity was 1000 U for both the low and high uptake forms. For the inserted Ochterlony immunodiffusion gel, 1500 U each of low uptake (I_1) and high uptake (I_2) enzyme were used; (S) represents saline control wells.

FIGURE 19

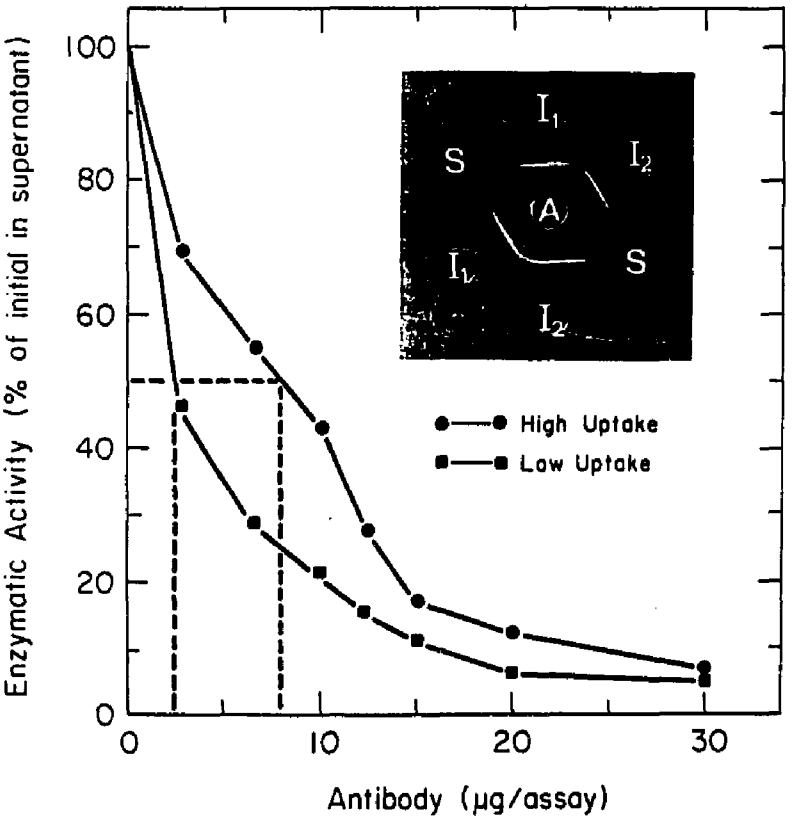
Enzymatic Activity (% of initial in supernatant)
100
80
60
40
20
0
0
10
20
30
Antibody (µg/assay)
I1
S
I2
(A)
I1
S
I2
High Uptake
Low Uptake

C. Comparative Gene Mapping of Human and Feline α-L-Iduronidase:

1. Immunodiscrimination of Human and Murine α-L-Iduronidase:

Figure 20 shows an Ochterlony double immunodiffusion gel which demonstrated that the rabbit anti-human antibody, raised against purified low uptake human α-L-iduronidase, was not species specific, but cross-reacted with the enzyme from various sources. The precipitan bands shown in this Ochterloney gel also stained for α-L-iduronidase activity (photograph not shown). Therefore, immunoprecipitation and electrophoretic conditions that would discriminate the human and feline enzymes from their rodent counterparts were investigated. Figure 21 illustrates that when 75 units (picomoles 4MU/h/ml) of α-L-iduronidase activity was incubated with 2 µl of the ammonium sulfate concentrated antisera, less than 2% of the mouse enzyme was recovered in the immunoprecipitate. In contrast, over 60% of the human enzymatic activity was detected. Interestingly, both the mouse and human enzymes were depleted from the supernatant to an equal extent (data not shown). Mixing experiments were conducted to determine the reliability of the immunologic discrimination assay. Figure 22 illustrates that when the total activity in the assay was kept constant at 75 U and the amount of human enzyme varied from zero to 100 percent, the activity detected in the immunoprecipitate was directly proportional to the amount of human enzyme present in the mixture.

2. Chromosomal Assignment of the Structural Gene for Human α-L-Iduronidase:

The immunoprecipitation assay detailed above was used to discriminate mouse and human α-L-iduronidase activities in 14 mouse(RAG)-

Figure 20. Immunologic Cross-reactivity of Rabbit Anti-Human Antibodies with α-L-Iduronidase from Different Sources.

The procedures used for the preparation of the rabbit anti-low uptake human α-L-iduronidase antibodies are described in the Methods section; 1500 U (picomoles 4MU/h/ml) of each enzyme source was used. Human fibroblasts (H), Chinese hamster fibroblasts (CH), mouse RAG cells (M) and feline lymphoblasts (F); (S) represents saline controls.

FIGURE 20

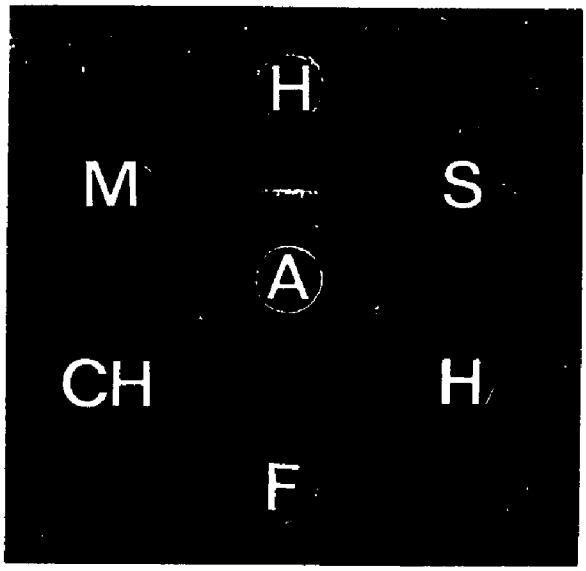

Figure 21. Immunodiscrimination Assay of Human and Mouse α-L-Iduronidase Activities.

The procedure used for the immunodiscrimination assay of α-L-iduronidase extracted from human fibroblasts and mouse RAG cells is described in the Methods section. ---- represents 75 picomole 4MU/h/assay, the point of optimal discrimination.

FIGURE 21

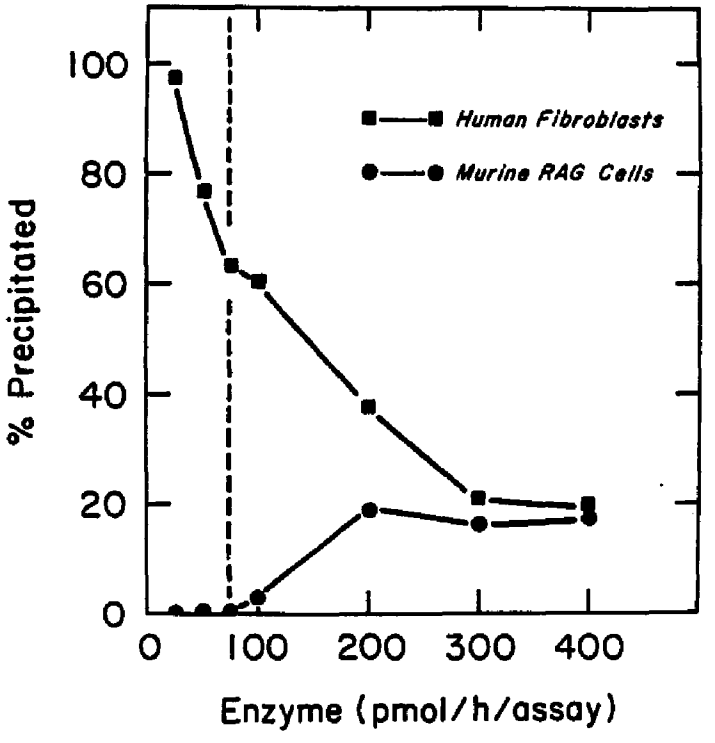
100
80
60
40
20
0
% Precipitated
Human Fibroblasts
Murine RAG Cells
0
100
200
300
400
Enzyme (pmol/h/assay)

Figure 22. Artificial Mixing and Immunoprecipitation of Human and Mouse α-L-Iduronidase Activities.

Artificial mixtures of α-L-iduronidase activity were made using enzyme extracted from human fibroblasts and mouse RAG cells; the total amount of enzyme present in each mixture was kept constant at 75 picomoles 4MU/h/ml. Immunoprecipitation using rabbit anti-human antibodies and subsequent determinations of enzymatic activity were performed as described in the Methods section.

FIGURE 22

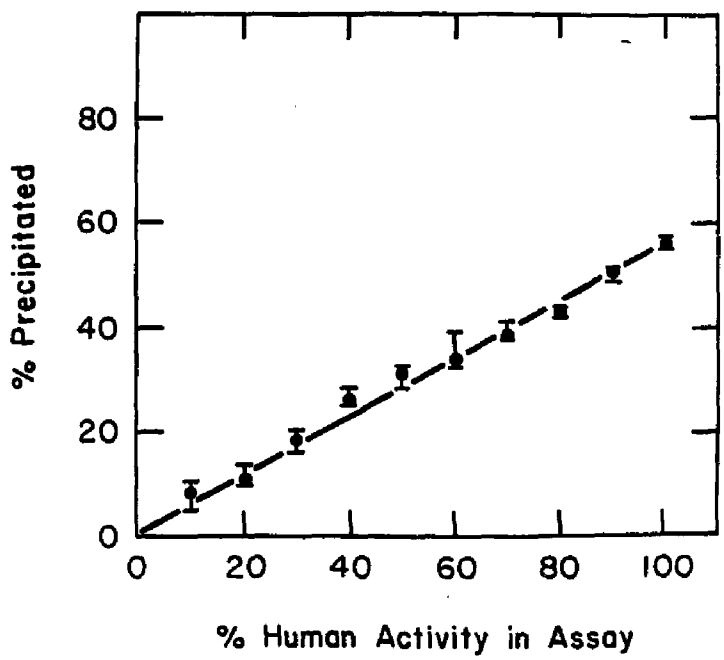
% Precipitated
0
20
40
60
80
0
20
40
60
80
100
% Human Activity in Assay

human fibroblast somatic cell hybrids (Table 21). Based on the percent discordancy, these data indicated that the structural gene for human α-L-iduronidase was on either chromosome 21, or more likely, chromosome 22.

Since hybrid clone R-G-21 contained both chromosomes 21 and 22 and only three other human autosomes, it was selected for further subcloning. Of the secondary R-G-21 hybrids, subclones K and J were positive for human α-L-iduronidase but did not have chromosome 21, thereby localizing the structural gene to human chromosome 22 (Table 22). Further support for these data was obtained when hybrid R-G-21J, which contained four human chromosomes, was subcloned further and nine tertiary hybrids were examined. Of these, two, J-40 and J-46, had only human chromosome 22 and were positive for human α-L-iduronidase activity.

Figure 23 shows a metaphase chromosome spread of tertiary hybrid J-15, which was banded with Trypsin-Giemsa stain; note the presence of only the two indicated human chromosome 22's. The absence of other human chromosomes or human-mouse rearrangements was confirmed by subsequent G-11 staining (data not shown).

Figure 24 illustrates that the level of human α-L-iduronidase activity was correlated with the average number of human chromosome 22's per cell in the tertiary subclones derived from R-G-21. Note that R-G-21J-15, which contained an average of 1.7 chromosome 22's per cell and only one other human chromosome, Y, expressed human α-L-iduronidase at a level approximately 30% of that in normal diploid fibroblasts. From these data it was determined that, on the average, at least one chromosome 22 must be present per cell for the immunoprecipitation assay to significantly detect the presence of human α-L-iduronidase.

TABLE 21

SEGREGATION ANALYSIS OF HUMAN α-L-IDURONIDASE AND HUMAN CHROMOSOMES IN 14 MOUSE-HUMAN SOMATIC CELL HYBRIDS

Human Chromosome	Concordant		Discordant		Percent Discordant
	+/+	-/-	+/-	-/+	
1	9	1	2	2	28.6
2	1	2	1	10	78.6
3	9	1	2	2	28.6
4	6	1	2	5	50.0
5	7	0	3	4	50.0
6	6	0	3	5	57.2
7	7	1	2	4	42.8
8	7	1	2	4	42.8
9	1	3	0	10	71.4
10	3	1	2	1	21.4
11	3	1	2	8	71.4
12	5	2	1	6	50.0
13	4	2	1	7	57.1
14	7	1	2	4	42.8
15	8	0	3	3	42.8
16	3	0	3	8	78.6
17	4	3	0	7	50.0
18	6	2	1	5	42.8
19	4	3	0	7	50.0
20	2	2	1	9	71.4
21	11	1	2	0	14.2
22	11	3	0	0	0.0

TABLE 22

SEGREGATION ANALYSIS OF HUMAN α-L-IDURONIDASE AND HUMAN CHROMOSOMES IN SUBCLONES OF MOUSE-HUMAN SOMATIC CELL HYBRIDS

Hybrid Clone	Human Chromosomes							Human α-L-Iduronidase
	1	3	9	21	22	X	Y	
Primary:								
R-G21	+	+	+	+	+	+	+	+
Secondary:								
R-G21-A	+	+	+	+	+	+	+	+
-H	+	+	-	+	+	+	+	+
-K	+	-	+	-	+	-	+	+
-J	-	+	-	-	+	+	+	+
Tertiary:								
R-G21-J-29	-	-	-	-	-	+	-	-
-36	-	-	-	-	-	-	-	-
-13	-	-	-	-	+	-	+	+
-50	-	+	-	-	+	-	-	+
-14	-	+	-	-	+	-	+	+
-27	-	-	-	-	+	-	+	+
-15	-	-	-	-	+	-	+	+
-40	-	-	-	-	+	-	-	+
-46	-	-	-	-	+	-	-	+

Figure 23. Metaphase Chromosome Spread of Mouse-Human Hybrid R-G-21-J15 Stained with Trypsin-Giemsa.

Procedures used for the preparation and staining of chromosomes in this metaphase are described in the Methods section. Arrows indicate human chromosome 22s.

FIGURE 23

Figure 24. Human α-L-Iduronidase Activities in Mouse-Human Somatic Cell Hybrids with Varying Chromosome 22 Content.

Procedures used for the immunologic determination of human α-L-iduronidase activity and the cytologic identification of human chromosome 22 are described in the Methods section. For determination of the chromosome constitution of each tertiary hybrid cell line at least 75 metaphase spreads were examined.

FIGURE 24

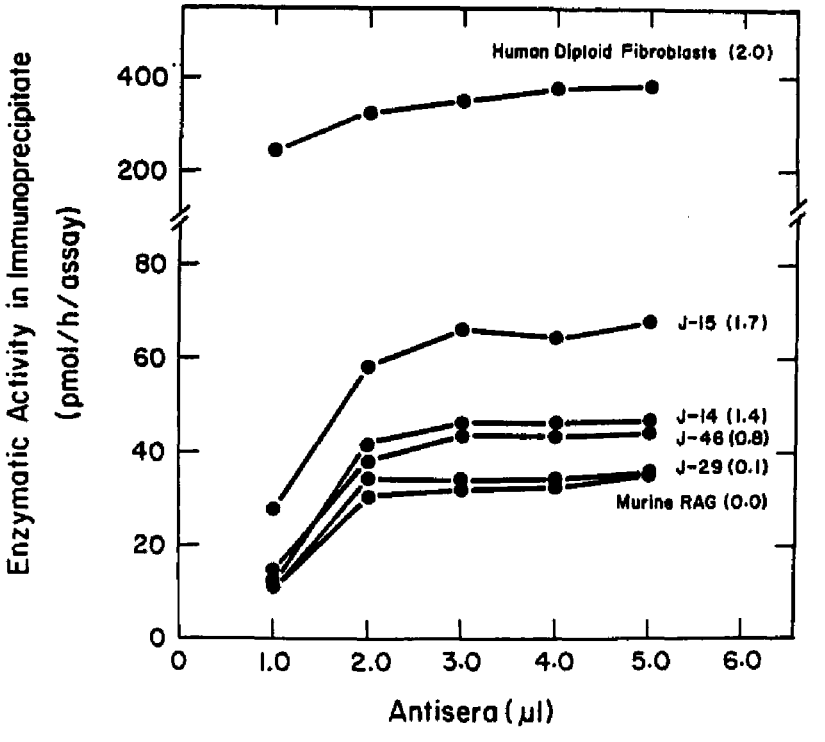
Enzymatic Activity in Immunoprecipitate
(pmol/h/assay)
Human Diploid Fibroblasts (2.0)
J-15 (1.7)
J-14 (1.4)
J-46 (0.8)
J-29 (0.1)
Murine RAG (0.0)
400
200
80
60
40
20
0
0
1.0
2.0
3.0
4.0
5.0
6.0
Antisera (µl)

Figure 25 (right) illustrates the expression of the total α-L-iduronidase specific activity in human fibroblasts, mouse RAG cells, and human-mouse somatic cell hybrid R-G-21J-15 as a function of days in culture. For this experiment cells were initially plated to the same cell density in 75 mm^2 flasks and allowed to grow under normal conditions (detailed in the Methods section); Figure 25 (left) shows the growth curves obtained for each line. Note that the variation of the enzyme levels in the hybrid cell resembled that observed in the mouse parental line throughout the experiment.

3. Regional Gene Assignment for Human α-L-Iduronidase:

In an attempt to regionally assign the human α-L-iduronidase structural gene, cell lines, some trisomic and others monosomic for regions of chromosome 22, were obtained from the Human Genetic Mutant Cell Repository. Although the specific activity of the control enzyme, β-hexosaminidase, was similar in these and the control fibroblast lines, the α-L-iduronidase levels were consistent with that expected from a gene dosage effect (Table 23). Note that the average ratio of α-L-iduronidase, IDA, in the trisomic lines to those of the controls was 1.63, while in the monosomic lines this ratio was 0.60. Comparative enzyme assays for each cell line were performed on cultures which were harvested at or near the same cell density. Based on these data the structural gene for human α-L-iduronidase was preliminarily localized to the region 22pter → 22q11 (Figure 26).

Figure 25. α-L-Iduronidase Enzyme Levels As A Function of Cell Growth in Human Fibroblasts, Mouse RAG Cells and A Mouse-Human Somatic Cell Hybrid.

Cells were initially plated to a density of 0.2-0.5 x 10^5 cells/75 mm^2 flask (left panel) and allowed to grow under standard conditions described in the Methods section. At the indicated times, the cells were harvested by trypsinization, washed twice with PBS and aliquots were removed for cell counting (left panel) and enzyme determinations (right panel).

FIGURE 25

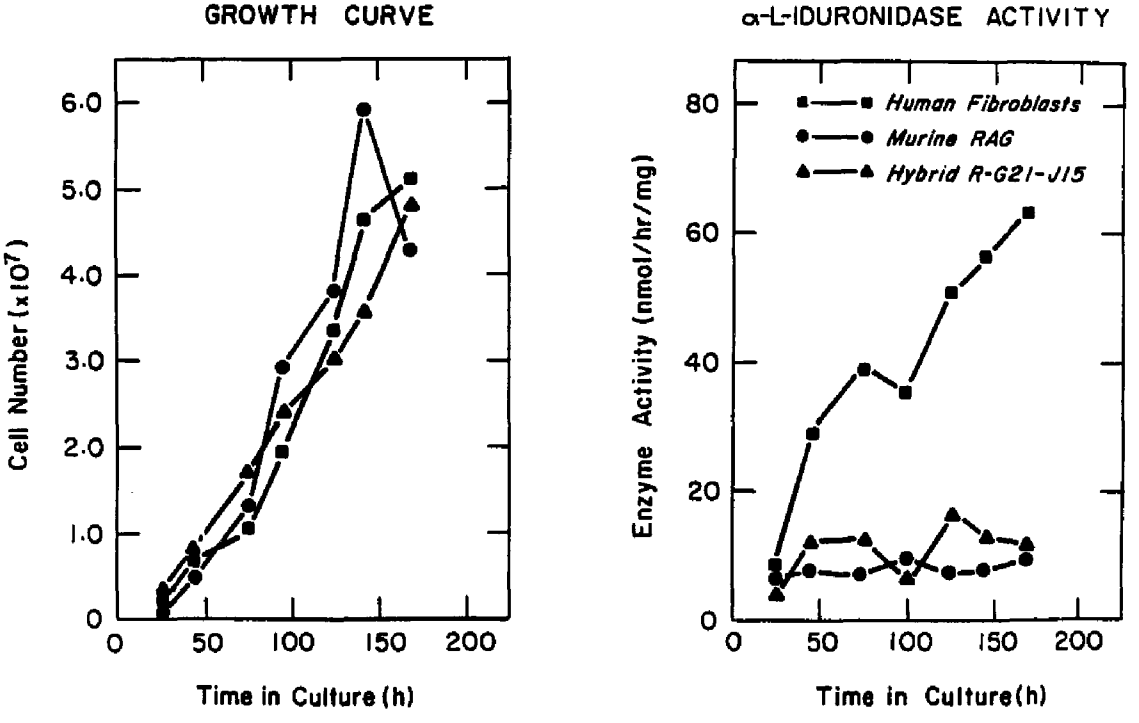
GROWTH CURVE
Cell Number (x10⁷)
6.0
5.0
4.0
3.0
2.0
1.0
0
0
50
100
150
200
Time in Culture (h)
α-L-IDURONIDASE ACTIVITY
Enzyme Activity (nmol/hr/mg)
80
60
40
20
0
Human Fibroblasts
Murine RAG
Hybrid R-G21-J15
Time in Culture(h)

TABLE 23

α-L-IDURONIDASE ACTIVITIES IN HUMAN CELL LINES
CONTAINING STRUCUTRAL REARRANGEMENTS OF CHROMOSOME 22

Cell Line	α-L-Id-uronidase	β-Hexos-aminidase	IDA[a]
			Mean Diploid IDA
	(nmol/h/mg)	(μmol/h/mg)	
Partial Trisomy 22 (22pter → 22q11)	92.8	23.6	1.63
Partial Monosomy 22 (22pter → 22q11)	34.3	19.9	0.60
Normal Diploid Fibroblasts Mean (n=4)	56.8	21.5	1.00

[a] IDA; α-L-Iduronidase. The data represents the average results obtained from six trisomic and two monosomic cell lines which have been subjected to the analyses detailed in the Methods section.

Figure 26. Regional Assignment of the Human α-L-Iduronidase Gene on Chromosome 22.

Schematic illustration of the regional chromosomal assignment of the structural gene for human α-L-iduronidase. This assignment was based on experiments detailed in the text. α-L-Iduronidase; IDA.

FIGURE 26

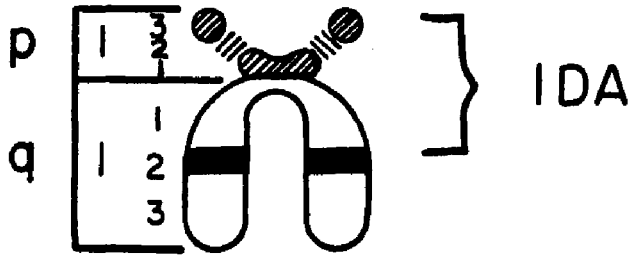

22 pter ⟶ q11

4. Electrophoretic Separation of α-L-Iduronidase Isozymes and Chromosomal Assignment of the Feline Structural Gene:

Additional confirmation for the assignment of the human gene for α-L-iduronidase to chromosome 22 was obtained by electrophoretic separation of the human and rodent enzymes. Figure 27 illustrates that when α-L-iduronidase from human, mouse and Chinese hamster parental lines was electrophoresed on cellulose acetate gels using 10 mM Tris/HCl buffer at pH 7.1, the gel sliced into 1.8 cm strips and the enzymatic activity eluted and assayed, the human and mouse enzymes co-migrated whereas the Chinese hamster activity was more electropositive. Furthermore, note that the feline enzyme was also electrophoretically separated from the Chinese hamster activity. Human-Chinese hamster hybrids positive and negative for human chromosome 22 were analysed for the presence of human α-L-iduronidase using this electrophoretic technique; the results of these studies further confirmed this gene assignment to human chromosome 22 (data not shown).

Using the electrophoretic method, the feline α-L-iduronidase structural gene has also been mapped. Thirteen feline-Chinese hamster somatic cell hybrids were analyzed for the presence of the feline enzyme. The segregation of feline α-L-iduronidase and each feline chromosome is shown in Table 24. Based on the percent discordancy, these data indicated that the structural gene for feline α-L-iduronidase was localized to feline chromosome D4 (Figure 28).

Figure 27. Electrophoretic Separation of Human, Feline and Rodent α-L-Iduronidase on Cellulose Acetate.

The procedure used for the electrophoresis of α-L-iduronidase on cellulose acetate gels and the determination of enzymatic activity are described in the Methods section. The cellulose acetate gel on the right has been stained with 100 μM 4MU α-Id as described for the isoelectrofocusing studies. The enzyme sources were: feline lymphoblasts (Lane A), Chinese hamster fibroblasts (Lane B) and Chinese hamster lymphoblasts (Lane C).

FIGURE 27

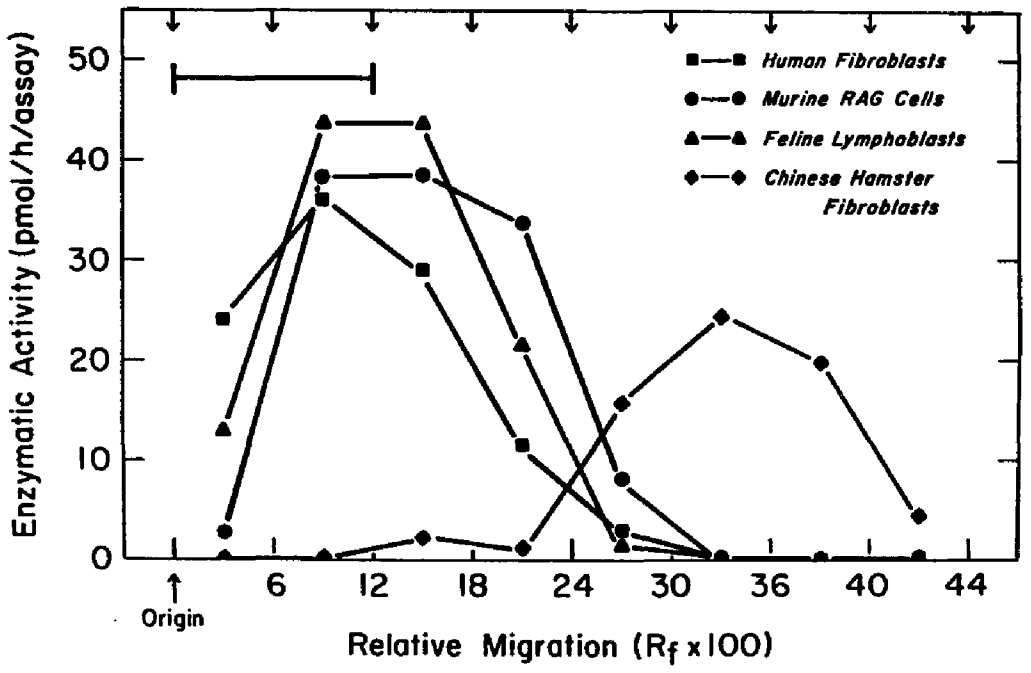
Enzymatic Activity (pmol/h/assay)
50
40
30
20
10
0
Origin
6
12
18
24
30
36
40
44
Relative Migration (R_f x100)
Human Fibroblasts
Murine RAG Cells
Feline Lymphoblasts
Chinese Hamster Fibroblasts

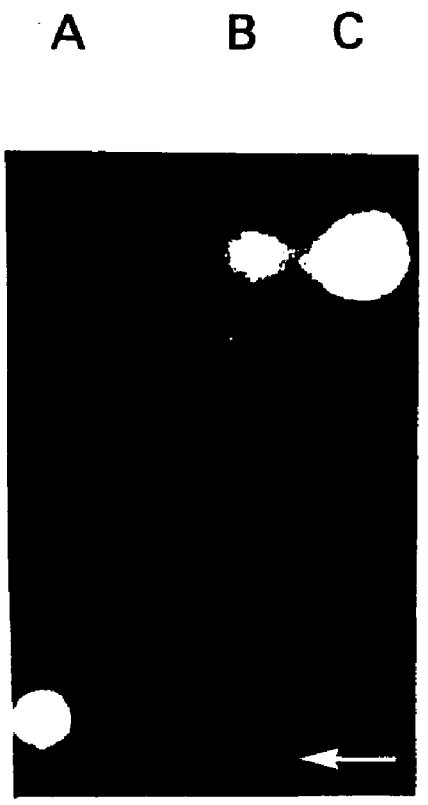
A
B
C

TABLE 24

SEGREGATION ANALYSIS OF FELINE α-L-IDURONIDASE AND FELINE CHROMOSOMES IN 13 HAMSTER-FELINE SOMATIC CELL HYBRIDS

Feline Chromosome	Concordant		Discordant		Percent Discordant
	+/+	-/-	+/-	-/+	
A1	1	4	7	1	61.5
A2	6	4	2	1	23.0
A3	4	2	4	3	53.8
B1	3	3	5	1	50.0
B2	3	4	5	0	41.8
B3	8	2	0	3	23.0
B4	4	2	4	3	53.8
C1	2	5	6	0	46.2
C2	5	2	3	3	46.2
D1	4	5	4	0	30.8
D2	1	5	7	0	53.8
D3	3	5	5	0	38.5
E1	0	5	8	0	61.5
E2	0	5	8	0	61.5
E3	1	3	7	1	66.8
F1	0	5	8	0	61.5
F2	3	4	5	1	46.2
X	8	2	0	3	23.0
D4	7	5	1	0	7.7

Figure 28. Comparative Gene Assignments for the Human and Feline α-L-Iduronidase Structural Genes.

Schematic summary of the comparative chromosomal assignments of the structural genes for human and feline α-L-iduronidase. α-L-Iduronidase (IDA); inorganic pyrophosphatase (PP); hexokinase (HK).

FIGURE 28

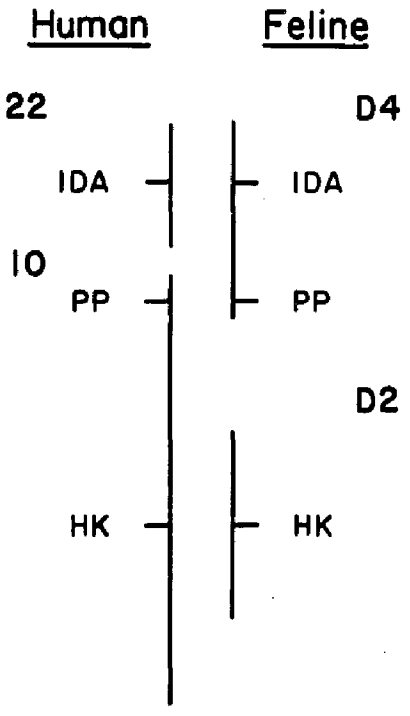

DISCUSSION

A. Glycosaminoglycan Analyses:

The analysis of GAGs in biologic materials has been markedly facilitated by the application of electrophoretic techniques. Since most of these methods do not completely resolve all of the major GAGs, electrophoresis in several different systems has been required to confirm the identification of the individual components of complex mixtures. Recently, a discontinuous electrophoretic method has been developed which permits the separation of all the mammalian GAGs in a monodimensional run (19). However, the two ethanol precipitation steps required to achieve complete separation of the GAGs in this system caused decreased and variable recoveries of individual GAGs when applied to the electrophoretic system described within this thesis (Table 8). In addition, this discontinuous method required a specially designed electrophoretic apparatus. Thus, the major advantages of the newly developed system were 1) the separation of six major GAGs in a single, continuous, monodimensional run, 2) the improved recovery allowing for more reliable quantitation of the individual GAGs, and 3) the use of commercially available equipment. In addition, the pattern of GAG separation was different in this system than those of previously reported electrophoretic methods, thereby providing a useful adjunct for the identification of GAGs in biological samples.

Sample application was extremely important for achieving optimal GAG resolution in the electrophoretic runs. Use of the Beckman microzone cellogel apparatus permitted sample application in narrow, 0.75 cm bands. Even so slight diffusion, presumably due to the heterogeneity

of the available standards, was observed after electrophoresis. The six GAGs may also be separated using the larger Chemitron electrophoretic tank and applicator. However, use of this equipment reduced the resolution. Recently, Cappelletti and co-workers achieved sharp bands by pre-equilibrating part of the gel in distilled water (19). Attempts to apply this technique in the system reported here resulted in reduced GAG separation.

It was noted that different preparations of chondroitin sulfate migrated to different locations; an observation which is possibly due to the various amounts of heterogeneous components present in the samples (11) which may effect the migration pattern. Most GAG preparations, especially C6S, C4S, HS and HP, are heterogeneous with respect to the proportion of sulfated uronic acid moieties. This variation is dependent on both the species and tissue from which the individual GAGs are isolated. Therefore, since the degree of sulfation may alter the linear charge density and subsequent ionic binding, the same GAG obtained from various sources may have slightly different electrophoretic mobilites. For example, a C6S sample (75% pure from river sturgeon cranial cartilage) migrated near HS but could not be consistently resolved from C4S. However, a different C6S preparation (from shark cartilage) co-migrated with HS and was readily distinguished from C4S (data not shown). The C4S standards used in these experiments included a 90% pure sample isolated from river sturgeon notochord and a commercial preparation from whale cartilage; both standards co-migrated in this system. It should also be noted that only highly purified GAG preparations should be used as standards to insure band sharpness and increased resolution, thereby enhancing the reliability of GAG identification in biologic samples.

Finally, it is important to realize that due to their complex structure the complete analysis of GAGs in biologic tissues requires a variety of electrophoretic, enzymatic and chemical techniques. Since the identification of individual GAGs by co-migration with reference standards in a single electrophoretic system has been considered inadequate (17), it is imperative that a variety of different separation procedures be cooperatively employed.

The preliminary data obtained upon examination of the stored GAGs in a variety of tissues and fluids of human and feline MPS I individuals emphasizes the value of this new analytical method. As expected, most of the samples examined from the human MPS I-H individuals showed substantial accumulation of both dermatan sulfate and heparan sulfate, the two predominant GAGs which are physiologic substrates for α-L-iduronidase (13). Surprisingly, the kidney specimen from one MPS I-H individual did not show substantial accumulation of either substrate, although excessive GAGs were excreted in the urine of this same patient (Table 9). Interestingly, the liver from a different MPS I-H homozygote stored only dermatan sulfate (Fig. 5); a number of speculative interpretations may be offered to account for these findings. Both dermatan sulfate and heparan sulfate contain uronic acid moieties and are potent inhibitors of human α-L-iduronidase activity (Fig. 17), however, it is possible that the mutant α-L-iduronidase(s) present in these (and/or other) MPS I individual(s) retains differential residual catalytic activity towards one GAG, but not another. Furthermore, it is also possible that differentiated cells (i.e., hepatocytes) possess alternative GAG-specific catabolic pathways which may bypass the necessity for normal α-L-iduronidase activity. Further support for these hypotheses requires addition-

al analyses of specimens from a number of different MPS I-H individuals and a comprehensive survey of the stored GAGs in other tissues of these same patients.

The preliminary data obtained with the feline MPS I homozygote further emphasizes the need to investigate the substrate specificity of the feline, as well as human, α-L-iduronidase enzymes. In each of the tissues examined dermatan sulfate, but not heparan sulfate, could be shown to accumulate; however, analysis of the urine sample revealed that small amounts of heparan sulfate may be excreted. It is also intriguing to note that heparin, an iduronic acid containing GAG which is the most potent inhibitor of human α-L-iduronidase activity (Table 17), did not accumulate in any of the tissues or fluids of human or feline MPS I homozygotes; perhaps additional degradative pathways exist for this essential metabolite. Finally, this new analytical tool may now be employed to precisely characterize, for the first time, the stored GAGs in visceral and neuronal tissues from MPS I-S (Scheie) and MPS I-H/S (Hurler/Scheie) individuals in an attempt to biochemically decipher the dramatic phenotypic variations observed within the α-L-iduronidase deficiency diseases.

B. Purification and Characterization of Low and High Uptake Forms of Human α-L-Iduronidase:

α-L-iduronidase has served as a prototypic model for studies of lysosomal enzyme processing and transport. In 1971, Barton and Neufeld reported the first purification of the "Hurler corrective factor" from normal human urine (53). This purification was monitored by measuring the ability of the "factor" to degrade accumulated $^{35}[SO_4]$ glycosamino-

glycans in cultured Hurler fibroblasts; on the basis of this assay the "factor" (high uptake form) was enriched 100-fold (approximately 10% pure) in the final preparation. Some intriguing observations were generated by this early work. At high salt concentrations (0.5 M NaCl) the enzymes apparent molecular weight as determined by gel filtration was estimated at 87,000; however, at low salt concentrations (0.1 M NaCl) it tended to aggregate and become inactive. In addition, the corrective activity could be resolved into two peaks by hydroxyapatite chromatography. On the basis of binding to the cation exchange resin, carboxymethylcellulose, and polyacrylamide gel electrophoresis the isoelectric point was estimated to lie between pH 4.5 and 6.3.

Later, in 1976, with the availability of the phenyl-α-L-iduronide substrate Rome et al. (54) undertook the purification of human kidney α-L-iduronidase. Their final preparations were judged to be ∿ 70% pure on the basis of polyacrylamide gel electrophoretic studies. Fifty percent of the initial enzyme activity was never solubilized from the membranes in these preparations and therefore very limited yields (∿150 to 200 μg purified protein) were obtained. The partially purified enzyme was postulated to be a dimer with a native molecular weight of 60,000 ± 6,500 and a subunit molecular weight of 31,000 ± 6,500. All of the purified enzyme was of the low uptake, non-corrective form.

In this thesis, a novel purification procedure for the isolation of α-L-iduronidase from a human tissue is described. Lung was chosen as the enzyme source because it had more than four times the starting activity of other tissues tested (other than cultured skin fibroblasts), was available in large quantities and a majority of the contaminating protein was hemoglobin, which could be easily separated from the enzyme

by Con A-Sepharose chromatography. The initial conditions that were established for the tissue homogenization were optimized for the coisolation of another connective tissue enzyme, proline hydroxylase (126). However, the use of an alkaline homogenization buffer, pH 7.3, did not destabilize the α-L-iduronidase activity in the early stages of the purification. In addition, the use of the non-ionic detergent, nonidet P-40, afforded greater than 90% recovery of the total α-L-iduronidase activity from the membranes.

Initial experiments were designed to test the behavior of the solubilized enzyme on the anion exchange resin, DEAE-cellulose. It was observed that the total activity which bound to the column at pH 7.3 could be resolved into two major peaks, one which eluted at ∿ 0.075 M NaCl and another that eluted at ∿ 0.32 M NaCl when linear salt gradients were established. It must be noted that, after homogenization, the pH of the supernatant was reduced to ∿ 6.50, presumably due to the release of endogenous acids; if the pH was readjusted to 7.3 prior to applying the samples to the DEAE-cellulose, the respective fractions eluted at ∿ 0.18 M and ∿ 0.45 M NaCl. Preliminary studies indicated that the enzyme from both fractions quantitatively bound Con A-Sepharose and had molecular weights below 100,000. Isoelectric focusing studies using crude homogenates and the fluorimetric 4MU α-Id substrate to visualize the enzyme revealed that the total activity ran as a broad band with a pI range of 5.85-7.35; two major peaks of activity were detected and other minor bands could be visualized. This was the first indication that, using the presently described homogenization procedure, multiple forms of α-L-iduronidase activity might be present in human lung.

For the purpose of the large scale purification (typically with

8-10 kg wet weight of tissue) a gradient elution from the DEAE-cellulose could not be practically employed; therefore, the homogenizations were done in the presence of 0.1 M NaCl. The low uptake, less electronegative α-L-iduronidase fraction (∿ 80% of the total initial activity) was recovered in the column flow-through and wash while the high uptake enzyme fraction (∿ 20% of the total initial activity) was batch eluted using buffer containing 0.6 M NaCl.

The α-L-iduronidase activity which was present in the 0.1 M NaCl eluant co-eluted with hemoglobin from the DEAE-cellulose column. In addition, a small amount of hemoglobin was also found in the high salt eluant and therefore the next step in the purification was Con A-Sepharose, which readily separated this ubiquitous protein from α-L-iduronidase. This step resulted in a large purification of the low uptake enzyme (∿ 350-fold) and a smaller, yet significant, purification of the high uptake enzyme (∿ 25-fold). The specific activities of the two fractions at this stage in the enzyme purification were similar. Hydroxyapatite chromatography was performed essentially as described by Rome et al. (54). A slight amount of enzyme trailing was observed with this column and maximal purity was achieved by collecting only the peak fractions. Both forms of the enzyme became increasingly unstable after this step and a variety of techniques were evaluated for optimizing the stability. Addition of 0.1 M D(+)mannose to the preparations, together with the high salt environment (100 mM NaPi, 0.5 M NaCl) substantially increased the stability. In addition, at this stage it was advantageous to change the buffer to citrate phosphate, pH 4.0; these conditions were maintained throughout the remainder of the purification.

The molecular weight findings reported here are consistent with

what has been reported previously (53,54). The high uptake enzyme's molecular weight estimate of 85,000 by gel filtration (90,000 for the highest, consistently present molecular weight component when determined by SDS polyacrylamide gel electrophoresis) was similar to what Barton and Neufeld determined for the urinary "Hurler Corrective Factor". Although it was not found that the high uptake enzyme could be fractionated into two peaks by hydroxyapatite chromatography (53), a significant amount of trailing was observed using this column. The molecular weight estimate for the low uptake enzyme of 68,000 (72,000 by SDS gel electrophoresis) was consistent with the value reported for the partially purified human kidney enzyme, 60,000 ± 6,500. Recently, Myerowitz and Neufeld (46) reported that the molecular weights determined after immunoprecipitation and SDS polyacrylamide gel electrophoresis of the high and low uptake enzymes from human fibroblasts were 76,000 and 66,000, respectively.

The previous estimate of the isoelectric point of α-L-iduronidase (53) using ion exchange column chromatography and polyacrylamide gel electrophoresis was also consistent with the findings presented here. The existence of multiple, catalytically active forms of α-L-iduronidase in the human lung crude homogenates may be due post-translational modifications (i.e., glycoslyation and/or proteolysis) events. This observation has been previously made with a number of other lysosomal enzymes (42-46) although none of the intermediate enzyme forms have been isolated, purified or characterized previously. The two major bands (pI's of 6.00 and 6.85) may correspond to the high and low uptake enzymes, respectively; further studies are underway to confirm these findings.

The gel electrophoresis and HPLC data may be summarized as follows.

Both the low and high uptake forms of the pre-HPLC purified enzymes (SA of 105,000 U/mg Lowry protein) ran as single bands on native 7% polyacrylamide disc gels when 150 µg of each protein was applied. However, when these same samples were run under denaturing conditions on 10% SDS polyacrylamide gels, a number of discrete bands were visualized with Coomassie Blue stain. Surprisingly, for the same enzyme preparation all or some combination of these bands were identified in each different electrophoretic experiment and, in addition, their ratio varied. Furthermore, a number of these bands (72,000 and 43,000) were consistently present in both forms of the enzyme while others (88,000 and higher aggregates) were present only in the high uptake enzyme. Occassionally, other bands (55,000 and 28,000) were identified in both enzyme preparations (data not shown). When these samples were run on the HPLC a number of protein peaks were recovered; when assayed with the 4MU α-Id substrate each protein peak had catalytic activity. Furthermore, the specific activity in each peak was fairly constant. When the enzymes were stored for various lengths of time at 4°C during early stages in the preparation additional, intermediate MW SDS bands appeared in the final preparations. This may be due to endogeneous proteolysis since the low levels of PMSF (0.01 mM) employed may not be suitable to completely inhibit the proteolytic enzymes present in this rich source, human lung (28).

A model may be advanced to explain these data. It is proposed that the initial α-L-iduronidase gene product is an 85-90,000 peptide which possesses 4MU α-Id catalytic activity; this initial product contains the lysosomal "signal peptide" and is subsequently glycosylated. It is this form of the enzyme which is high uptake and is slowly post-translation-

ally processed into low uptake forms; proteolytic and carbohydrate processing of lysosomal enzymes has been observed previously (42,45). Myerowitz and Neufeld (46), after pulse-chasing normal fibroblasts, immunoprecipitating with anti-human α-L-iduronidase antibodies and V8 protease digesting the precipitated proteins have observed a prominent 46,000 band derived from the 66,000, low uptake enzyme which replaces a band of 56,000 derived from the larger high uptake forms. It is possible that the prominent 43,000 band that was observed in the purified lung preparations was the result of a similar, endogenous type of proteolysis. Furthermore, using a modified affinity purification method a prominant 55,000 species in the high uptake enzyme preparations has been observed (data not shown). The present data indicate that upon storage of the partially purified high uptake enzyme fraction at 4°C for 1 week it was converted into the low uptake forms. In this model it is proposed that any of the intermediate, proteolytically modified forms which retain a catalytic site will possess 4MU α-Id activity. To date, the smallest MW species isolated by HPLC which retained catalytic activity is ∿ 28,000 (data not shown). The occasional appearance of coincident SDS bands in each enzyme preparation indicates either incomplete separation of the high and low uptake forms by DEAE-cellulose chromatography, conversion of high uptake into low uptake enzyme during the purification, or alternatively, the existence of a common peptide backbone in both enzyme forms. Finally, it should be noted that the high uptake enzyme consistently had molecular weight species which were greater than those found in the low uptake enzyme. One which was predominant in each of the high uptake preparations has a MW ∿ 90,000; other higher aggregates were occasionally observed.

The kinetic, pH and thermal stability properties of the low uptake lung enzyme fraction using the artificial substrate, phenyl α-Id and the natural substrate anhydro[^{3}H]man were similar to those previously reported by Rome et al. (54) for the partially purified low uptake kidney enzyme. In addition, this is the first report of the physicochemical characterization of any α-L-iduronidase species using the recently synthesized 4MU α-Id substrate. The pH optimum of 3.50 for the low uptake lung enzyme using phenyl α-Id was slightly lower than that previously reported (4.00). However, this is within the variability expected between different laboratories. While the K_m determinations using this substrate were virtually identical to those obtained in the kidney preparations (54), the apparent V_{max} was considerably higher for the lung preparation (83 vs. 6.00 μmoles/mg/min). Interestingly, the K_m determination for the lung preparation using the natural substrate was substantially lower than that reported for the kidney enzyme (0.86 vs. 9.0 mM) while the apparent V_{max} values were nearly identical. A number of possibilities may be proposed for these discrepancies including differences in substrate preparations and assay buffers, tissue specificity and degree of enzyme purity.

The kinetic and thermal stability data obtained for the lung high uptake enzyme fraction were remarkably similar to those for the low uptake enzyme. In addition, although the pH optima were slightly higher for the high uptake enzyme, they were within 0.5 pH units of those obtained for the low uptake enzyme. Catalytic similarities between high and low uptake enzyme forms have been previously reported (48).

Despite these similarities the two purified enzyme fractions interacted quite differently with various glycosaminoglycans. Although most

GAGs inhibited both enzymatic activities, the effect was much less extreme on the high uptake enzyme fraction; Heparin was the most potent inhibitor of both enzymes. Chondroitin sulfates, which do not contain uronic acid moities, inhibited both enzymatic activities and hyaluronic acid, which contains a high percentage of uronates but is not sulfated, partially inhibited the low uptake enzyme but did not effect the high uptake form. Dermatan sulfate and heparan sulfate, the two predominant GAGs excreted in MPS I-H urine, were not very potent inhibitors of the high uptake enzyme. Together, these results indicate that the catalytic sites of the two enzyme forms present in these two fractions may be recognizing a complex conformational property of the polymerized GAG, rather than the iduronic acid residue alone. In addition, the 4MU α-Id active site of the two purified enzyme forms seem to be displaying differential specificities. Finally, since the low and high uptake enzymes behave similarly towards the artificial substrates (and one "natural substrate") but quite differently with the GAGs, their physiologic substrates, two distinct recognition sites may be involved; this concept is supported by the observation that the inhibition of α-L-iduronidase by GAGs was non-competitive when tested with the 4MU α-Id substrate.

The amino acid compositions argue that these two forms of α-L-iduronidase have distinct, structural differences. By analysis of these data it is not clear why the high uptake enzyme was more tightly membrane bound (11), since there is no obvious predominance of hydrophobic amino acids in this form; in fact, the two major amino acids which were elevated in the high uptake enzyme, glycine and arginine, are neutral and hydrophilic, respectively. Presumably, the hydrophobic nature of the high uptake enzyme is an intrinsic property of the molecules con-

formation. Similarly, the meaning of the other minor amino acid differences between the two enzymatic forms is not clear. Interestingly, leucine, a predominant amino acid in most hormonal signal peptides which have been analyzed to date (127), was slightly elevated in the high uptake enzyme (nine residue difference). There were also a number of differences between the amino acid composition presented for the low uptake form of the human lung enzyme and that which has been previously reported for the low uptake human kidney enzyme (54). Intriguingly, five of the seven amino acids which are significantly different, leucine, glycine, alanine, proline and arginine, are also different between the high and low uptake forms which have been purified from human lung. In each case there are more of these residues reported in the low uptake kidney enzyme than in the lung and, similarly, we have found that they are also elevated in the high uptake form of the lung enzyme. Perhaps the kidney preparation contained a small amount of the high uptake form.

C. Comparative Gene Mapping of Human and Feline α-L-Iduronidase:

As detailed in the Results section of this thesis, the structural genes for human and feline α-L-iduronidase have been assigned to chromosomes 22 and D4, respectively. Furthermore, the human gene has been localized to the small region 22pter → 22q11. Although α-L-iduronidase is the third lysosomal enzyme which has been mapped to this small chromosome, it is important to remember that the fourteen other human lysosomal hydrolases which have been previously mapped are dispersed throughout the genome (Table 2); therefore, it is speculative to comment on the significance of this correlation. However, it is interesting to note that both the high and low uptake forms of human α-L-iduronidase may be

mapped to chromosome 22, since the antibodies used in the immunoprecipitation discrimination assay cross-reacted with both enzyme forms (Fig. 19). Therefore these data support the hypothesis that high and low uptake forms of lysosomal hydrolases are coded by the same structural gene, and the differences in recognition and uptake properties are a result of post-translational modification events (i.e., proteolysis, glycosylation). However, these results do not rule out the possibility that there are multiple, transcriptionally functional α-L-iduronidase structural genes in the chromosomal region 22pter → 22q11. Undoubtedly, the availability of an α-L-iduronidase-specific nucleic acid probe will help to clarify this issue, as well as identify non-functional coding sequences (i.e., pseudogenes) and other temporal genes which may not be active in the cell hybrids used for these studies.

As discussed earlier in the Background and Rationale section, it would be interesting to know whether each lysosomal hydrolase structural gene contains sequences coding for its own lysosmal "signal peptide" or, alternatively, if this peptide is encoded by a separate, unlinked gene and is added onto the individual hydrolases post-translationally. Since the polyclonal antibodies used for these studies recognize common components of the high and low uptake α-L-iduronidase forms, it would not be useful in this pursuit. However, the availability of a monoclonal antibody specific for the α-L-iduronidase signal peptide would facilitate these investigations. The ability to isolate and homogeneously purify milligram quantities of high uptake α-L-iduronidase by the methods described in this thesis enhances the feasibility of these experiments.

Throughout the gene mapping studies, it was observed that the

levels of human enzyme expression in the human-rodent hybrid cell lines were significantly lower than that expected if the human structural gene was being faithfully transcribed and the resultant mRNA properly processed and translated. In fact, Figure 24 demonstrates that even in tertiary hybrid, R-G-21-J15, which contained an average of 1.7 human chromosomes 22/cell, the human α-L-iduronidase activity was only ∿ 30% of that observed in normal diploid human fibroblasts (n = 2.0). Furthermore, this graph illustrates that for the immunodiscrimination assay to significantly detect human α-L-iduronidase activity, a minimum of one human chromosome 22 must be present on the average per cell. Figure 25 demonstrates that in the tertiary mouse-human somatic cell hybrid, R-G-21-J15, which contained only human chromosomes 22 and Y, the expression of the total α-L-iduronidase activity as a function of cell density seemed to mimic the pattern observed in the mouse RAG parental cell line, as opposed to that observed in a normal human fibroblast line. Although the growth patterns of the three lines used in this experiment were similar (Fig. 25, left), the level of enzyme activity in the human fibroblast line increased linearly as a function of density, whereas the activity in the mouse RAG cells and hybrid R-G-21-J15 remained at or near the initial basal level (Fig. 25, right).

A number of possibilities may account for these observations. First, it may be argued that to achieve normal expression of the human enzyme activity, regulatory sequences present on human chromosomes other than 22 must be present in the cell nucleus. Secondly, it is possible that the low levels of human enzyme expression observed in the somatic cell hybrids throughout these studies were an artifact of the immunochemical detection technique. Figure 21 demonstrates that when seventy-

five units or less of human or mouse enzyme activity were independently immunoprecipitated and the precipitates subsequently sonicated and assayed for α-L-iduronidase activity, significant amounts of human enzyme (60-100% of initial) could be detected, however, no mouse activity was measured. Surprisingly, analysis of the supernatants of these reactions revealed that both the human and mouse enzyme activities were depleted to the same extent (data not shown). Support for the observation that the anti-human antibodies used in this study cross-reacted with the mouse isozyme may be seen in the Ochterloney immunodiffusion gel shown in Figure 20. Apparently, either the immunoprecipitated mouse enzyme activity was inhibited during the formation of the antigen-antibody complex to a greater extent than the human or, alternatively, it was less stable than the human enzyme under these conditions. In the hybrid cell lines the possibility exists that a hybrid enzyme molecule is produced which behaves similar to the native mouse isozyme. Therefore, although normal amounts of human enzyme protein is produced, the human-mouse hybrid product would not be recognized efficiently by the anti-human antibodies. Although to date it is not clear that α-L-iduronidase is indeed a polymeric enzyme, this explanation cannot be ruled out. Lastly, it is also possible that mouse regulatory elements present in the nucleus of the hybrid cell may be surpressing the human enzyme activity.

Support for the first hypothesis comes from the observation that in primary hybrids, most of which contained many human chromosomes, the levels of human enzyme expression were significantly higher than those observed in secondary and tertiary hybrids which contained single or few human chromosomes (data not shown). Furthermore, the mouse genetic

background in all of the hybrid cells examined throughout these studies was constant, minimizing its role in the differential expression of the human enzyme activity. Finally, since the immunodetection technique discussed above was employed throughout the entire study (i.e., primary, secondary and tertiary hybrid analyses), it is unlikely that the observed low levels of human enzyme expression in hybrid R-G-21J-15 were a result of a methodology artifact.

As mentioned previously, the feline structural gene for α-L-iduronidase has been assigned to feline chromosome D4 using a novel electrophoretic separation technique. This is the first human gene on chromosome 22 to be comparatively mapped in another mammalian species (Fig. 28). Although no obvious banding similarities may be observed between chromosomes 22 and D4, it is interesting that the feline gene for inorganic pyrophosphatase also resides on chromosome D4, whereas, the human counterpart is on chromosome 10; surprisingly, another human gene on chromosome 10, hexokinase, has been comparatively mapped to feline chromosome D2 (76). Together, these data indicate that there may be a distant evolutionary relationship between these four mammalian chromosomes (Homo sapiens and Felis catus diverged ∿ 60 million years ago), however, a complete understanding of these findings must await additional cytological and molecular studies.

CONCLUDING REMARKS

A series of investigations were undertaken to examine some of the biochemical and genetic characteristics of human and feline mucopolysaccharidoses I (α-L-iduronidase deficiency diseases); three objectives were outlined. First, I intended to develop new biochemical tools which would be used for the quantitative analysis of the glycosaminoglycan tissue distribution in normal, as well as, human and feline mucopolysaccharidosis I individuals. Secondly, I wished to purify to homogenity and comprehensively characterize the biochemical properties of the multiple, catalytically active forms of normal human α-L-iduronidase, a prototypic lysosomal enzyme which is defective in these individuals. Lastly, I desired to comparatively map the human and feline α-L-iduronidase structural genes and investigate the regulation of the human enzyme in human-rodent somatic cell hybrids. Each of these three objectives have been met.

A new analytical electrophoretic system was developed which allowed, for the first time, complete resolution of the six major mammalian glycosaminoglycans in a single, continuous, monodimensional run. This new tool was employed to quantitatively investigate the tissue distribution of the stored glycosaminoglycans in both human and feline mucopolysaccharidoses I. In the future this novel analytical method may be used to study a variety of intriguing avenues including 1) the ability to perform prenatal diagnosis by rapid GAG analysis in amniotic cells and fluid, 2) the development of new screening techniques for the fifteen delineated human mucopolysaccharidoses and their respective animal models, and 3) the ability to study the basic metabolism of GAGs in normal

and pathologic mammalian tissues.

Both the low and high uptake forms of human α-L-iduronidase have been purified to homogenity by a combination of conventional and high performance liquid chromatographic techniques. These approaches have allowed the comprehensive biochemical characterization of each catalytically active species of α-L-iduronidase, highlighting significant differences which were specific to each type. Furthermore, this thesis reports the first purification and characterization of the "high uptake" form of a lysosomal hydrolase. It is my hope that this work has laid the foundations for many fruitful investigations into 1) the nature of the enzyme defect(s) in both human and feline mucopolysaccharidoses I, and 2) the complex processing and transport events which are unique to lysosomal enzymes.

Finally, the structural genes for human and feline α-L-iduronidase have been mapped using mammalian-rodent somatic cell hybrids; in addition, the human gene has been localized to the small chromosomal region 22pter → 22q11. A number of significant observations have also been made regarding the expression of the human enzyme in the somatic cell hybrids which were used for these studies. These findings should enhance the role of α-L-iduronidase as a model for future investigations into the organization and evolution of the lysosomal gene family. Most importantly, it is anticipated that the results will provide a tool for many additional studies of this enzyme's gene structure and regulation.

BIBLIOGRAPHY

1. Hurler, G. (1919), Z. Kinderheilk 24:220

2. McKusick, V.A. (1972), Heritable Disorders of Connective Tissue, Fourth Edition, St. Louis: C.V. Mosby

3. Scheie, H.G., Hambrick, G.W., and Barness, L.A. (1962), Amer. J. Ophthal. 53:753

4. Brante, G. (1952), Scand. J. Clin. Lab. Invest. 4:43

5. Dorfman, A., and Lorincz, A.E. (1957), Proc. Natl. Acad. Sci. USA 43:443

6. Hers, H.G. (1965), Gastroenterology 48:625

7. Fratantoni, J.C., Hall, C.W., and Neufeld, E.F. (1969), Proc. Natl. Acad. Sci. USA 64:360

8. Harris, H. (1981), The Principles of Human Biochemical Genetics, Third Edition, New York: American Elsevier

9. McKusick, V.A., Howell, R.R., Hussels, I.E., Neufeld, E.F., and Stevenson, R. (1972), Lancet 1:933

10. Bach, G., Friedman, R., Weissmann, B., and Neufeld, E.F. (1972), Proc. Natl. Acad. Sci. USA 69:2048

11. Roden, L. (1980), in The Biochemistry of Glycoproteins and Proteoglycans (Lennarz, W., ed.), New York: Plenum Press, p. 267

12. Comper, W.D., and Laurenct, T.C. (1978), Physiol. Rev. 58:255

13. McKusick, V.A. (1978), Am. J. Hum. Genet. 30:105

14. Kobayashi, N. (1959), Amer. J. Path. 35:591

15. Denny, W., and Dutton, G. (1962), Brit. Med. J. 1:555

16. Diferrante, N.M., Nichols, B.L., Donnelly, P.V., Neri, G., Hargovoc, R., and Beiglund, R.K. (1971), Proc. Natl. Acad. Sci. USA 68:303

17. Capelletti, R., Del Rosso, M., and Chiarugi, V.P. (1979), Anal. Biochem. 93:37

18. Dietrich, C.P., McDuffie, N.M., and Sampaio, L.O. (1977), J. Chrom. 130:299

19. Cappelletti, R., DelRosso, M., and Chiarugi, V.P. (1979), Anal. Biochem. 99:311

20. Hata, R., and Nagay, Y. (1972), Anal. Biochem. 45:462

21. Nader, H.B., McDuffie, N.M., and Dietrich, C.P. (1974), Biochem. Biophys. Res. Commun. 57:488

22. Dietrich, C.P., and Dietrich, S.M. (1976), Anal. Biochem. 70:645

23. Neufeld, E.F., and Cantz, M.J. (1971) Ann. NY Acad. Sci. 179:580

24. Neufeld, E.F., Lim, T.W., and Shapiro, L.J. (1975) Ann. Rev. Biochem. 44:357

25. Bell, C.E., Sly, W.S., and Brot, F.E. (1977), J. Clin. Invest. 59:97

26. Kaplan, A., Achord, D.T., and Sly, W.S. (1977), Proc. Natl. Acad. Sci. USA 74:2026

27. Hickman, S., Shapiro, L.J., and Neufeld, E.F. (1974), Biochem. Biophys. Res. Commun. 57:55

28. Kaplan, A., Fischer, D., Achord, D., and Sly, W.S. (1977), J. Clin. Invest. 60:1088

29. Ullrich, K., Mersmann, G., Weber, E., and Von Figura, K. (1978), Biochem. J. 170:643

30. Von Figura, K, and Klein, U. (1979), Eur. J. Biochem. 94:347

31. Natowitz, M.R., Chi, M.M.-Y., Lory, O.H., and Sly, W.S. (1979), Proc. Natl. Acad. Sci. USA 76:4322

32. Kaplan, A., Fischer, D., and Sly, W.S. (1978), J. Biol. Chem. 253:647

33. Sando, G.N., and Neufeld, E.F. (1977), Cell 12:619

34. Weismann, U.N., Di Donato, S., and Herschkowitz, N.N. (1975), Biochem. Biophys. Res. Commun. 66:1338

35. Sando, G.N., Titus-Dillon, P., Hall, C.W., and Neufeld, E.F. (1979), Exp. Cell Res. 119:359

36. Tietze, C., Schlesinger, P., and Stahl, P. (1980), Biochem. Biophys. Res. Commun. 93:1

37. Wilcox, P., and Rattray, P. (1979), Biochim. Biophys. Acta 586:442

38. Neufeld, E.F., and McKusick, V.A. (1982), in The Metabolic Basis of Inherited Disease (Stanbury, J.B., Wyngaarden, J.B., Fredrickson, D.S., Goldstein, J.L., and Brown, M.S., eds.) Fifth Edition, New York: McGraw-Hill, p. 751

39. Gonzalez-Noriega, A., Grubb, J.H., Talkad, V., and Sly, W.S. (1980), J. Cell Biol. 84:77

40. Helenius, A., Kartenbeck, J., Simons, K., and Fries, E. (1980), J. Cell Biol. 84:404

41. Fischer, H.D., Gonzalez-Noriega, A., Sly, W.S., and Morre, D.J. (1980), J. Biol. Chem. 255:5069

42. Skodlarek, M.D., and Swank, R.J. (1979), J. Biol. Chem. 254:9939

43. Erickson, A.H., Conner, G.E., and Blobal, G. (1981) J. Biol. Chem. 256:11224

44. Hasilik, A., Von Figura, K., Conzelmann, E., Nehrkorn, H., and Sandhoff, K. (1982), Eur. J. Biochem. 125:312

45. Hasilik, A., and Neufeld, E.F. (1980), J. Biol. Chem. 255:4937

46. Myerowitz, R., and Neufeld, E.F. (1981), J. Biol. Chem. 256:3044

47. Huang, J.S., Huang, S.S., and Tang, J. (1979), J. Biol. Chem. 254:11405

48. Shapiro, L.J., Hall, C.W., Leder, I., and Neufeld, E.F. (1976), Arch. Biochem. Biophys. 172:156

49. Brot, F.E., Glaser, J.H., Roozen, K.J., Sly, W.S., and Stahl, P. (1974), Biochem. Biophys. Res. Commun. 57:1

50. Wall, D.A., Wilson, G., and Hubbard, A.L. (1980), Cell 21:79

51. Weissmann, B. (1978), in Methods in Enzymology (Ginsberg, V., ed.), 50:141

52. Leder, I. (1978), in Methods in Enzymology (Ginsberg, V., ed.), 50:150

53. Barton, R.W., and Neufeld, E.F. (1975), J. Biol. Chem. 246:7773

54. Rome, L.H., Garvin, J.A., and Neufeld, E.F. (1978), Arch. Biochem. Biophys. 189:344

55. Hall, C.W., and Neufeld, E.F. (1973), Arch. Biochem. Biophys. 158:817

56. Liem, K.O., and Hooghwinkel, G.J. (1975), Clin. Chim. Acta 60:259

57. Thompson, J.N., Finley, S.C., Lorincz, A.E., and Finley, W.H. (1975), in Disorders of Connective Tissue, Vol.XI (Bergsma, D., ed.), New York: National Foundation-March of Dimes, p. 341

58. Hopwood, J.J., and Muller, V. (1979), Clin. Sci. 57:265

59. Carlson, E.A. (1966), The Gene: A Critical History, Philadelphia: W.B. Saunders Co.

60. Bridges, C.B. (1925), Am. Nat. 59:127

61. Creighton, H.B., and McClintock, B. (1931), Proc. Natl. Acad. Sci. USA 17:485

62. McKusick, V.A., and Ruddle, F.H.(1977), Science 196:391

63. Harris, H., and Watkins, J.F. (1965), Nature 205:640

64. Poste, G. (1972), Int. Rev. Cytol. 33:157

65. VII International Workshop on Human Gene Mapping, Oslo, Norway, 1981.

66. Paigen, K. (1981), in Lysosomes and Lysosomal Storage Diseases (Callahan, J.W. and Lowden, J.A., eds.), New York: Raven Press, p. 1

67. Paigen, K. (1979), Annu. Rev. Genet. 13:417

68. Paigen, K. (1961), Proc. Natl. Acad. Sci. USA 47:1641

69. Lusis, A.H., and Paigen, K. (1975), Cell 6:371

70. Paigen, K., Meisler, M., Felton, J., and Chapman, V. (1976), Cell 9:533

71. Daniel, W.L. (1976), Biochem. Genet. 14:1003

72. Daniel, W.L. (1976), Genetics 82:477

73. Berger, F.G., Breen, G.A.M., and Paigen, K. (1979), Genetics 92:1187

74. Waheed, A., Hasilik, A., and Von Figura, K. (1981), J. Biol. Chem. 256:5717

75. Frisch, A., and Neufeld, E.F. (1981), J. Biol. Chem. 256:8242

76. O'Brien, S.J., and Nash, W.G. (1982), Science 216:257

77. De Grouchy, J., Turleau, C., and Finaz, C. (1979), Ann. Rev. Genet. 12:289

78. Francke, U., and Taggart, R.T. (1980), Proc. Natl. Acad. Sci. USA 77:3595

79. Pearson, P.L., Roderick, T.H., Davisson, M.T., Lalley, P.A., and O'Brien, S.J. (1982), Cytogenet. Cell Genet., in press

80. Essex, M. (1975), Adv. Cancer Res. 21:175

81. Robinson, R. (1977), Genetics for Cat Breeders, 2nd Ed., New York: Pergamon Press

82. Haskins, M.E., Jezyk, P.M., Desnick, R.J., McDonough, S.K., and Patterson, D.F. (1979), Pediatr. Res. 13:1294

83. McKusick, V.A. (1978), Mendelian Inheritance in Man, Baltimore: Johns Hopkins University Press

84. Andrews, E.J., Ward, B.L., and Altman, N.J. (1979), Spontaneous Animal Models of Human Disease, Vol.II., New York: Academic Press

85. Hommes, F.A. (1979), Models for the Study of Inborn Errors of Metabolism, Amsterdam: Elsevier/North Holland Biomedical Press

86. Richards, R.B., Edwards, J.R., Cook, R.D., and White, R.R. (1977), Neuropathol. Appl. Neurobiol. 3:45

87. Hocking, J.D., Jolly, R.D., and Batt, R.D. (1972), Biochem. J. 128:69

88. Jones, M.Z., and Dawson, G. (1981), J. Biol. Chem. 256:5185

89. Baker, H.J., Lindsey, J.R., McKhann, G.M., and Farrell, D.F. (1978), Science 174:838

90. Cork, L.C., Munnell, J.F., Lorenz, M.D., Murphy, J.V., Baker, H.J., and Rattazzi, M.C. (1977), Science 196:1014

91. Rattazzi, M.C., Appel, A.M., Nestu, J.A. (1979), Am. J. Hum. Genet. 30:59A

92. Haskins, M.E., Jezyk, P.F., Patterson, D.F. (1979b), Pediatr. Res. 12:1203

93. McGovern, M.M., Vine, D.T., Haskins, M.E., and Desnick, R.J. (1981), Enzyme 26:206

94. Bundza, A., Lowden, J.A., and Charlton, K.M. (1979), Vet. Pathol. 16:530

95. Suzuki, Y., Austin, J., Armstrong, D., Suzuki, K., Schlenkr, J., and Fletcher, T. (1970), Exp. Neurol. 29:65

96. Duchen, L.W., Eicher, E.M., Jacobs, J.M., Scaravilli, F., and Teixeira, F. (1980), Brain 103:695

97. Jones, M., and Laine, R.A. (1981), J. Biol. Chem. 256:5181

98. Phillips, N.C., Robinson, D., and Winchester, B.G. (1974), Clin. Chim. Acta. 55:11

99. Burditt, L.J., Chotai, K., Hirani, S., Nugent, P.G., and Winchester, B.G. (1980), Biochem. J. 189:467

100. Sung, J.H., Hayano, M., and Desnick, R.J. (1977), J. Neuropath. Exp. Neurol. 36:807

101. Desnick, R.J., Sharp, H.L., Grabowski, G.A., Brunning, R.D., Sung, J.H., Quie, P.G., and Ikonne, J.U. (1976), Pediatr. Res. 10:985

102. Van de Water, N.S., Jolly, R.D., and Farrow, B.R.H. (1979), Aust. J. Exp. Biol. 57:551

103. Farrow, B.R.H., Hartley, W.J., Pollard, A.C., Grabowski, G.A., Fabbro, D., and Desnick, R.J. (1982), in Gaucher Disease: A Century of Delineation and Research (Desnick, R.J., Grabowski, G.A. and Gatt, S., eds.) New York: Alan R. Liss, Inc.

104. Wenger, D.A., Sattler, M., Kendoh, T., Snyder, S.P., and Kingston, R.S. (1980), Science 208:1471

105. Yoshida, A., Beutler, E., and Motulsky, A.G. (1971), Bull. Wld. Hlth. Org. 45:243

106. Yoshida, A., and Beutler, E. (1978), Ann. Hum. Genet. Lond. 41:347

107. Beutler, E., and Yoshida, A. (1973), Ann. Hum. Genet. Lond. 37:151

108. Bunn, H.F., Forget, B.G., and Ranney, H.M. (1977), Human Hemoglobins, Philadelphia: W.B. Saunders

109. Kimura, A., Tsurumi, K., and Ogane, S. (1978), in The Biochemistry and Pathology of Connective Tissue (Otaka, Y., ed.), Tokyo: Igaku Sloin Ltd., p. 36

110. Rome, L.H., Weissmann, B., and Neufeld, E.F. (1979), Proc. Natl. Acad. Sci. USA 76:2331

111. Hall, C.W., Liebaers, I., Dinataele, P., and Neufeld, E.F. (1978), in Methods in Enzymology, Vol. 50, (Wood, W.A., ed.), New York: Academic Press, p. 439

112. Bishop, D.F., and Desnick, R.J. (1981), J. Biol. Chem. 256:1307

113. Lowry, O.H., Rosenbrough, N.J., Farr, A.L., and Randall, R.J. (1951), J. Biol. Chem. 193:265

114. Reisfeld, R.A., Lewis, U.J., and Williams, D.F. (1962), Nature 195:281

115. Blakesle, R.A., and Boets, J.A. (1977), Ann. Biochem. 82:580

116. King, J., and Laemmli, U.K. (1971), J. Mol. Biol. 62:465

117. Guzman, N.A., Graves, P.N., and Prockop, D.J. (1978), Biochem. Biophy. Res. Comm. 84:591

118. Edelhoch, H. (1967), Biochemistry 6:1948

119. Vaughan, V.L., Hansen, D., and Stadler, J. (1976), Somatic Cell Res. 2:437

120. Littlefield, J.W. (1966), Exp. Cell Res. 41:190

121. Han, B.G., and Puck, T.T. (1962), Proc. Soc. Exp. Biol. Med. 111:67

122. Harris, H., and Hopkinson, D.A. (1976), The Handbook of Enzyme Electrophoresis in Human Genetics, Amsterdam: North Holland

123. Smith, M., Gold, P., Freedman, S.O., and Shuster, J. (1975), Ann. Hum. Genet. 39:21

124. Friend, K.K., Dorman, B.P., Kucheclapati, R.R., and Ruddle, F.H. (1976), Exp. Cell Res. 99:31

125. Breg, W.R. (1972), Stain Technol. 47:87

126. Berg, R.A., and Prockop, D.J. (1973), J. Biol. Chem. 248:1175

127. Hemmings, B.A., Zubenko, G.S., Hasilik, A., and Jones, E.W. (1981), Proc. Natl. Acad. Sci. USA 78:435